Science AAAS

Supplementary Materials for

Low-temperature mineralization of perfluorocarboxylic acids

Brittany Trang *et al*.

Corresponding authors: K. N. Houk, [redacted]@chem.ucla.edu; William R. Dichtel, [redacted]@northwestern.edu

Science **377**, 839 (2022)
DOI: 10.1126/science.abm8868

The PDF file includes:

Materials and Methods

Materials

Reagents were purchased in reagent grade from commercial suppliers and used without further purification, unless otherwise described. Anhydrous DMSO was obtained by drying with activated 4Å molecular sieves. Reagents were purchased from Fisher or Sigma unless specified.

4,4′-difluorobenzophenone NMR standard (Merck) was prepared by diluting to 0.095 M in DMSO-d_6 and adding 60–80 µL of solution to a coaxial NMR tube insert (Wilmad-Lab Glass, WGS-5BL). Each ^{19}F NMR sample was referenced to 4,4′-difluorobenzophenone (-106.5 ppm) by inserting the coaxial tubes containing the external NMR standard into the NMR sample tube before NMR analysis. ^{13}C NMR samples were quantified using a sodium acetate standard in D_2O (50 µL, 5.33 M). ^{1}H NMR samples were quantified using 4,4′-dihydroxybiphenyl dissolved in DMSO-d_6 (0.68 M). Quantification of samples was conducted by integrating each NMR peak and normalizing with the external standard peak integration, then converting to molar concentration using the known molar amount of the external standard. 25 mL PTFE round bottom flasks were purchased from Ace Glass (United States, 13438-16).

PFCA degradation reactions were conducted on 0.5 mmol or 1 mmol scales.

Instruments

Proton nuclear magnetic resonance (^{1}H NMR) spectra and fluorine nuclear magnetic resonance (^{19}F NMR) spectra were recorded at 25 °C on a 400 MHz Bruker Avance III HD Nanobay equipped with a BBFO Smart probe w/ Z-Gradient (unless stated otherwise). Fluorine-decoupled carbon nuclear magnetic resonance (^{13}C NMR) spectra and two-dimensional C–F spectra were recorded on a Bruker Neo 600 MHz system with a QCI-F cryoprobe w/ Z-Gradient. Quantitative ^{13}C NMR spectra were recorded on a Bruker Avance III 500 MHz system equipped with a 5mm DCH CryoProbe w/Z-Gradient using a 40 second D1 delay. Other spectra were recorded on a Bruker Avance III 600 MHz with a BBFO Smart Probe w/ Z-Gradient. Experiments used pulse programs adapted from standard Bruker pulses library.

Ion chromatography was performed using a Thermo Scientific Dionex ICS-5000+ equipped with a Dionex AS-DV autosampler and using a Dionex IonPac AS22 column (Product No. 064141, Thermo Scientific, California, USA). The analysis was run using an eluent of 4.5 mM sodium carbonate and 1.4 mM sodium bicarbonate (Product No. 063965 from Thermo Scientific, California, USA) and a Dionex AERS 500 Carbonate 4 mm Electrolytically Regenerated Suppressor (Product No 085029 from Thermo Scientific, California, USA). A flow rate of 1.2 mL/min was used, giving the following retention times: fluoride = 3.3 min; formate = 3.8 min. Elemental standards containing 1000 µg/mL F^-, and 1000 ug/mL $HCOO^-$ (ICF1, ICHCO1, respectively, from Inorganic Ventures, Christiansburg, VA, USA) were mixed to make quantitative standards consisting of 50, 25, 12.5, 6.25, 3.125, 1.56, 0.78 ug/mL of each anion in ultra-pure H_2O (18.2 MΩ·cm). Ultra pure H_2O was used as the calibration blank. Validation experiments indicated an error of approximately 10% for ion chromatography results.

APCI-MS was collected on an Agilent 6545 QTOF Mass Spectrometer equipped with Atmospheric Pressure Chemical Ionization (APCI) source coupled with Agilent 1200 series LC running in direct injection mode. Data acquisition and analysis were done on Agilent Mass Hunter software.

GC/MS analysis was performed in the Reactor Engineering and Catalyst Testing (REACT) core facility at Northwestern University using an Agilent 6850 GC system coupled to an Agilent 5975C MS system. Helium (Airgas, 99.999%) was purified using an Agilent "Big Universal Trap"

(Model RMSH-2) and used as a carrier gas. Gas separation was performed using a HP-Plot Q column (19091P-Q04E, 30m x 0.320 mm x 20 um) starting at 50 °C for 4 minutes. The temperature was then ramped to 220 °C at 30 °C/min and held for 3 minutes. The flow rate of He was maintained at 1.2 mL/min (inlet split ratio of 10:1). The MS was operated in scan mode (Gain factor = 1, EM voltage = 2518, MS Source = 250 °C, MS Quad = 150 °C) from m/z = 5 to m/z = 300. A solvent delay was not used.

Kinetic traces for PFOA degradation at different temperatures were fitted to the equation $y = ae^{-x/b} + c$ in MATLAB using the Curve Fitting application.

Geometry optimizations, frequency analyses, and single-point energies were calculated at the theoretical M06-2X/6-311+G(2d,p)-SMD-(DMSO) level (*36*, *37*) using the Gaussian 16 package (*38*) with default convergence criteria. M06-2X functional gives refined energies for organic systems (*39*). Frequency outcomes were examined to confirm stationary points as minima (no imaginary frequencies) or transition states (only one imaginary frequency). Paton's GoodVibes (*40*) was used to correct entropy and enthalpy by Grimme's quasi-harmonic approximation (*41*) and Head-Gordon's method (*42*). 3D structures of molecules were generated by CYL view (*43*). All energies are in kcal/mol if not labeled otherwise. All bond lengths are in Angstroms (Å).

Synthetic Procedures and NMR Characterization of Synthesized Compounds

General PFCA Destruction Procedure: Perfluorooctanoic acid (207 mg, 0.500 mmol) and sodium hydroxide (0.600 g, 15.0 mmol) were added to a 25 mL PTFE round bottom flask along with a PTFE-coated magnetic stirbar. 5 mL DMSO was added to the reaction vessel, followed by 0.625 mL distilled or de-ionized water. The vessel was sonicated for approximately 15 seconds, then the t = 0 aliquot was taken by diluting a 50 µL aliquot into 500 µL of deuterated solvent. The vessels were sealed with a rubber septum and pierced with a needle that was left in the septum to prevent overpressure. The vented vessels were then added to an oil bath preheated to 120 °C and stirred at 500 RPM for the specified time, usually 24 hours. Liquid aliquots for reactions monitored over time were taken using a syringe inserted through the rubber septum and diluted as above with solids removed by centrifugation if necessary. The reactions were removed from the heat and cooled for at least 40 minutes before workup. The entire contents of the reaction were diluted with distilled or deionized water until the solids at the bottom were completely dissolved (typically 20–40 mL water added) and were transferred to a polypropylene centrifuge tube. The resulting fluoride- and formate- containing solution was further diluted in water 100x–500x for ion chromatography analysis. For carbonaceous products quantification, the contents of the reaction were added to a 15 mL polypropylene centrifuge tube, centrifuged, and the DMSO solvent was decanted. The remaining solids were rinsed and centrifuged 2x with dichloromethane, then dried overnight at 120 °C on high vac. A portion of the solids (~30 mg) was dissolved (750 µL D_2O + 50 µL NaOAc standard in D_2O) for quantitative ^{13}C NMR analysis.

Scheme S1

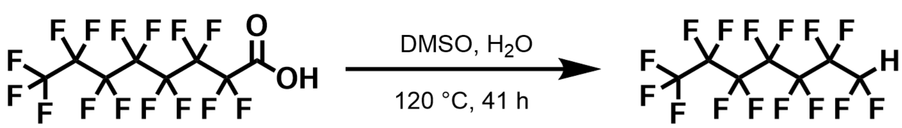

General procedure to decarboxylate perfluorocarboxylic acids and synthesis of perfluoro-1H-heptane **(2)**. PFOA (1.035 g, 2.500 mmol) was added to a glass pressure vessel with PTFE screw-top and PTFE-coated magnetic stirbar and dissolved in a mixture of DMSO (5.00 mL) and deionized H_2O (0.625 mL). The solution was heated to 120 °C for 41 h, then was removed from heat and allowed to cool to room temperature for 2 h. The product phase-separated as a clear liquid on the bottom of the vessel and was decanted via micropipette to provide **2** as a colorless oil (0.703 g, 76% yield). ^{19}F NMR (564 MHz, DMSO) δ -83.614, -123.990, -124.648, -125.218, -128.289, -131.643, -140.332. ^{13}C NMR (151 MHz, DMSO) δ 116.223, 109.800, 109.315, 109.196, 109.152 (d, J^2_{CH} = 7.5 Hz), 107.548, 107.498, 106.194 (d, J^1_{CH} = 197.7 Hz). ^1H NMR (400 MHz, DMSO) δ 5.94 (tt, J = 51.4, 5.1 Hz, 1H).

Scheme S2

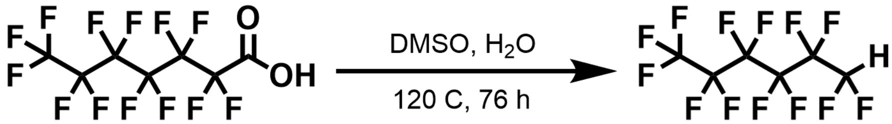

<u>Perfluoro-1H-hexane</u> **<u>(S1).</u>** **S1** was obtained using the above procedure as a colorless oil (0.654 g, 84% yield). ^{19}F NMR (564 MHz, DMSO) δ -83.73 (tt, J = 10.4, 2.4 Hz), -124.955, -125.559, -128.487, -131.875, -140.31 (d, J = 51.7 Hz). ^{13}C NMR (151 MHz, DMSO) δ 116.282, 109.757, 109.340, 109.13 (d, J = 6.6 Hz), 107.560, 106.81 (d, J = 195.8 Hz). ^{1}H NMR (600 MHz, DMSO) δ 5.85 (tt, J = 51.7, 5.1 Hz, 1H).

Supplementary Text

Experimental Determination of $\Delta G^{\ddagger}$

Using the Eyring equation:

$$k = \frac{\kappa k_B T}{h} e^{-\frac{\Delta G^{\ddagger}}{RT}}$$

where

κ is the transmission coefficient, assumed to be 1 in this case
k_B is the Boltzmann constant (1.38×10^{-23} J/K)
T is the temperature in Kelvin
h is Planck's constant (6.626×10^{-34} J•s)
$\Delta G^{\ddagger}$ is the Gibbs energy of activation
R is the gas constant (8.3145 J/mol•K, or 1.987 cal/mol•K)

$\Delta G^{\ddagger}_{393} = 30.0$ kcal/mol

Quantification of Carbon-Containing Byproducts

Quantitative ^{13}C NMR spectroscopy of the precipitate accounted for almost all of the carbon-containing species generated by the PFOA degradation reaction, none of which contain C–F bonds besides trifluoroacetate ions (**Table S4**). The byproducts were identified as a distribution of one-carbon (carbonate, formate), two-carbon (oxalate, glycolate, trifluoroacetate), and three-carbon products (tartronate). Quantification by ^{13}C NMR spectroscopy of the precipitate and ^{1}H NMR spectroscopy of the reaction solution indicated 2.5 ± 0.3 equivalents of formate per mol of PFOA starting material (**Table S4**). The formate ions were independently quantified by ion chromatography and corresponded to 2.1 ± 0.2 equivalents of formate per mol of PFOA starting material (**Figure 2D**). There are several potential pathways for the generation of some of these carbon-containing products that are not further explored in this work. However, the formation of non-fluorinated, relatively oxidized 1–3 carbon products is generally consistent with the proposed mechanism, while accounting for all of the carbon balance of the PFOA degradation reaction.

One Carbon Products: Under the basic reaction conditions, the carbon dioxide reacts with excess hydroxide ions to provide sodium carbonate within the precipitate. 2.1 ± 0.3 equivalents of carbonate ions per mol of PFOA were detected by quantitative ^{13}C NMR spectroscopy. 2.5 ± 0.3 equivalents of formate per mol PFOA were detected, as measured by ^{1}H NMR spectroscopy of the liquid reaction mixture and ^{13}C NMR spectroscopy of the precipitate. It should be noted that the carbonate ion concentration could not be independently measured by ion chromatography because available IC capabilities were run in carbonate-based buffers, precluding the detection of this ion.

Two Carbon Products: 0.32 ± 0.04 mols of trifluoroacetate per mol of PFOA were detected by ^{19}F NMR spectroscopy of the reaction solution at 24 h reaction time; only trace $CF_3CO_2^-$ was found in the precipitate by ^{19}F NMR spectroscopy. 0.6 ± 0.1 mols of glycolate ions per mol of PFOA were detected, some of which might be formed from the degradation of fluoroacetic acid, which was observed in low-temperature experiments (see main text). Oxalate ions were detected at concentrations corresponding to 0.7 ± 0.1 mols per mol of PFOA.

Three Carbon Products: We assign another carbon-containing product as sodium tartronate (0.2 ± 0.1 equiv per mol PFOA) based on its ^{13}C NMR resonance at 177 ppm, which correlates with a ^{1}H NMR resonance at 4.2 ppm **(Fig. S32**). These chemical shifts match literature reports (*29*, *44*), and the correlation is consistent with an intermediate we propose in the mechanism (**Figure 3**). We propose that tartronate is formed in pathway D because it was observed in greater amounts in the degradation of PFBA (C = 4), likely from hydrolysis of INT8 (**Figure 3**).

Unidentified Product: An unidentified product (4.9 ± 2.4 mol% C) is likely derived from the reaction of glycolic acid with another intermediate in the pathway, as it was formed in higher concentration when glycolic acid and PFOA were subjected to the degradation conditions together. However, the unknown product did not form when glycolic acid was subjected to the degradation conditions in the absence of PFOA. The unidentified compound has two ^{13}C NMR resonances, one at 177.9 ppm and one at 69.4 ppm (**Fig. S30**). The two resonances integrate 1:1 with each other, making it likely that it contains either two or four carbons.

Further analysis of the reaction precipitates from degrading the C = 2, 4, 5, and 6 acids (**Fig. S30**) showed that the presence of oxalate was correlated with the presence of TFA, but it is not a direct degradation product of TFA, whose only carbon-containing degradation products were carbonate ions. The amount of oxalate appeared to increase slightly for PFCA with longer perfluoroalkyl chains, such that we speculate that it is formed, at least in part, within the B/C pathways, as are formate ions. Once the fluorocarbon intermediate is protonated, though, as in

INT31 (**Figure 3**), it is difficult to get the correct oxidation state for oxalate except through Cannizzaro reactivity or disproportionation, which could be possible under the extremely basic reaction conditions. We think it is likely that the oxalate either originates from a process in the B pathway preceding INT31 or from further degradation of carbonaceous byproducts.

Computational Mechanistic Investigations of PFCA Degradation

As shown in **Fig. S44**, decarboxylation is the rate-determining step of thermolysis with an energy barrier of 27.7 kcal/mol. This is also consistent with the experimental conditions that decarboxylation requires 120°C to initiate. Relaxed-scan comparisons of the decarboxylation energy profiles in both gas and liquid phase show that the solvent effect plays a significant role (**Fig. S45**). The energy profile in the liquid phase has a maximum value, while the energy profile in the gas phase keeps rising, indicating that in the gas phase, the products formed by decarboxylation will return to the reactant with a very low energy barrier. Hydroxide in the solvent may play a significant role in promoting decarboxylation.

Perfluoroanion INT1 can eliminate a fluoride to become a perfluoroalkene INT2 or be protonated by water to become a polyfluoroalkane. Since S_N2 reactions on saturated fluoroalkane carbons require a high energy barrier (**Fig. S46**), INT1 is more likely to generate perfluoroalkene INT2.

The resulting alkene INT2 is easily hydroxylated; our calculations also suggest that the hydroxylation is specifically favored at the terminal position, As shown in **Fig. S47**, the relaxed-scan addition energy profiles on the internal side and the terminal side show that the addition on the internal side of the alkene has a barrier of 8.9 kcal/mol, whereas addition on the terminal side does not have an enthalpic barrier.

After the formation of hydroxylated perfluoroanion INT3, two consecutive fluoride ion eliminations produce α,β-unsaturated acyl fluoride INT6. The carbon–oxygen bond length scanning coordinates of INT7 and INT13 do not have inflection points but continuously rise, showing that neither 1,2-addition nor 1,4-addition have enthalpic barriers (**Fig. S48**).

1,4-addition produces 1,3-diketone compound INT8. **Fig. S49** shows that subsequent hydroxide addition is favored to occur on the ketone carboxyl side of INT8 rather than the acyl fluoride side.

While 1,4-addition leads to the formation of shorter PFCAs such as $CF_3CO_2^-$ (**Fig. S44**), 1,2-addition can lead to the eventual formation of byproduct HCOOH. The 1,2-hydroxylation produces α,β unsaturated perfluorocarboxylic acid INT14 (**Fig. S51**), then generates an alkene anion INT30. Several pathways for generating INT30 from INT14 exist (**Fig. S50**).

We propose two possible pathways for the transformation of INT14 to INT30 (**Fig. S50**). In Pathway B″ (**Fig. S54**), hydroxide addition to the alpha carbon allows an acid fluoride equivalent of oxalate to be generated, eliminating a fluoroalkene anion five carbons in length (for PFOA; generalized to other PFCAs, the alkene is three carbons shorter than the original PFCA length) with a barrier of 24.8 kcal/mol. In Pathway B′ (**Fig. S51, Fig. S52**), 1,4 addition of the hydroxide to INT14 leads to a Darzens-type decarboxylation through an epoxide intermediate INT19 via TS11 with a barrier of 19.4 kcal/mol. Interestingly, though carbonate INT18 has a similar structure to acid fluoride INT9, they have different reactivity (**Fig. S53**). INT9 tends to fragment, while INT18 tends to form the epoxide because it cannot form a dianion through fragmentation. For longer PFCAs (original PFCA C > 6), the unsaturated aldehyde intermediate can eliminate a fluoride and pass through a Pathway C-like process (Pathway C′; **Fig. S52**) where hydroxide adds to the carbonyl and eliminates off an alkene four carbons shorter than the original PFCA (for PFOA, four carbons in length) and an equivalent of glyoxylate, which can disproportionate into an equivalent of oxalate and an equivalent of glycolate (*45*).

The mechanisms explicitly proposed in **Fig. S50** and its supporting figures show many classes of reactivity at the possible bifurcation points. For example, the C and C′ reactivity modes are the same, even though the resulting byproducts are different; similarly, pathway D-type retroaldol reactions could occur at other 1,3-dicarbonyl intermediates to create a PFCA + carboxylic acid byproduct equivalent. We expect that the reactivity motifs we have explored through computation may be active at intermediates in the mechanism other than what we have explicitly shown.

Calculation results show that protonating the alkene anion INT30 is more favorable than eliminating a fluoride to generate the alkyne, the hydroxide addition is more likely to happen on the terminal side of INT31 (**Fig. S56**) as it was for the fully fluorinated INT2, and solvent effects can reduce the energy barrier for protonation (**Fig. S58**). Likewise, two consecutive eliminations of fluoride ions generates α,β-unsaturated aldehyde INT35, an analogue to the α,β-unsaturated acid fluoride INT6. The scanning coordinates of carbon–oxygen bonds length of INT36 and INT37 show that neither 1,2-addition or 1,4-addition to INT35 have enthalpic barriers (**Fig. S57**). The 1,2-addition leads to the production of formate through elimination (**Fig. S55**), while the 1,4-addition can exit the cycle and generate shorter PFCAs through pathway D (**Figure 3, S59**). As with analogue INT8, hydroxide addition is more favorable on the ketone carboxyl side of 1,3-diketone compound INT38 (**Fig. S60**).

Computational Investigations Into Alternate Mechanisms

Finally, to show that the mechanism we proposed is the most reasonable at present, we calculated the α-lactone mechanism proposed by Pellerite (*33*) and a difluorocarbene mechanism we proposed. Selecting some intermediates to calculate the energy, we found that neither of these hypothetical mechanisms are feasible for our system (**Fig. S61 and Fig. S62**).

Computational Mechanistic Investigations of PFECA Degradation

We also used computational tools to investigate the GenX degradation pathway. GenX goes through a mechanism much like Pathway A for PFCAs before forming INT45 (**Fig. S63**). However, INT45 cannot eliminate a fluoride like PFCAs. Instead, sequential hydrolysis reactions generate **5**, which was experimentally observed.

5 does not easily decarboxylate (**Fig. S65**). Instead, it is attacked by hydroxide and eliminates a perfluoroether tail, which can be transformed into a corresponding PFCA through hydrolysis in pathway F (**Fig. S64**). **Fig. S66** shows which side of **5** hydroxide more easily attacks.

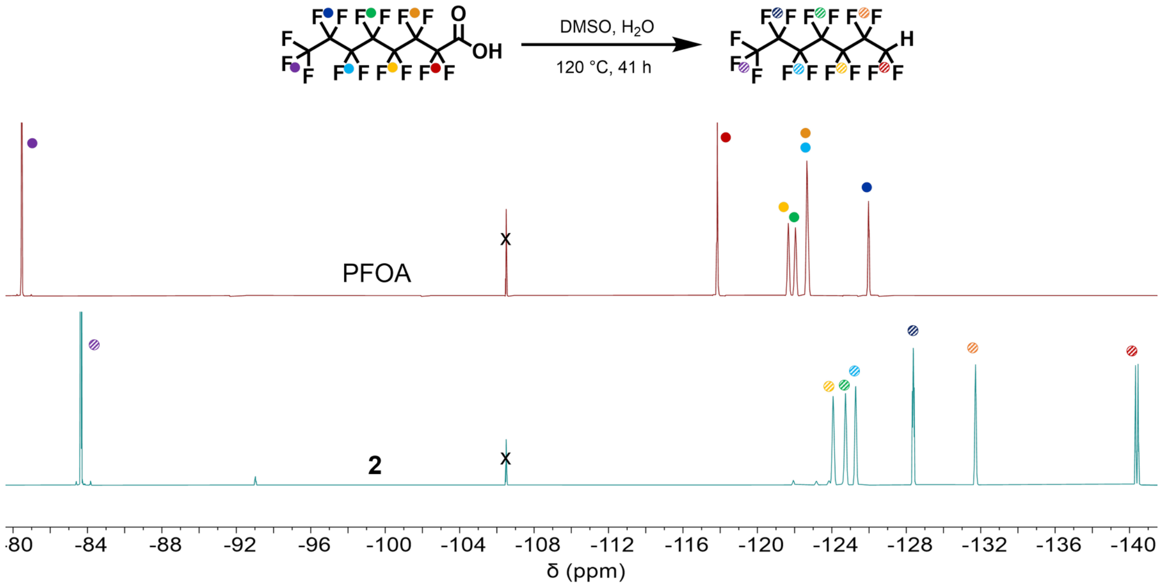

Fig. S1. ^{19}F NMR spectra of PFOA (top, DMSO-d_6, 400 MHz) and **2** (bottom, DMSO-d_6, 600 MHz). **2** is insoluble in DMSO, so it was analyzed as a neat oil in an inner coaxial insert tube with a solution of a 4,4′-difluorobenzophenone standard (-106.5 ppm) dissolved in DMSO-d_6 in an outer tube.

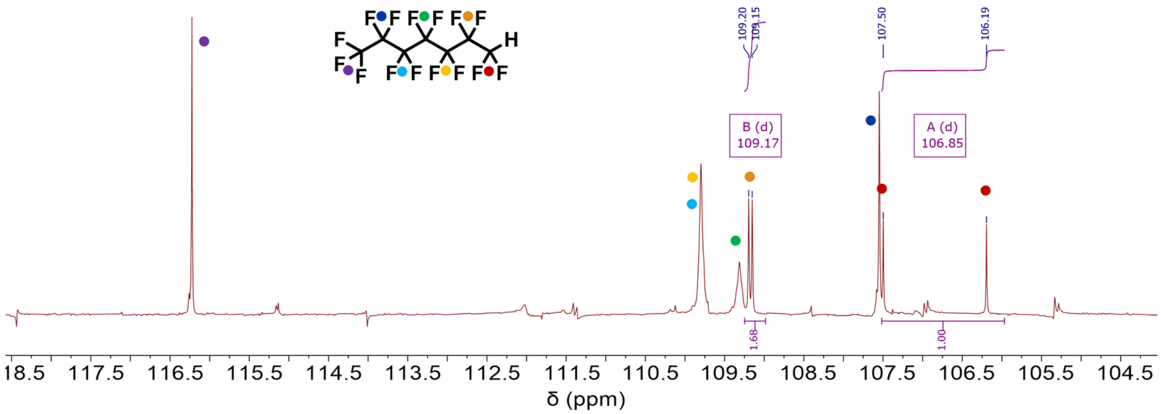

Fig. S2. Fluorine-decoupled ^{13}C NMR spectrum of perfluoro-1H-heptane, calibrated to DMSO-d_6 (39.52 ppm). **2** is insoluble in DMSO, and so it was analyzed as a neat oil in an inner coaxial insert tube with a solution of a 4,4′-difluorobenzophenone standard (-106.5 ppm) dissolved in DMSO-d_6 in an outer tube.

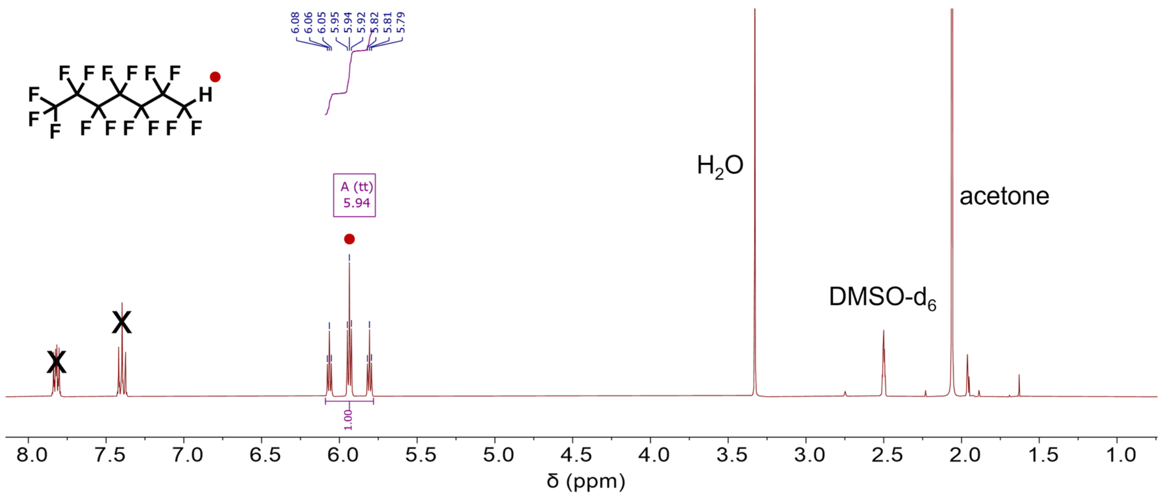

Fig. S3. ^1H NMR spectrum of perfluoro-1H-heptane (DMSO-d_6, 600 MHz). **2** is insoluble in DMSO, so it was analyzed as a neat oil in an inner coaxial insert tube with a solution of a 4,4′-difluorobenzophenone standard (7.3–7.8 ppm, marked with X) dissolved in DMSO-d_6 in an outer tube.

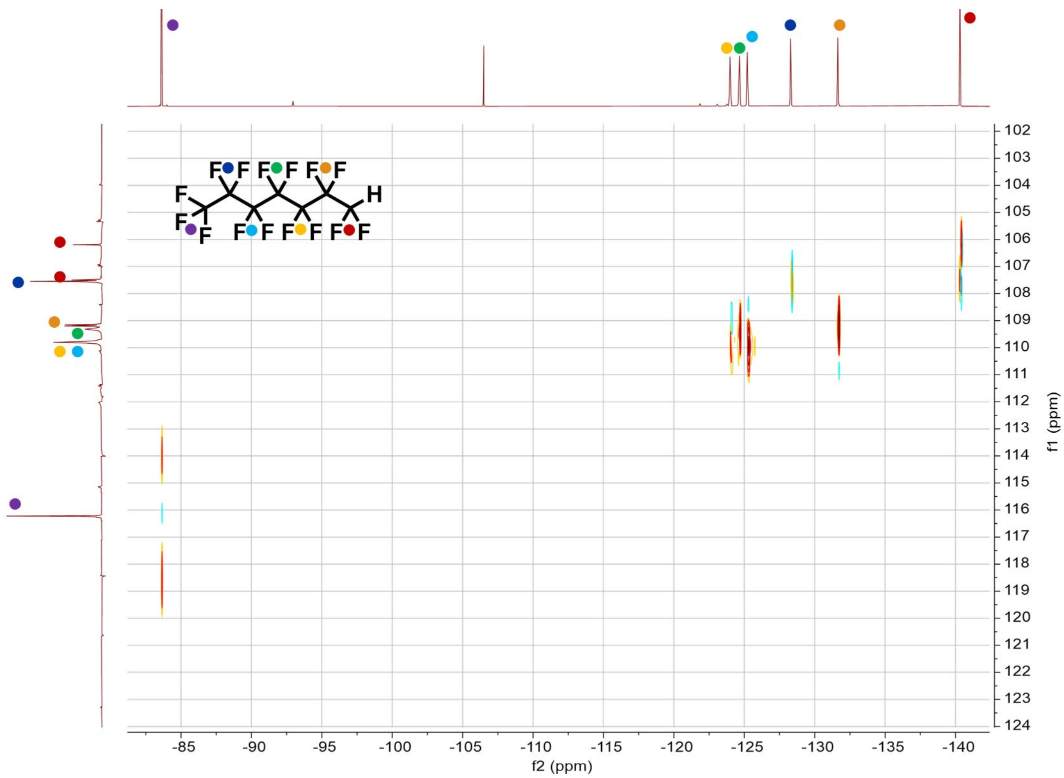

Fig. S4. ^{19}F–^{13}C HSQC spectrum of perfluoro-1H-heptane used to assign the ^{13}C resonances. The ^{19}F resonances were assigned by comparison to PFOA.

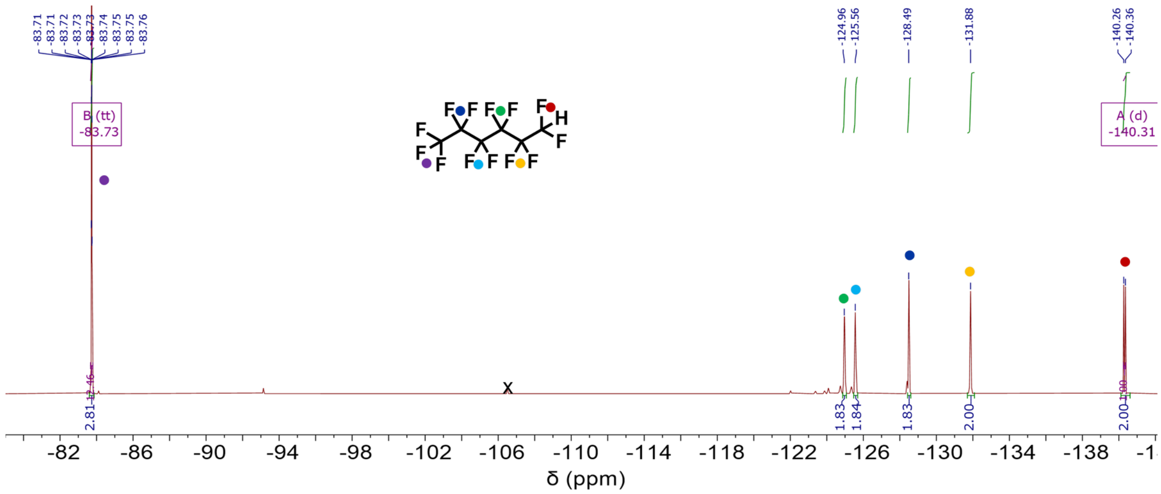

Fig. S5. [19]F NMR spectra of perfluoro-1H-hexane (DMSO-d_6, 600 MHz). **S1** is insoluble in DMSO, and so it was analyzed as a neat oil in an inner coaxial insert tube with a solution of a 4,4′-difluorobenzophenone standard (-106.5 ppm) dissolved in DMSO-d_6 in an outer tube.

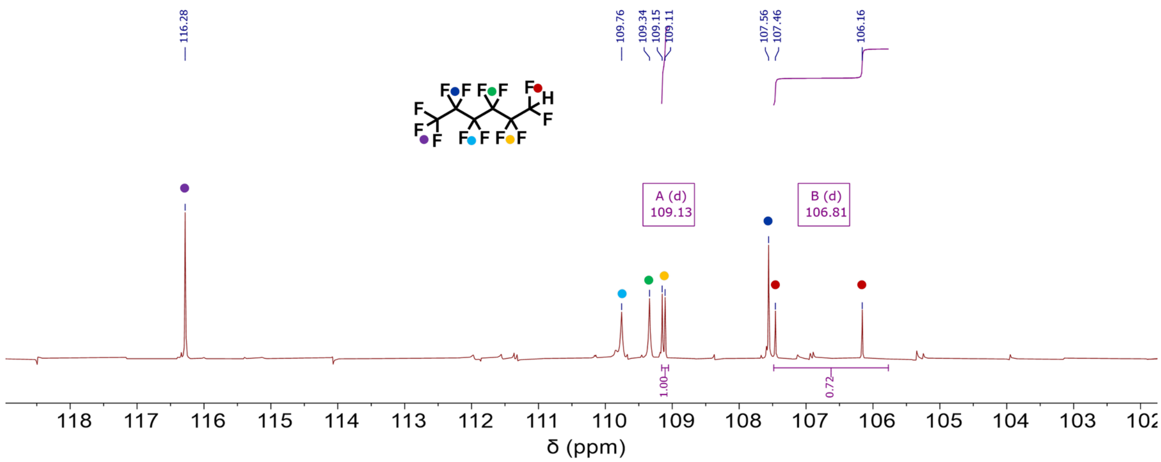

Fig. S6. Fluorine-decoupled ^{13}C NMR spectrum of perfluoro-1H-hexane, calibrated to DMSO-d_6 (39.52 ppm). **S1** neat in coaxial insert tube with 4,4′-difluorobenzophenone standard dissolved in DMSO-d_6 in outer tube.

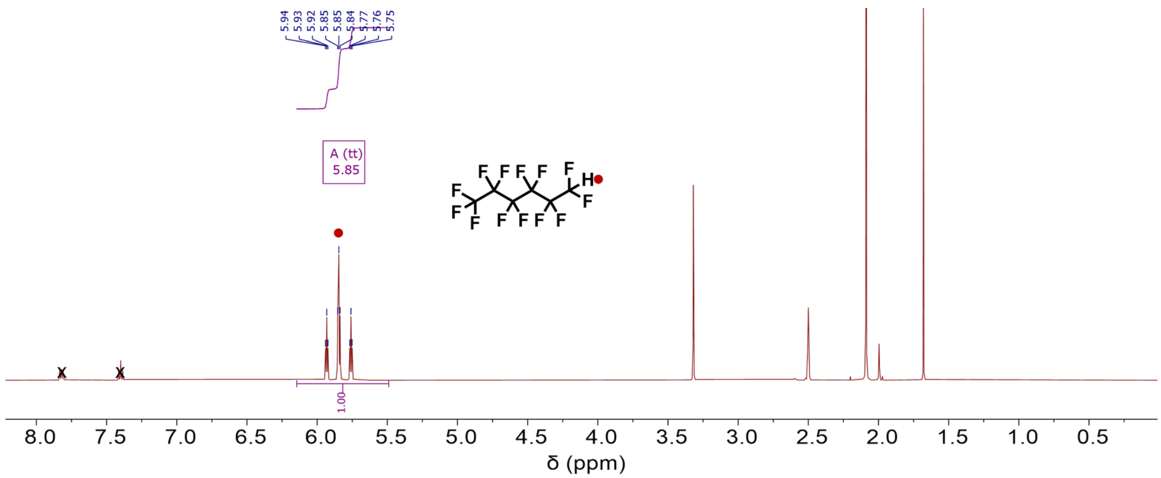

Fig. S7. ^{1}H NMR spectrum of perfluoro-1H-hexane (DMSO-d_6, 600 MHz). **S1** is insoluble in DMSO, so it was analyzed as a neat oil in an inner coaxial insert tube with a solution of a 4,4′-difluorobenzophenone standard (7.3–7.8 ppm, marked with X) dissolved in DMSO-d_6 in an outer tube.

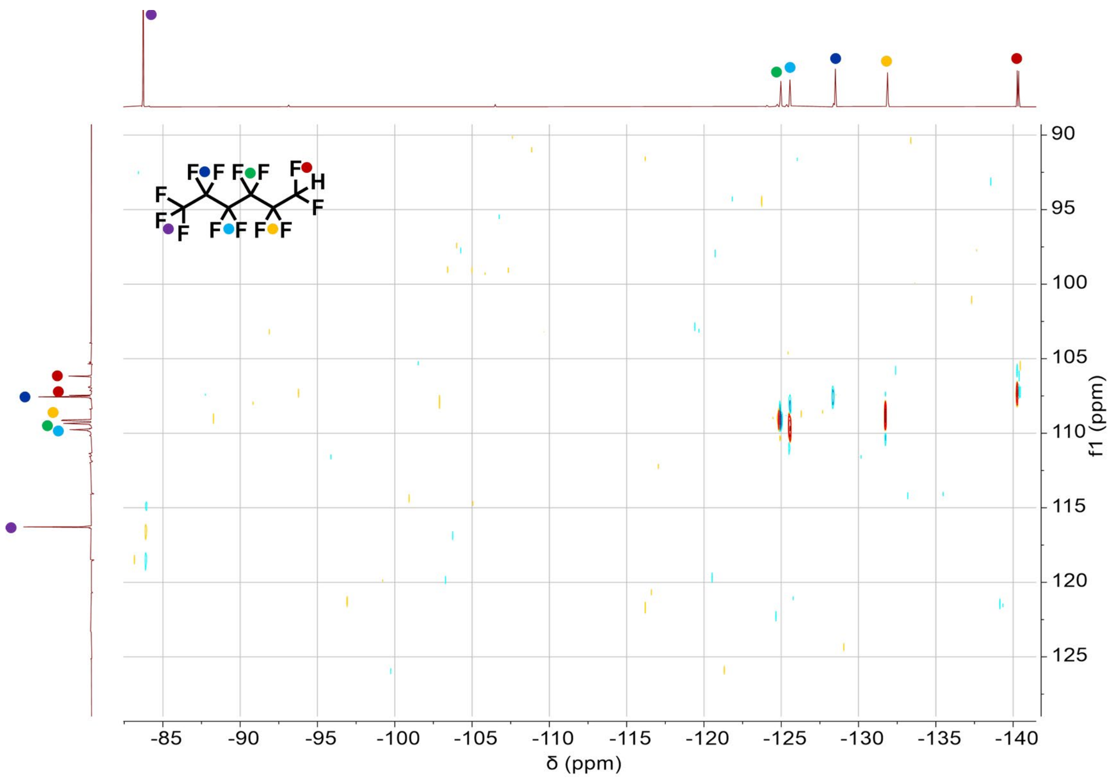

Fig. S8. ^{19}F–^{13}C HSQC of perfluoro-1H-hexane used to assign carbon peaks. Fluorine peaks assigned based on PFOA and literature.

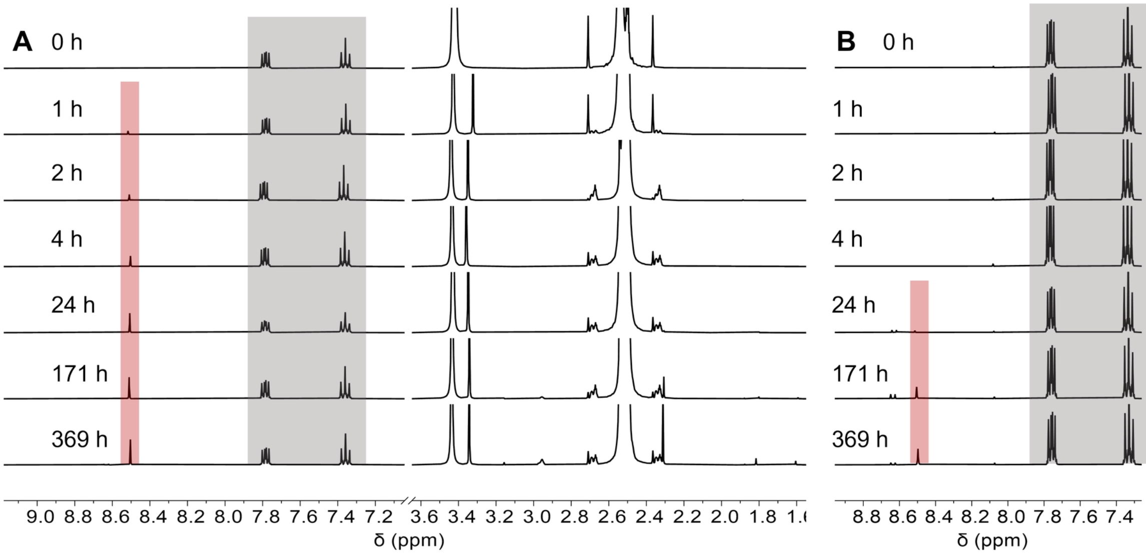

Fig. S9. ^{1}H NMR spectra to monitor formate ion formation at 120°C as a function of reaction time. Peaks highlighted in gray correspond to the 4,4′-difluorobenzophenone external standard, and peaks highlighted red correspond to formate ions. A) PFOA degradation reaction: the formate ion concentration increases steadily over the course of the reaction, even after all PFOA has been degraded (24 h) and only TFA remains. B) Control reaction of water, DMSO, and NaOH in the absence of PFOA demonstrates a slower background reaction that also produces a small amount of formate, presumably from the degradation of the DMSO solvent. In both cases, formate production was confirmed by ion chromatography. However, ^{1}H NMR spectroscopy is not sufficient for formate quantification, as much of the formate precipitates out of the reaction and cannot be detected in solution.

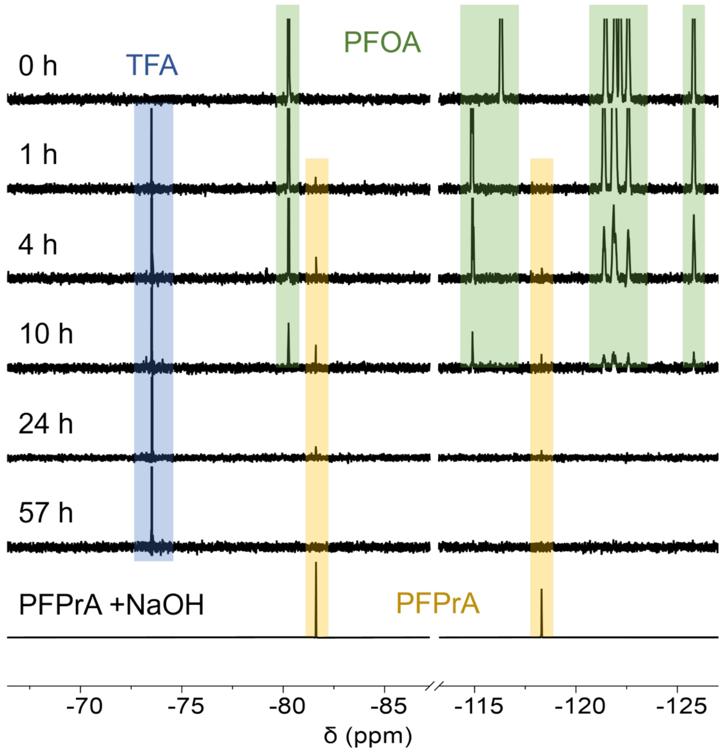

Fig. S10. Appearance and disappearance of perfluoropropionic acid (PFPrA) during the degradation of PFOA at 120°C as a function of reaction time. Bottom spectrum: authentic sample of PFPrA and NaOH heated to 120°C for 1 h. Blue highlighted peaks correspond to trifluoroacetate (TFA), green highlighted peaks correspond to PFOA, and yellow highlighted peaks correspond to PFPrA. PFPrA is observed as a trace byproduct (in the 10 h spectrum, its concentration is approximately 1–2% of the initial PFOA concentration) that subsequently degrades between reaction times of 24–57 h.

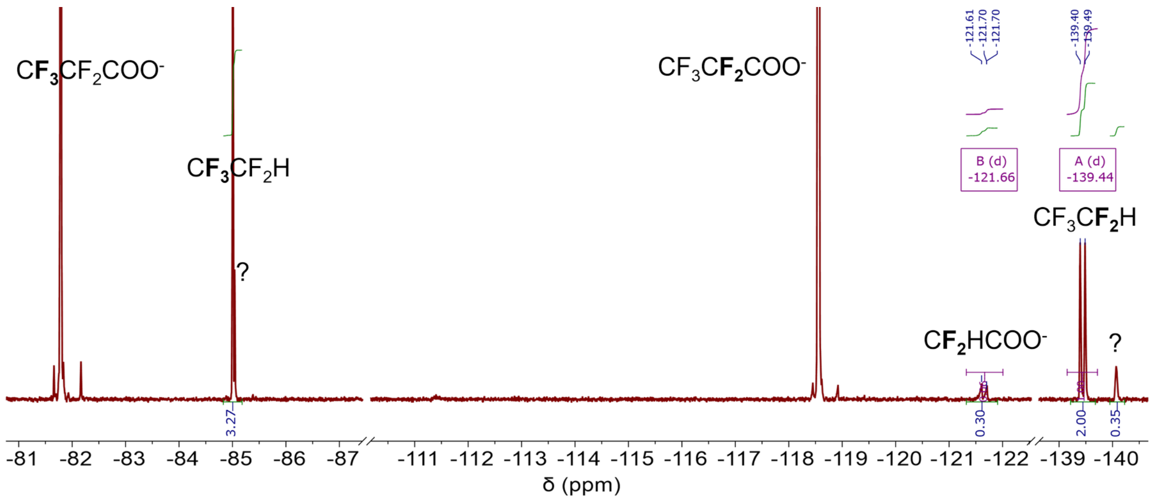

Fig. S11. ^{19}F NMR (565 MHz, DMSO) spectrum of concentrated aliquot of PFPrA degradation reaction (30 equiv NaOH in 8:1 DMSO:H_2O). The degradation of PFPrA provides evidence for the formation of a volatile protodecarboxylated fluorocarbon CF_3CF_2H, along with difluoroacetate ions.

CF_2HCOO^- Actual: -121.66 (d, $J = 53.5$ Hz)

Literature (*46*): (solvent not specified): -123.63 d, J = 56.5 Hz.

CF_3CF_2H Actual: δ -85.00 (s, 3F), -139.44 (d, $J = 51.4$ Hz, 2F).

Literature (*47*): $(CD_3)_2SO$: −139.5 (2F, dq, $^2J_{HF} = 51.1$, $^3J_{FF} = 3.0$ Hz, HCF_2), −85.1 (3F, dt, $^3J_{HF} = {}^3J_{FF} = 3.0$ Hz, CF_3).

Unidentified peaks at -85.04 (s), -140.07 (s)

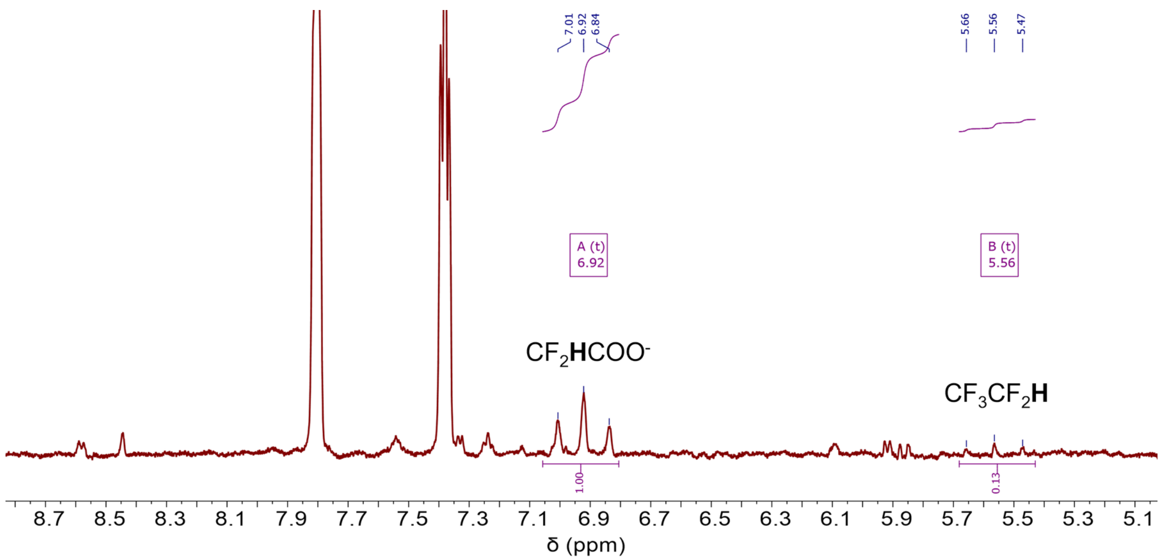

Fig. S12. ^{1}H NMR (600 MHz, DMSO) spectrum of concentrated aliquot of PFPrA degradation reaction (30 eq. NaOH in 8:1 DMSO:H_2O). The degradation of PFPrA provides evidence for the formation of a volatile protodecarboxylated fluorocarbon CF_3CF_2H, along with difluoroacetate ions.

CF_2HCOO^- Actual: δ 6.92 (t, J = 50.8 Hz)
Literature (*48*): (CF_2HCOOH, 299.949 MHz, solvent not specified): ^{1}H spectrum: 6.13 ppm, $^2J_{H,F}$ = 53.10 Hz.

CF_3CF_2H Actual: δ 5.56 (t, J = 55.8 Hz)
Literature (*49*): (neat, referenced to DMSO in D_2O) 5.80 (1H, tq, J = 52.31, 2.55 Hz)

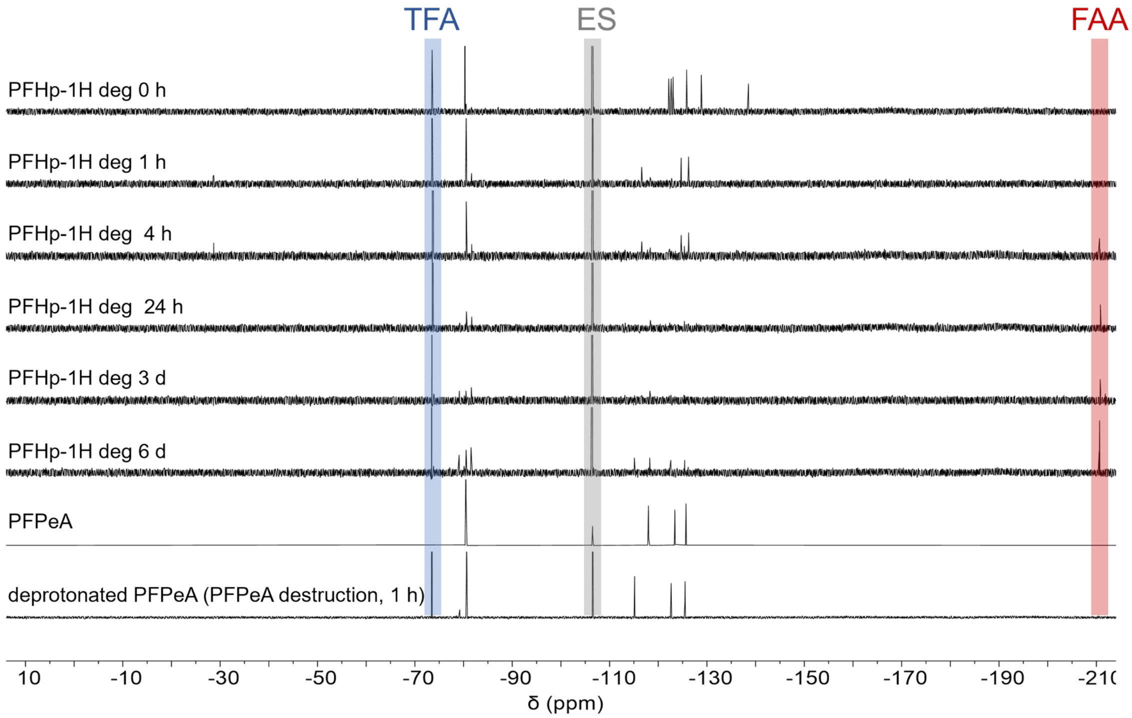

Fig. S13. ^{19}F NMR spectra (600 MHz) of aliquots from the 40°C degradation of PFHp-1H. When the degradation is run at this lower temperature, various fluorinated intermediates (fluoroacetic acid, INT8/9, perfluoropentanoic acid) are observed that are not seen in the spectra of degradation reactions run at higher temperatures. These intermediates are shown in greater detail below. TFA = trifluoroacetate, ES = external standard (4,4′-difluorobenzophenone), FAA = fluoroacetic acid.

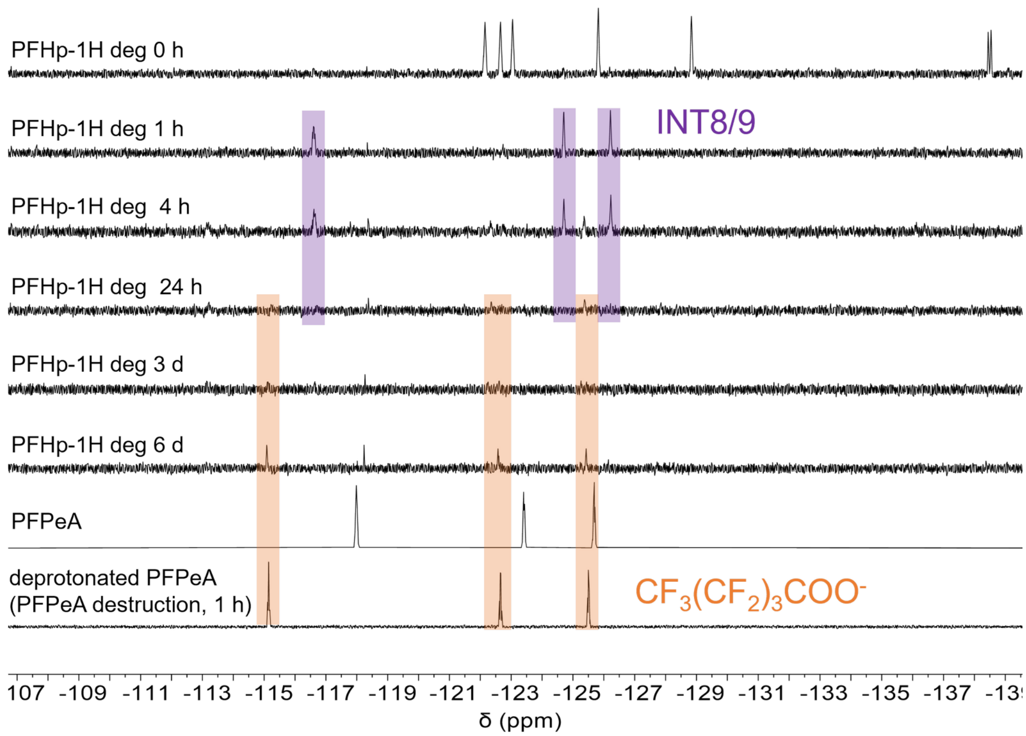

Fig. S14. Partial ^{19}F NMR spectra (600 MHz) of the 40°C degradation of **2**. In the first few hours of reaction, an intermediate with 3 CF_2 groups is observed (purple). We hypothesize that this intermediate is INT8 or 9; see **Fig. S15** for further assignment of these peaks. In spectra obtained at 24 h, 77 h, and 142 h, resonances corresponding to five-carbon PFPeA are observed (orange), in accordance with the three-carbon shortening process proposed in **Figure 3** Pathways A + D.

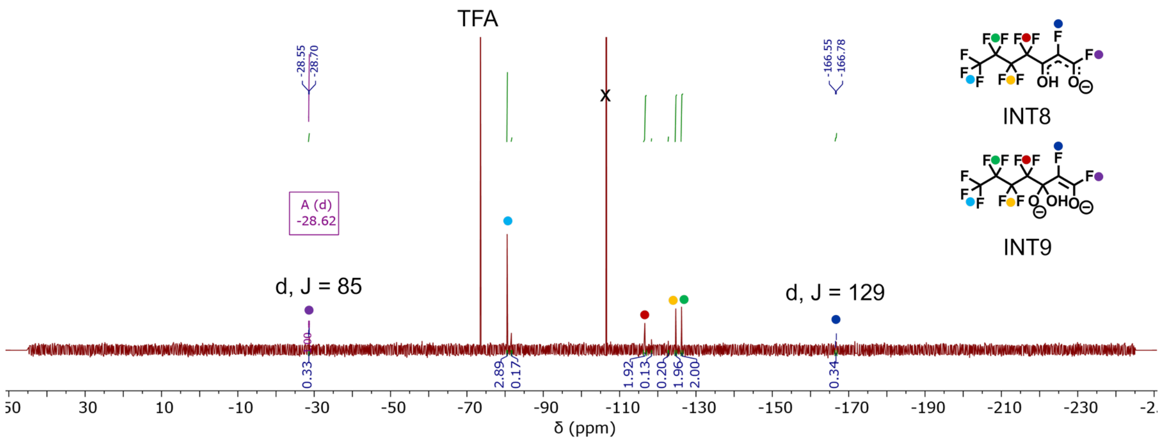

Fig. S15. Proposed assignment of ^{19}F NMR peaks corresponding to proposed intermediates INT8 or 9 from the ^{19}F NMR spectrum of 1 h aliquot of 40°C degradation of **2**. TFA = trifluoroacetate, x = 4,4′-difluorobenzophenone standard. Peak assignments marked with colored dots based on the spectrum of PFPeA and the assignment of enol fluorine (*50*). While the relative peak positions are relatively consistent with the proposed structures, the peak integrations and couplings are potentially inconsistent with these structures.

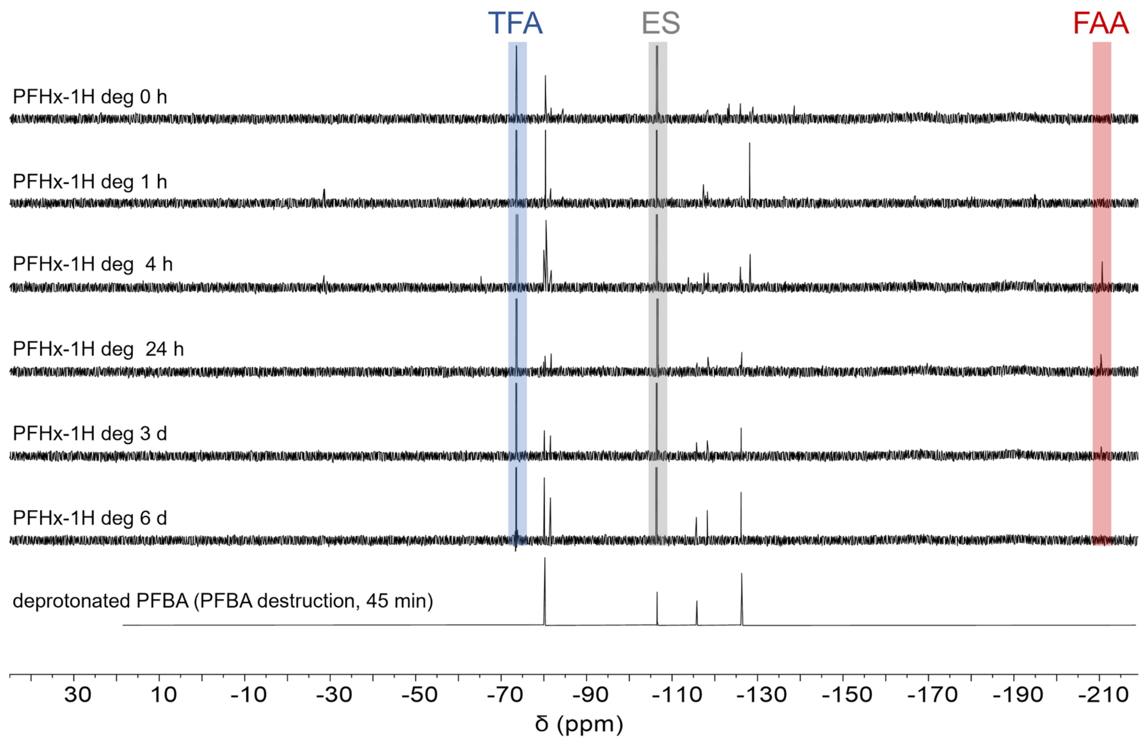

Fig. S16. ^{19}F NMR spectra (600 MHz) of aliquots from the 40 °C degradation of **S1**. When the degradation is run at this lower temperature, various fluorinated intermediates (fluoroacetic acid, INT8/9, perfluorobutanoic acid) are observed that are not seen in the spectra of degradation reactions run at higher temperatures. These intermediates are shown in greater detail below. TFA = trifluoroacetate, ES = external standard (4,4′-difluorobenzophenone), FAA = fluoroacetic acid.

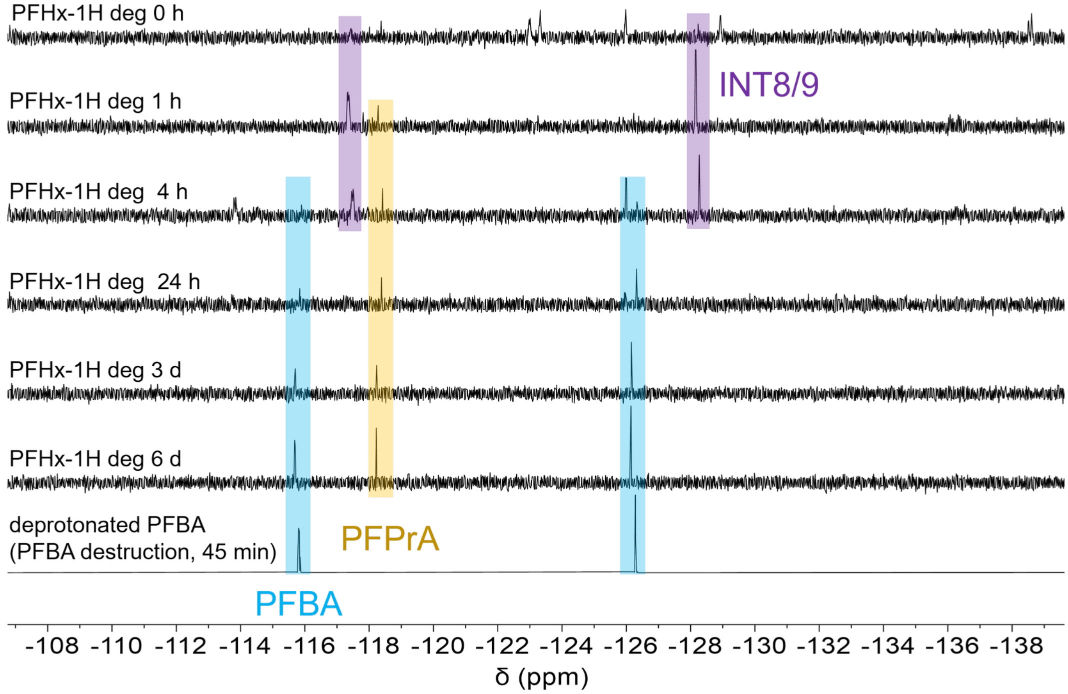

Fig. S17. Partial ^{19}F NMR spectra (600 MHz) degradation of **S1** performed at 40°C. In the first few hours of reaction, an intermediate with 3 CF_2 groups is observed (purple). We hypothesize that this intermediate is INT8 or 9; see **Fig. S18** for further assignment of these peaks. In spectra obtained at 24 h, 77 h, and 142 h, resonances corresponding to four-carbon PFBA are observed (blue), in accordance with the three-carbon shortening process proposed in **Figure 3** Pathways A + D. A peak corresponding to perfluoropropionic acid (PFPrA) is highlighted in yellow.

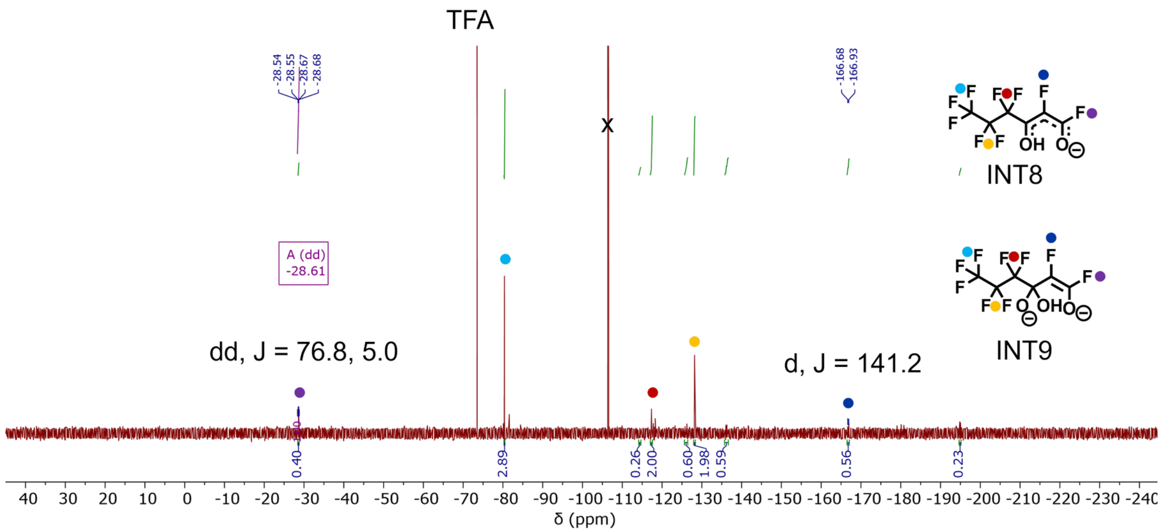

Fig. S18. Proposed assignment of ^{19}F NMR peaks corresponding to proposed intermediates INT8 or 9 from the ^{19}F NMR spectrum of 1 h aliquot of 40°C degradation of **S1**. TFA = trifluoroacetate, x = 4,4′-difluorobenzophenone standard. Peak assignments marked with colored dots based on the spectrum of PFBA and the assignment of enol fluorine (*50*). While the relative peak positions are relatively consistent with the proposed structures, the peak integrations and couplings are potentially inconsistent with these structures.

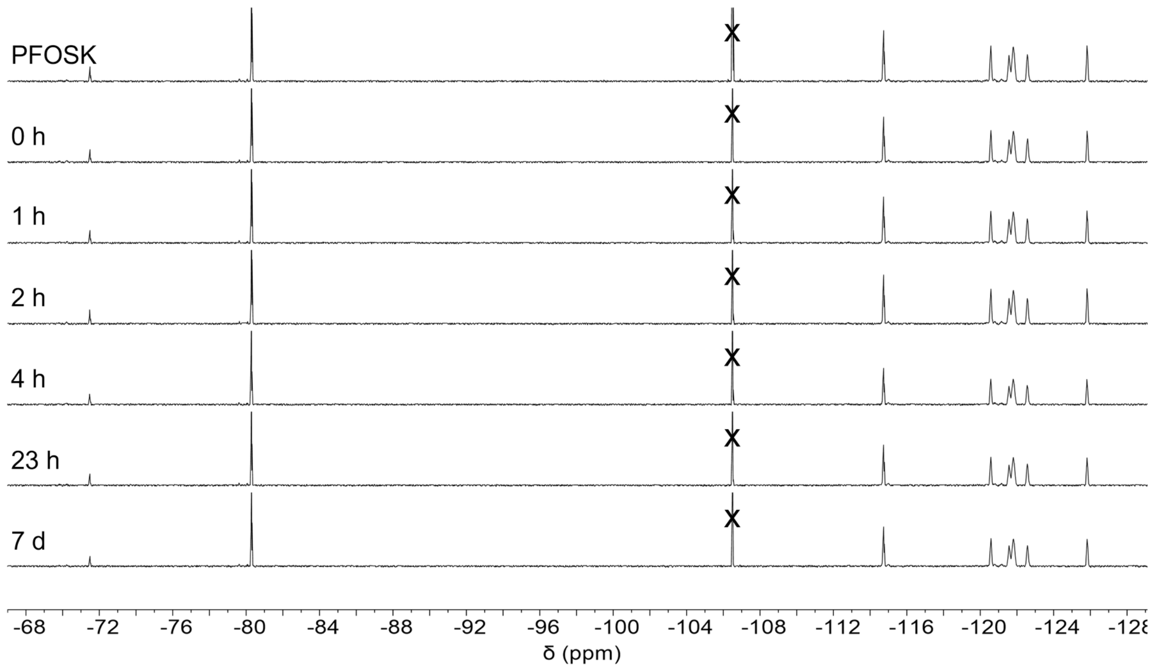

Fig. S19. [19]F NMR spectra of aliquots of perfluorooctanesulfonic acid potassium salt (PFOSK, 0.089 M) in DMSO:H_2O (8:1) in the presence of NaOH (30 equiv) and heated to 120°C. 4,4′-difluorobenzophenone was used as an external standard (X). No degradation of PFOSK is observed, implicating decarboxylation as the first step of PFCA degradation under these conditions.

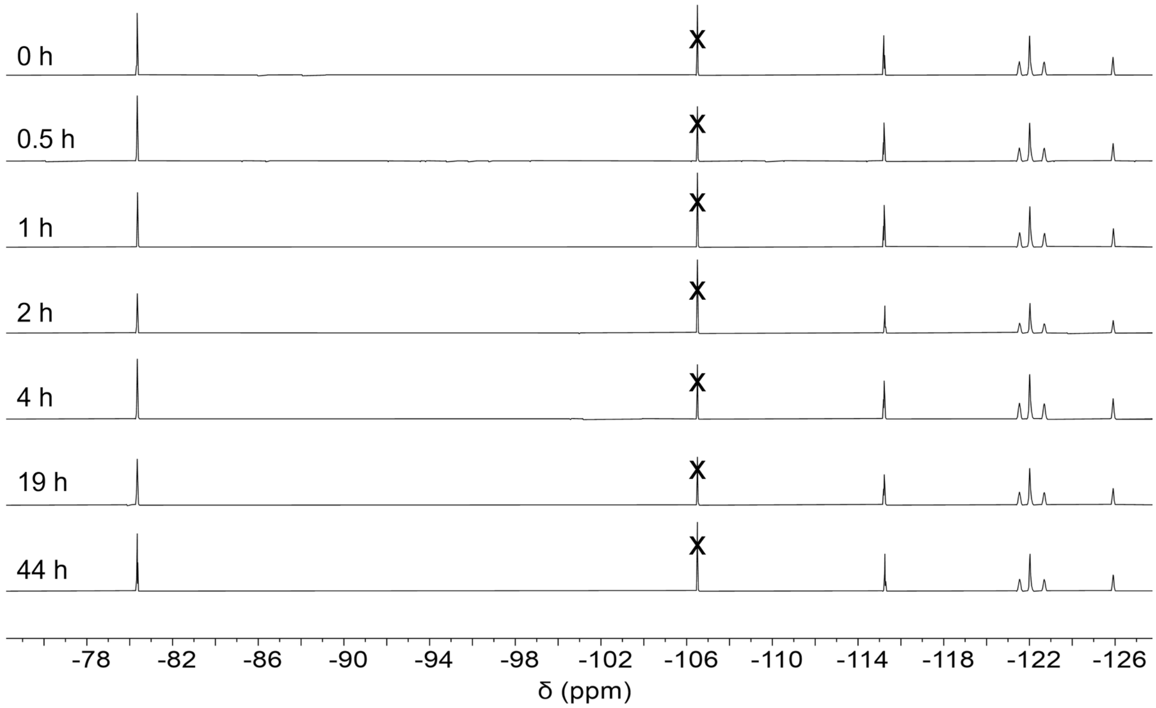

Fig. S20. ^{19}F NMR spectra of 0.089 M perfluorooctanoic acid (PFOA) in water with 30 equiv NaOH heated to 120°C. No change in the spectra over time shows that this decarboxylation needs polar aprotic solvent to occur. 4,4'-difluorobenzophenone standard is crossed out.

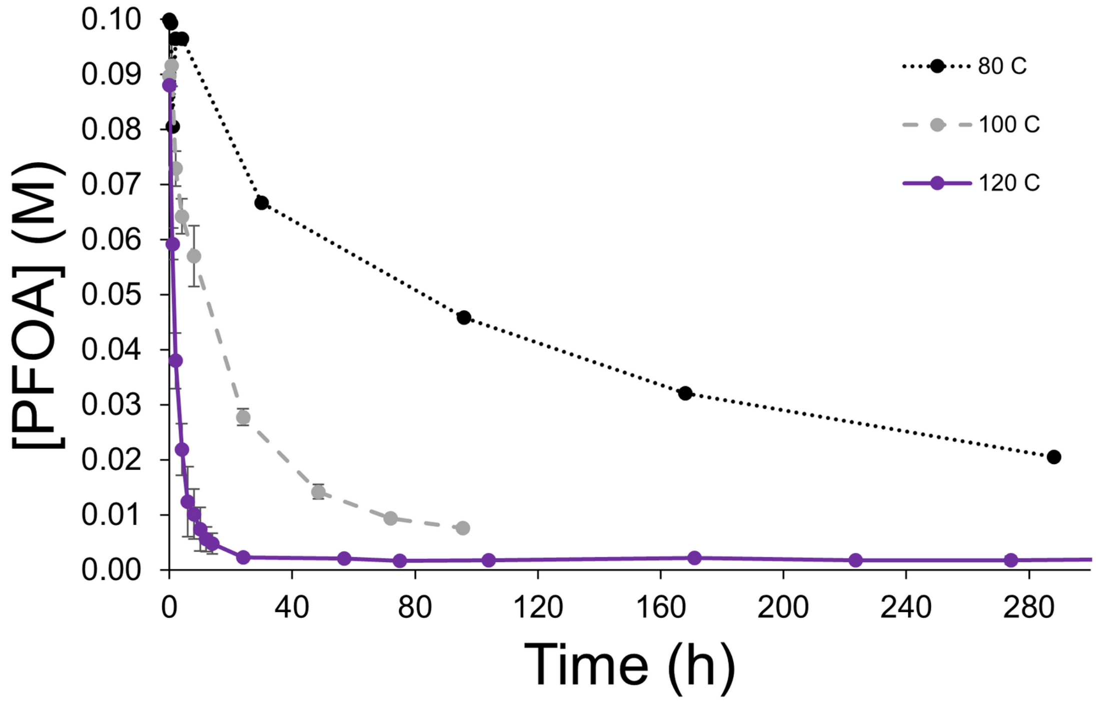

Fig. S21. Disappearance of PFOA over time at three different reaction temperatures as measured by ^{19}F NMR. [PFOA] = 0 mmol at < 24 h at 120°C (average of triplicates), 100 h at 100°C (average of triplicates), and >290 h for 80°C, showing the high temperature-dependence of the rate-limiting step.

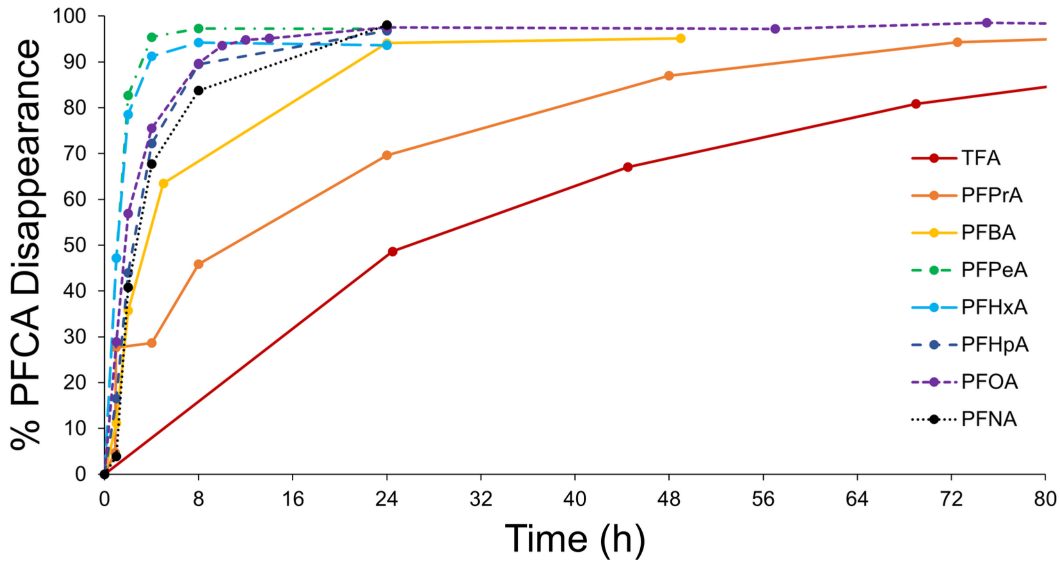

Fig. S22. Rates of PFCA degradation, as measured by ^{19}F NMR integration of the respective alpha-carbon fluorine resonances of each PFCA.

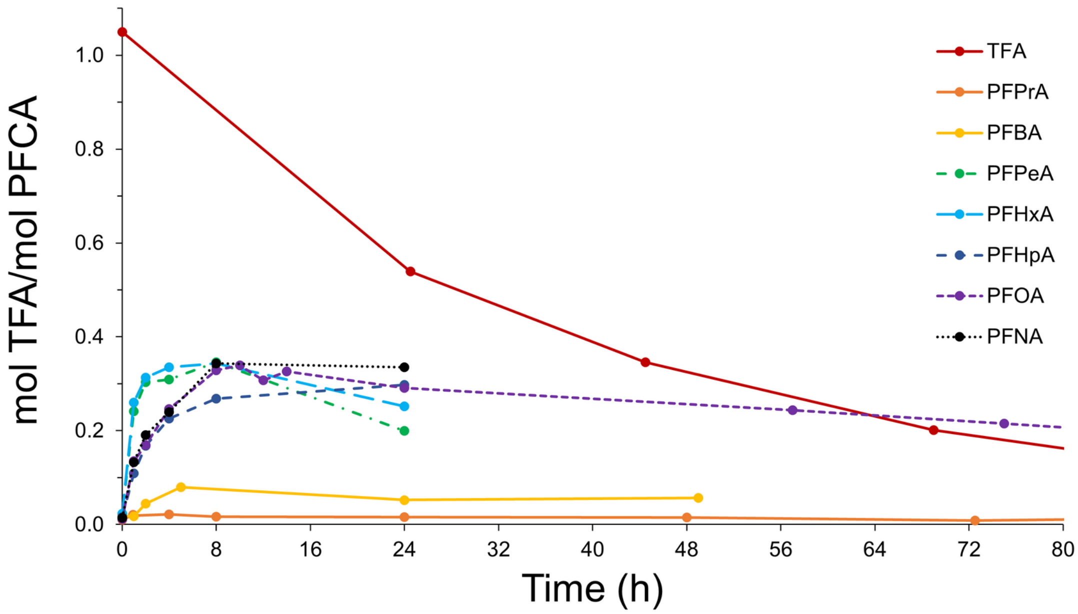

Fig. S23. Kinetic trace of mols of trifluoroacetate per mol of reactant PFCA, as measured by ^{19}F NMR spectroscopy. For TFA itself, the plot indicates its degradation rate. For PFPrA and PFBA, little or no TFA is formed. For PFCAs with five or more carbons, approximately 0.3 mol TFA/mol PFCA are formed in the early stages of the degradation reaction.

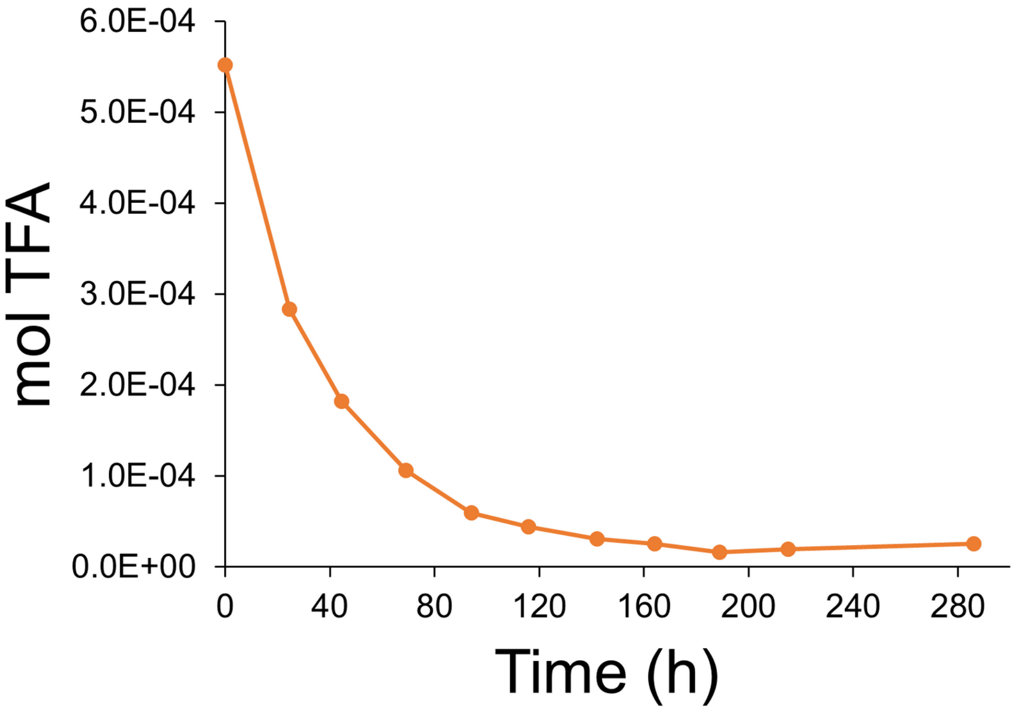

Fig. S24. Kinetic trace of the degradation of CF_3CO_2Na over time as calculated by NMR concentration. CF_3CO_2Na (0.089 M in DMSO) was degraded at 120°C with 30 equiv NaOH in 8:1 DMSO:H_2O.

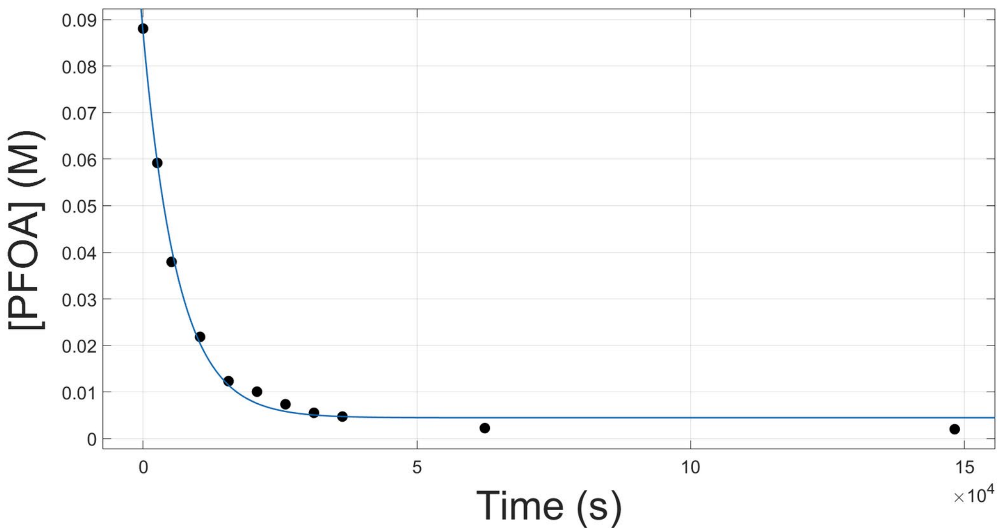

Fig. S25. Fitted curve for degradation of PFOA at 120°C as calculated from the integral of F2 in the ^{19}F NMR over time. Data is average of triplicate runs (see **Fig. S21**).

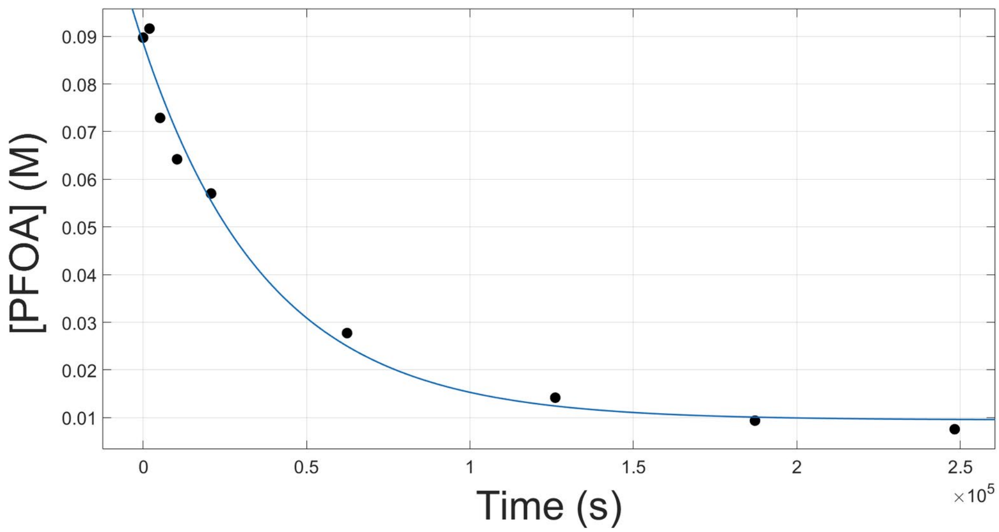

Fig. S26. Fitted curve for degradation of PFOA at 100°C as calculated from the integral of F2 in the ^{19}F NMR over time. Data is average of triplicate runs (see **Fig. S21**).

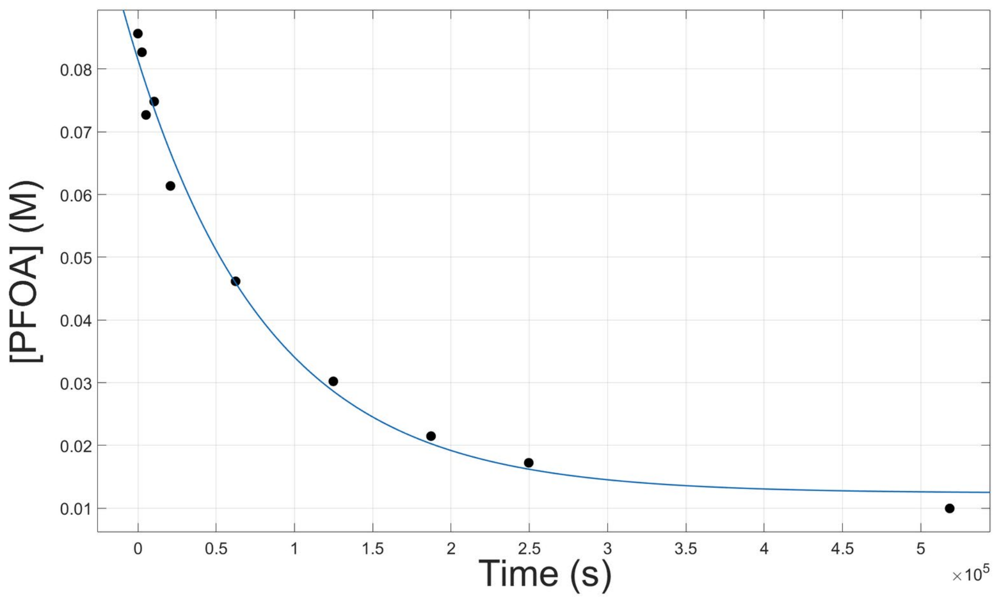

Fig. S27. Fitted curve for degradation of PFOA at 90°C as calculated from the integral of F2 in the ^{19}F NMR over time. Data is average of duplicate runs.

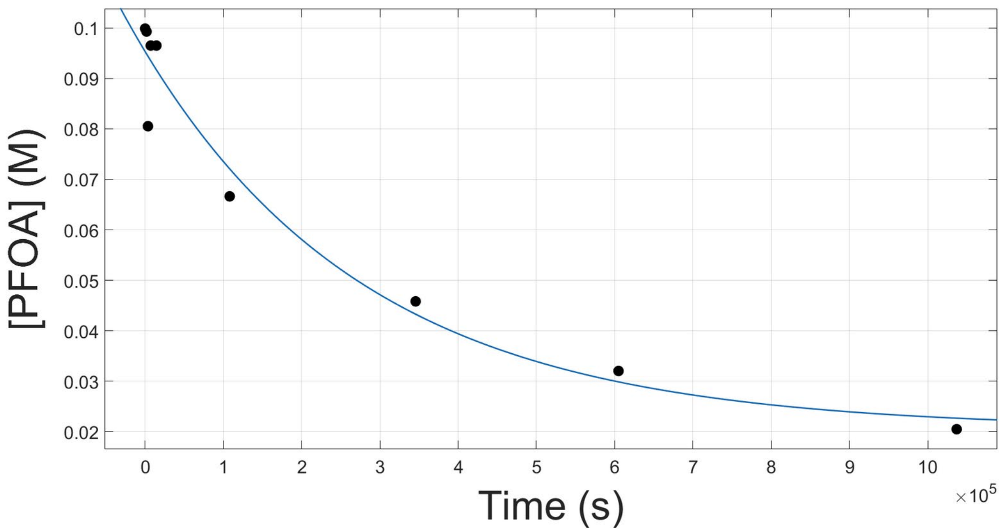

Fig. S28. Fitted curve for degradation of PFOA at 80°C as calculated from the integral of F2 in the ^{19}F NMR over time. Data from single trial.

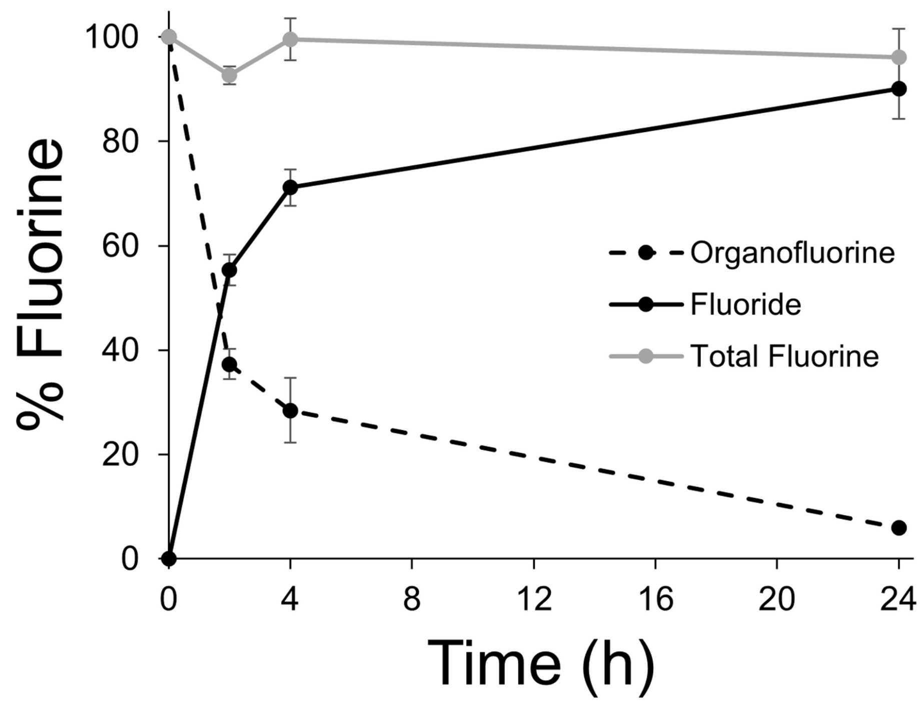

Fig. S29. Fluorine balance of PFOA degradation performed at 120°C at different reaction times. Organofluorine content (black dashed line) was measured by integrating all ^{19}F NMR peaks; the fluoride ion (black solid line) were measured by ion chromatography of entire reaction solution. The total fluorine (gray line) is calculated by adding the organofluorine and fluoride ion amounts and remains close to unity throughout the PFOA degradation reaction, indicating little to no loss of volatile organofluorine products.

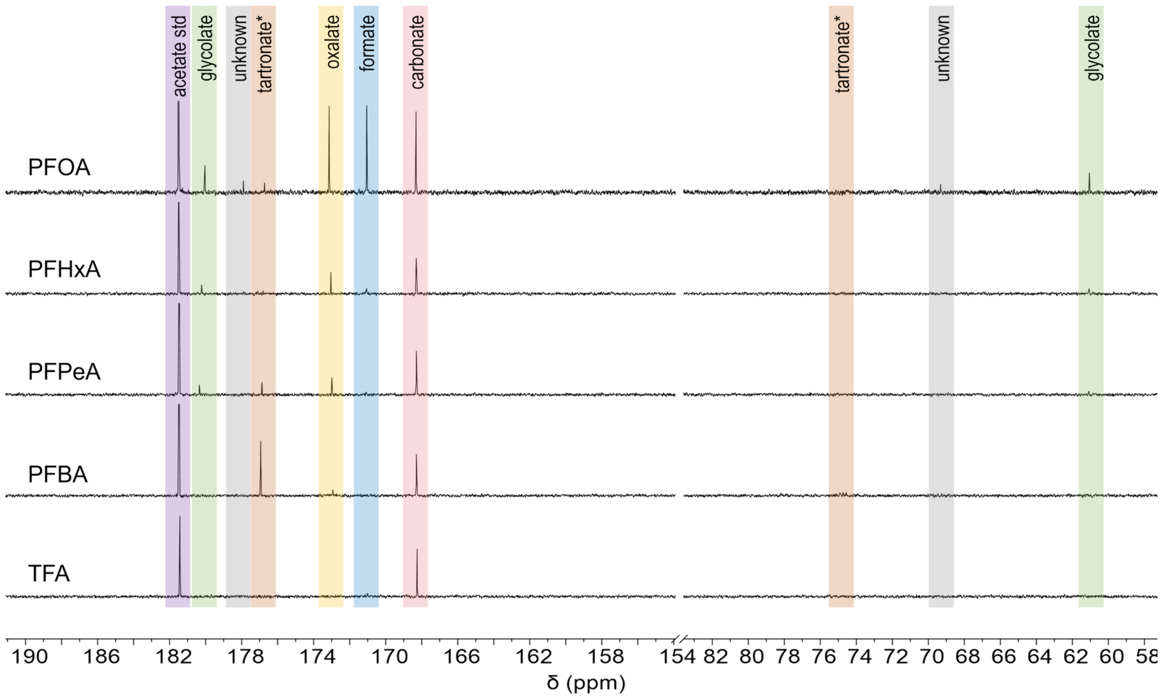

Fig. S30. Quantitative ^{13}C NMR of isolated reaction precipitate dissolved in D_2O [sodium acetate was used as an internal standard, (50 µL of a 0.68 M solution in D_2O). The PFOA sample was recorded with 900 scans at 40 s delay. Samples other than PFOA were recorded with 300 scans at 40 s delay and have imperfect proton decoupling from the extreme pH sample conditions. Sodium trifluoroacetate (TFA) shows only carbonate (168 ppm) as reaction byproduct. PFBA shows carbonate, trace oxalate ion formation, and enhanced tartronate ion formation compared to other samples. PFPeA shows glycolate (180 ppm, 61 ppm), tartronate, oxalate, and carbonate ion formation. PFHxA shows glycolate, oxalate, formate (present in proton NMR, ion chromatography, hard to see here due to proton coupling), and carbonate. PFOA shows glycolate, tartronate, oxalate, formate, carbonate, and two trace unknown peaks at 178 and 69 ppm. *Tartronate assigned based on literature references (*29*, *44*).

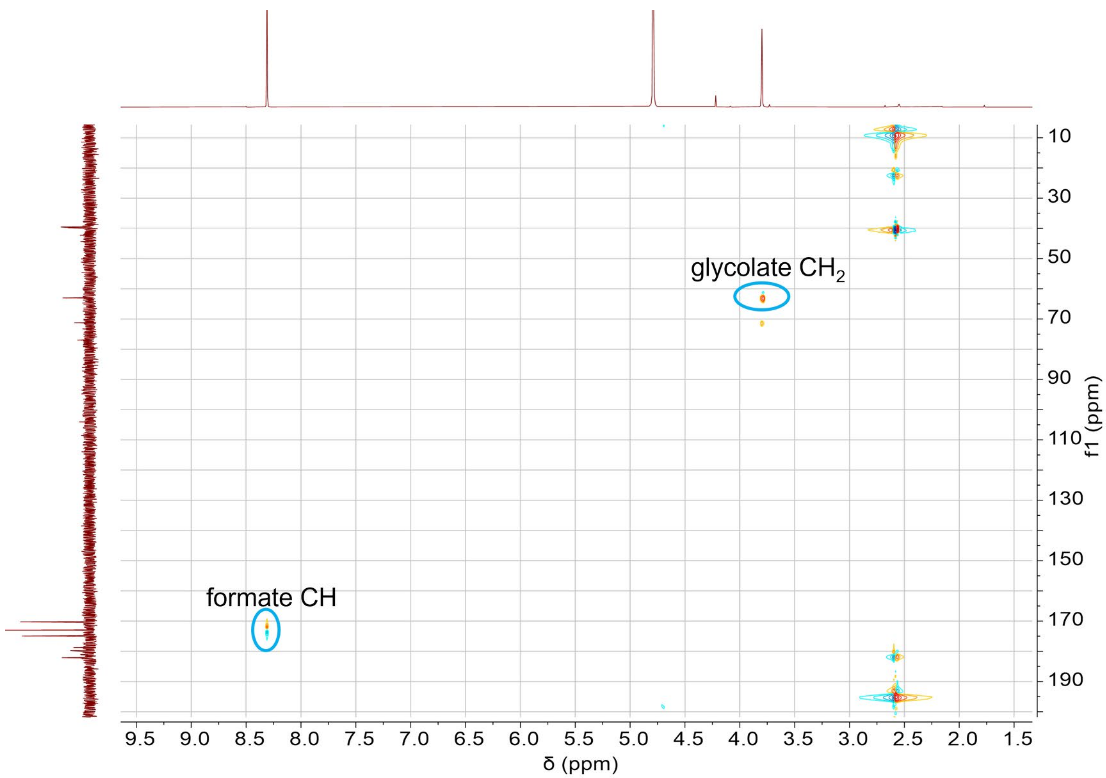

Fig. S31. HSQC of isolated PFOA reaction precipitate dissolved in D_2O with 30 μL DMSO standard allows for identification of some carbonaceous byproducts

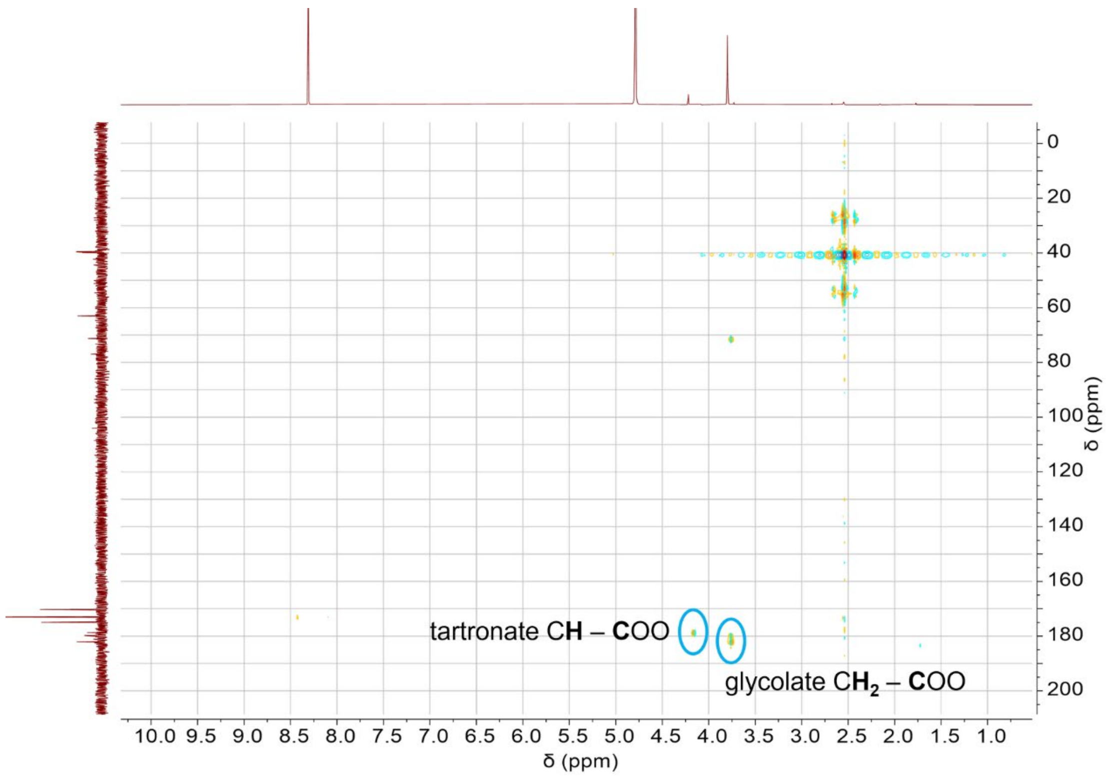

Fig. S32. HMBC of isolated PFOA reaction precipitate dissolved in D_2O with 30 μL DMSO standard allows for identification of some carbonaceous byproducts.

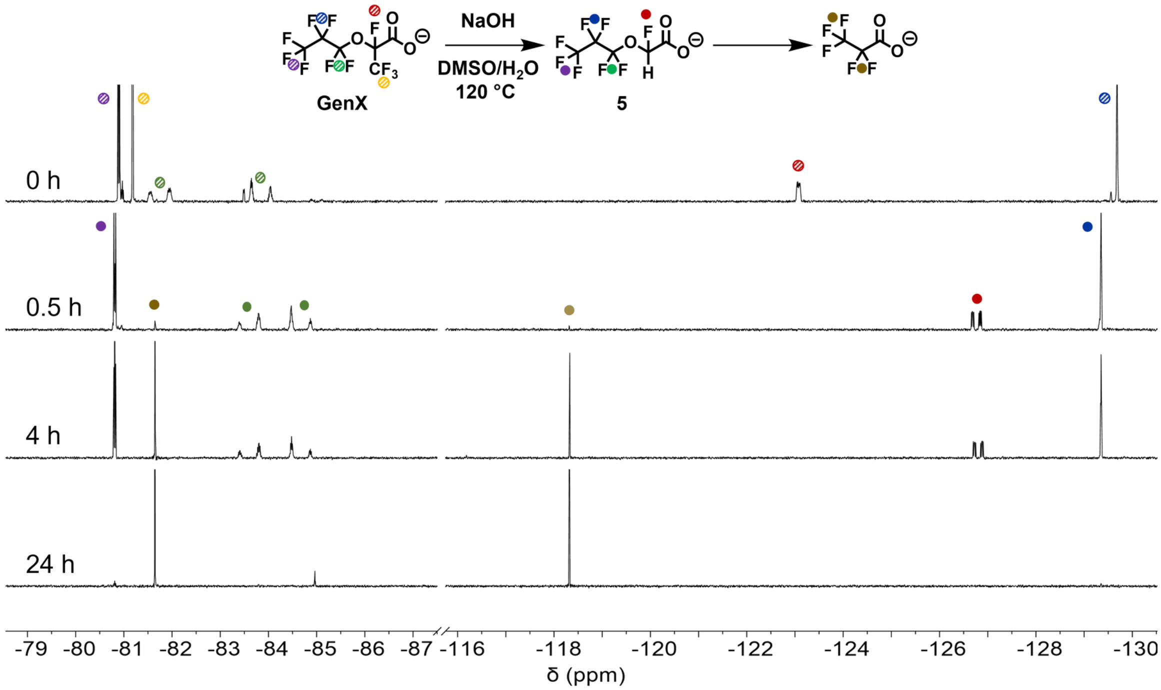

Fig. S33. ^{19}F NMR spectra of GenX degradation reaction at 120°C. The starting material (added as GenX ammonium salt) quickly decarboxylates and proto-de-trifluoromethylates to intermediate **5**, which was also detected by ESI-MS (**Fig. S42**). Over the course of several hours, **5** degrades to PFPrA, which subsequently degrades further, mainly to CF_3CF_2H, as described for the degradation of PFPrA (**Figure 2, Fig. S37**).

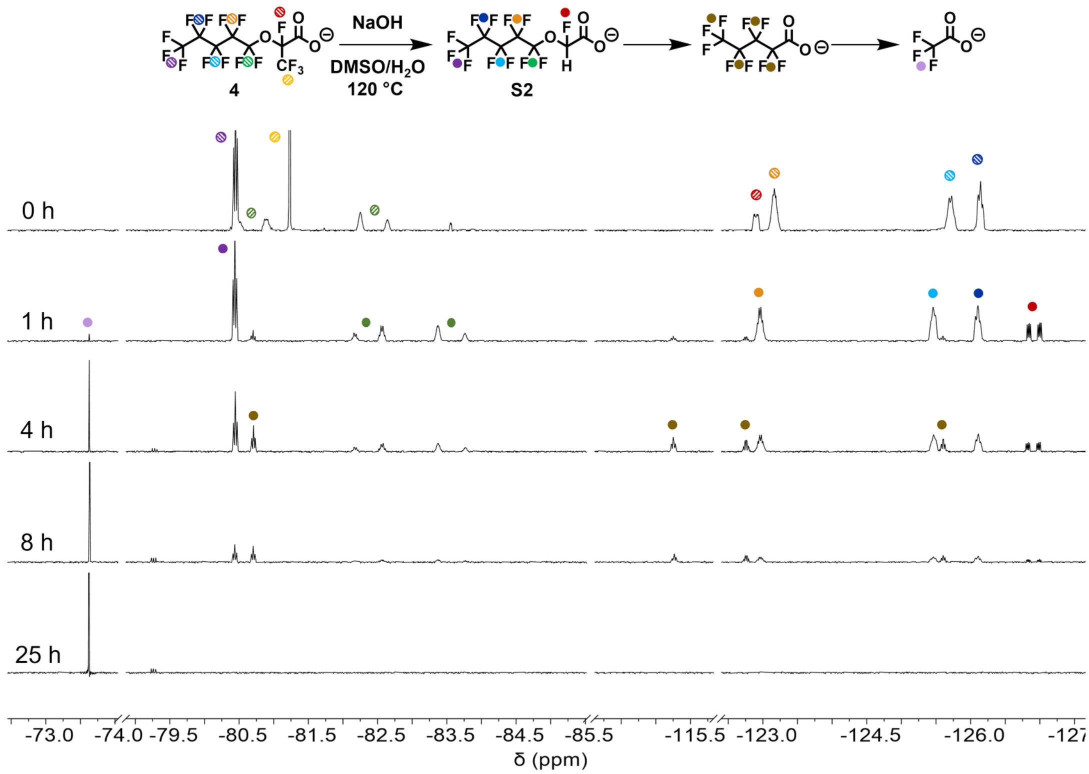

Fig. S34. [19]F NMR spectra of **4** degradation reaction at 120°C. The starting material (added as **4** ammonium salt) quickly decarboxylates and proto-de-trifluoromethylates to intermediate **S2**, which was also detected by APCI-MS (**Fig. S43**). Over the course of several hours, **S2** degrades to PFPeA, which subsequently degrades further, mainly to fluoride and $CF_3CO_2^-$, as described for the degradation of PFPeA (**Figure 2**).

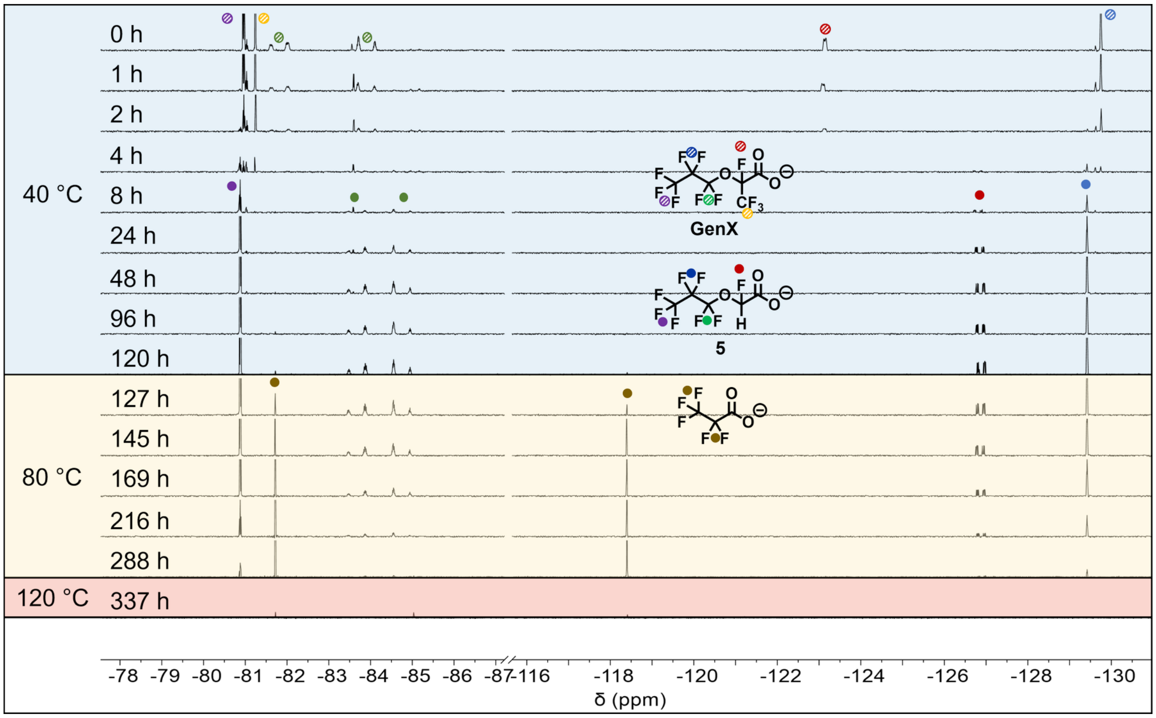

Fig. S35. [19]F NMR spectra of degradation of GenX over time at increasing temperature stages. Starting material for GenX (top, shaded dots) disappear as GenX is converted to compound **5** and falls out of solution, presumably because of an insoluble intermediate that is converted to intermediate **5** over time, causing **5** to slowly increase in concentration (brightly colored dots, until 120 h). When the temperature is increased to 80°C (121 h), peaks corresponding to PFPrA (brown dots) appear from **5** degradation as predicted, then disappear more quickly after the temperature is increased to 120°C (289 h).

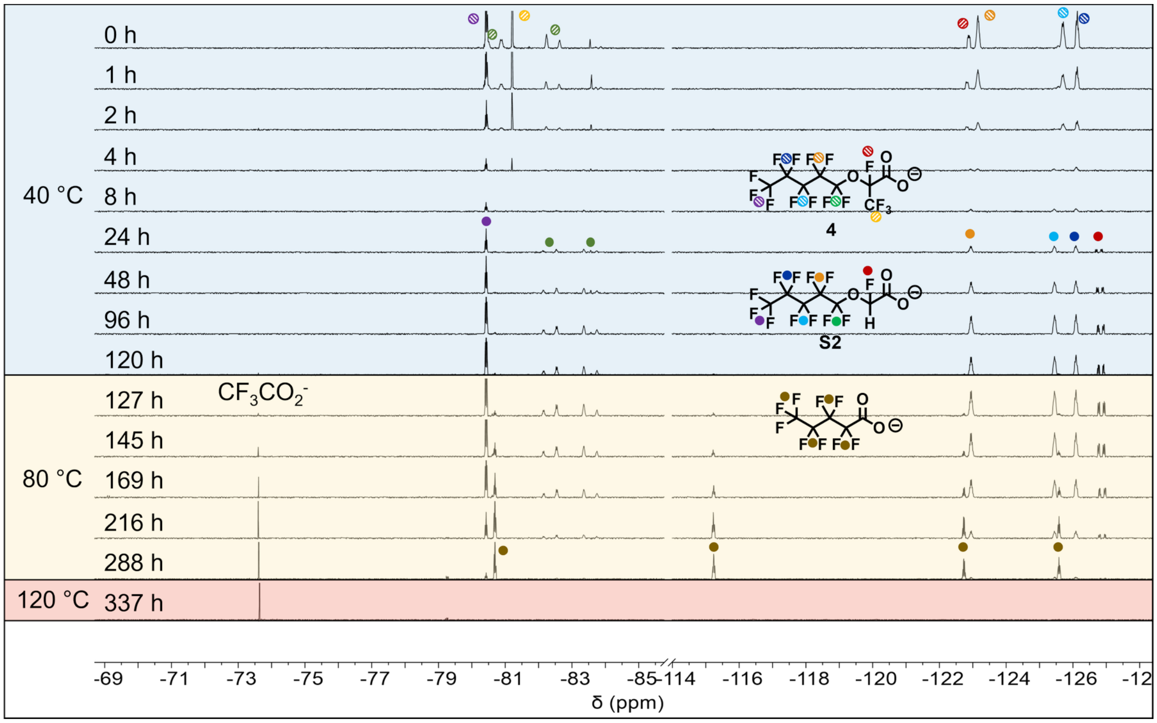

Fig. S36. [19]F NMR spectra of degradation of **4** over time at increasing temperature stages. Starting material for **4** (top, shaded dots) disappear as **4** is converted to intermediate **S2** and falls out of solution, presumably because of an insoluble intermediate that is converted to intermediate **S2** over time, causing **S2** to slowly increase in concentration (brightly colored dots, until 120 h). When the temperature is increased to 80°C (121 h), peaks corresponding to PFPeA (brown dots) and trifluoroacetate appear from **S2** degradation as predicted, then disappear more quickly after the temperature is increased to 120 °C (289 h).

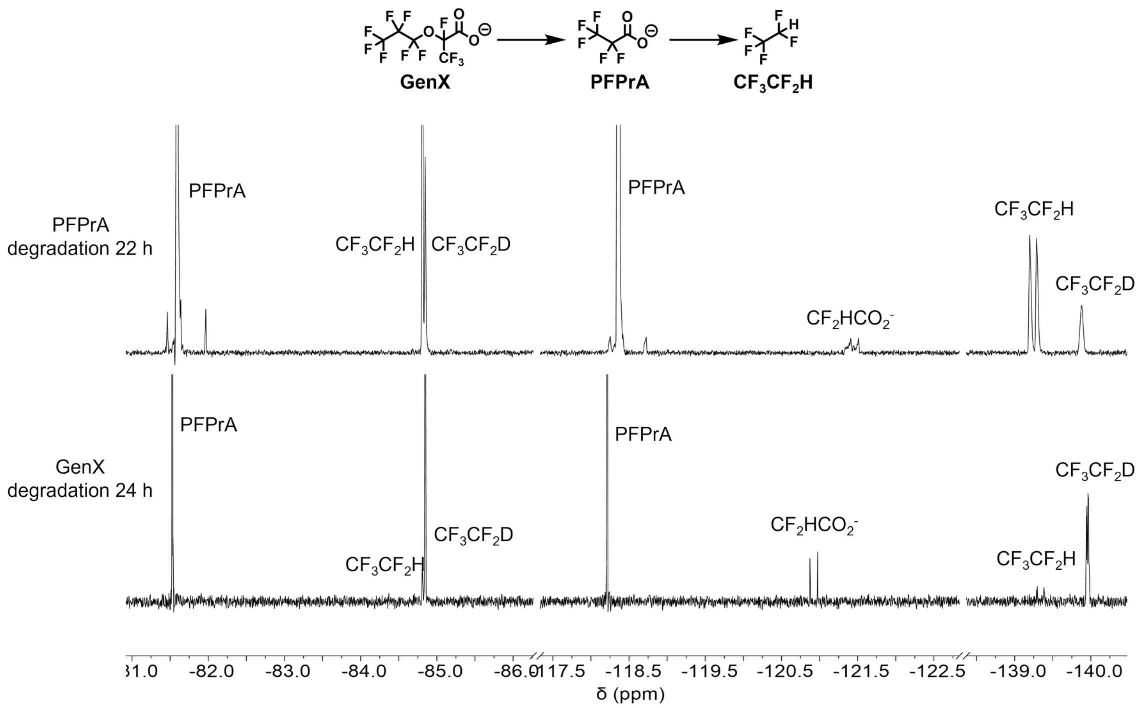

Fig. S37. ^{19}F NMR spectra of the degradation of perfluoropropionic acid (top) after 22 hours and GenX (bottom) after 24 hours at 120°C. Peaks corresponding to the same compounds appear in the degradation of each, indicating that GenX degrades to PFPrA and then follows the PFPrA degradation pathway, including producing CF_3CF_2H, which volatilizes and does not defluorinate, resulting in a lower fluoride recovery than for longer-chain analogues. Identity of CF_3CF_2D hypothesized.

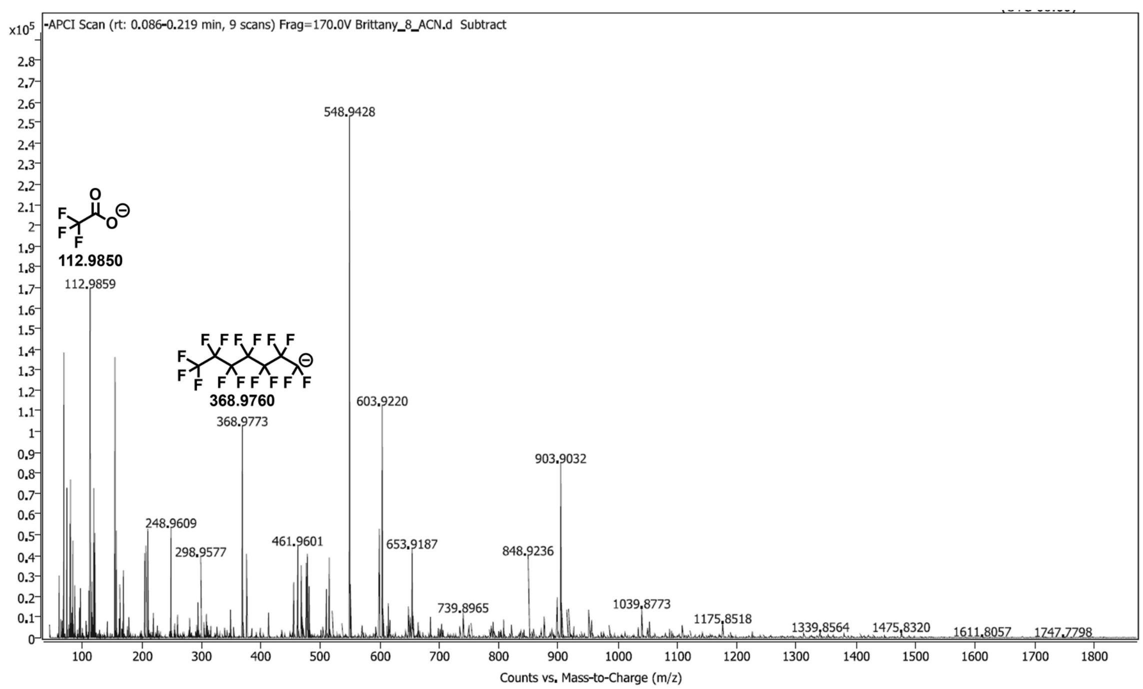

Fig. S38. APCI-MS spectrum of an aliquot of PFOA degradation reaction diluted in acetonitrile after 4 hours of heating at 120°C.

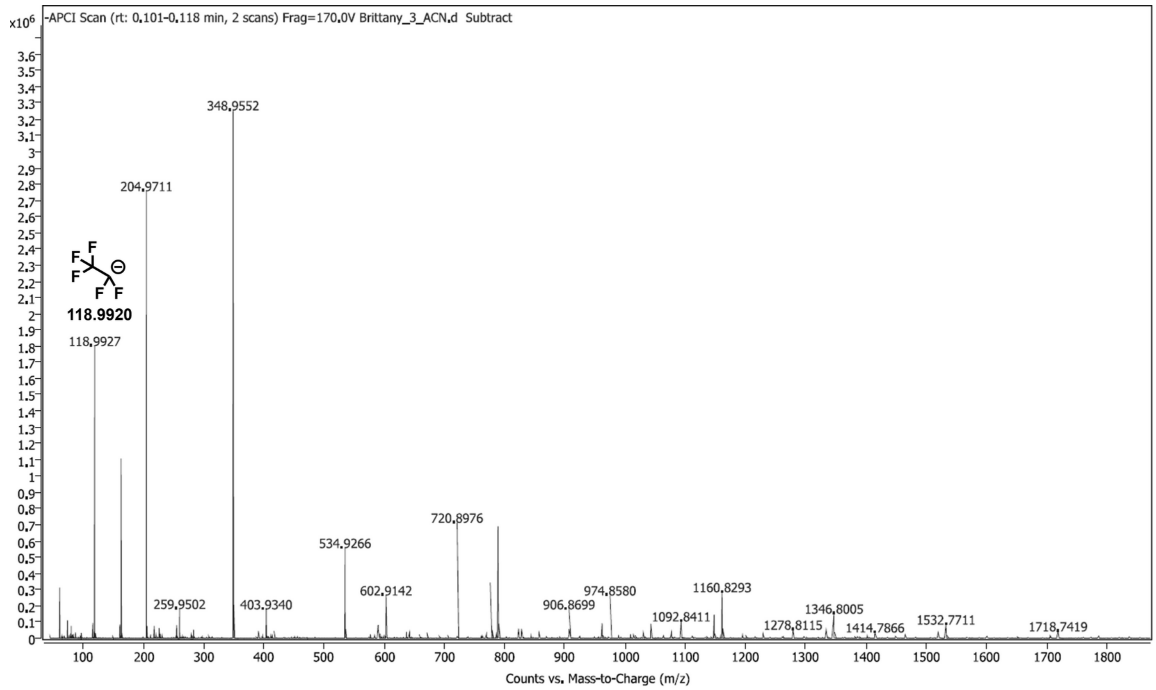

Fig. S39. APCI-MS spectrum of an aliquot of PFPrA degradation reaction diluted in acetonitrile after 4 hours of heating at 120°C. The prominent 118.9930 m/z peak identified in this reaction mixture is consistent with the proposed reaction mechanism as it corresponds to $CF_3CF_2^-$, which either comes from the decarboxylation of $CF_3CF_2CO_2^-$ or the deprotonation of CF_3CF_2H.

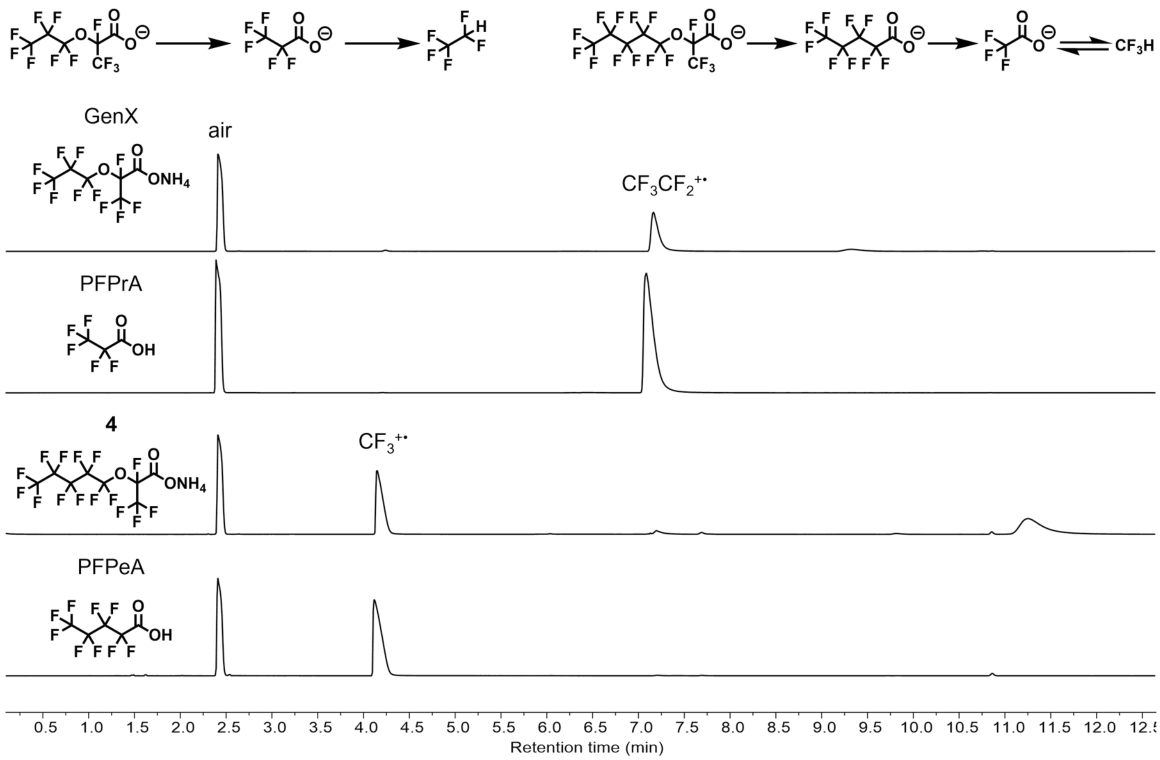

Fig. S40. GCMS-headspace total ion chromatograms after 4 hours of reaction for GenX (top), perfluoropropionic acid (second from top), **4** (second from bottom), perfluoropentanoic acid (bottom). Both PFPrA and GenX show evidence of $CF_3CF_2^{+\bullet}$ gas fragments, presumably derived from CF_3CF_2H, whereas PFPeA and **4** show only $CF_3^{+\bullet}$ fragments, presumably from an equilibrium between CF_3COOH and CF_3H.

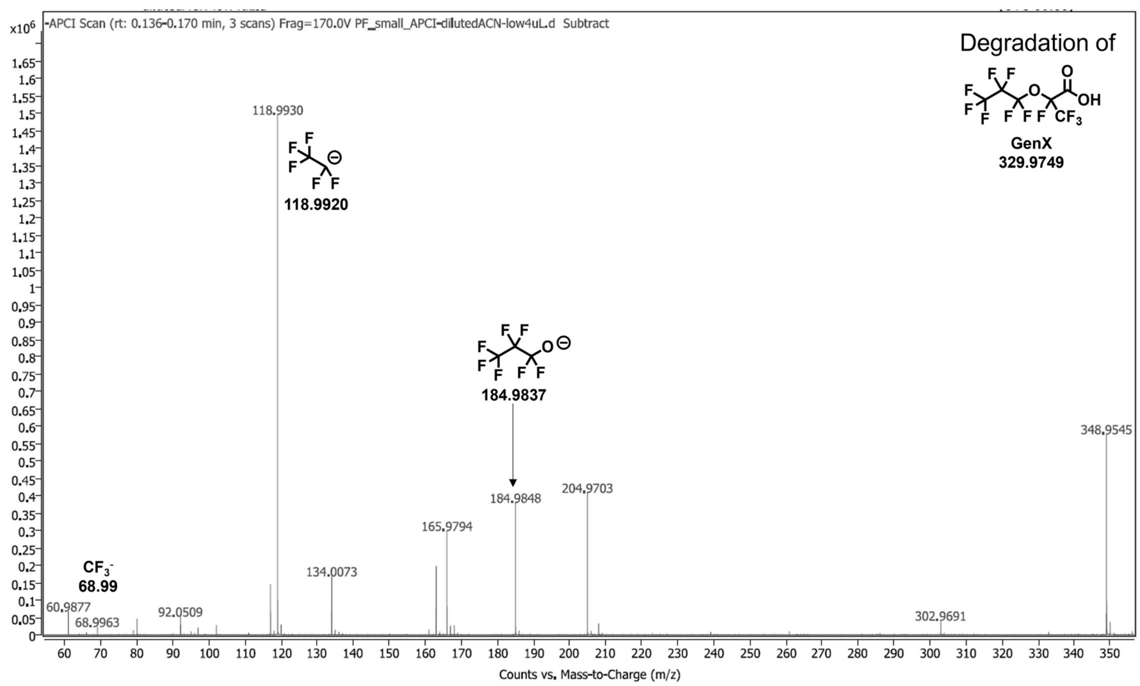

Fig. S41. APCI-MS spectrum of an aliquot of GenX degradation reaction diluted in acetonitrile after 7 hours of heating at 120°C. Molecular species identified from this reaction mixture are consistent with the proposed reaction mechanism, especially the prominent 118.9930 m/z peak corresponding to $CF_3CF_2^-$, which either comes from the decarboxylation of $CF_3CF_2CO_2^-$ or the deprotonation of CF_3CF_2H.

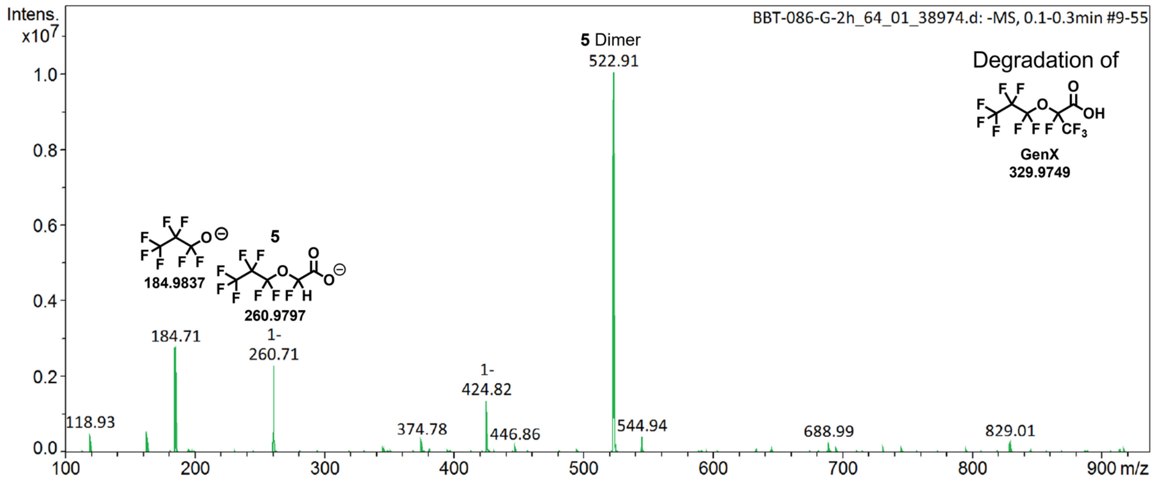

Fig. S42. ESI-MS of spectrum of an aliquot of GenX degradation reaction diluted in acetonitrile after 2 hours of heating at 120°C. Molecular species identified from this reaction mixture are consistent with the proposed reaction mechanism, especially the **5** and **5** dimer at 260.71 m/z and 522.91 m/z.

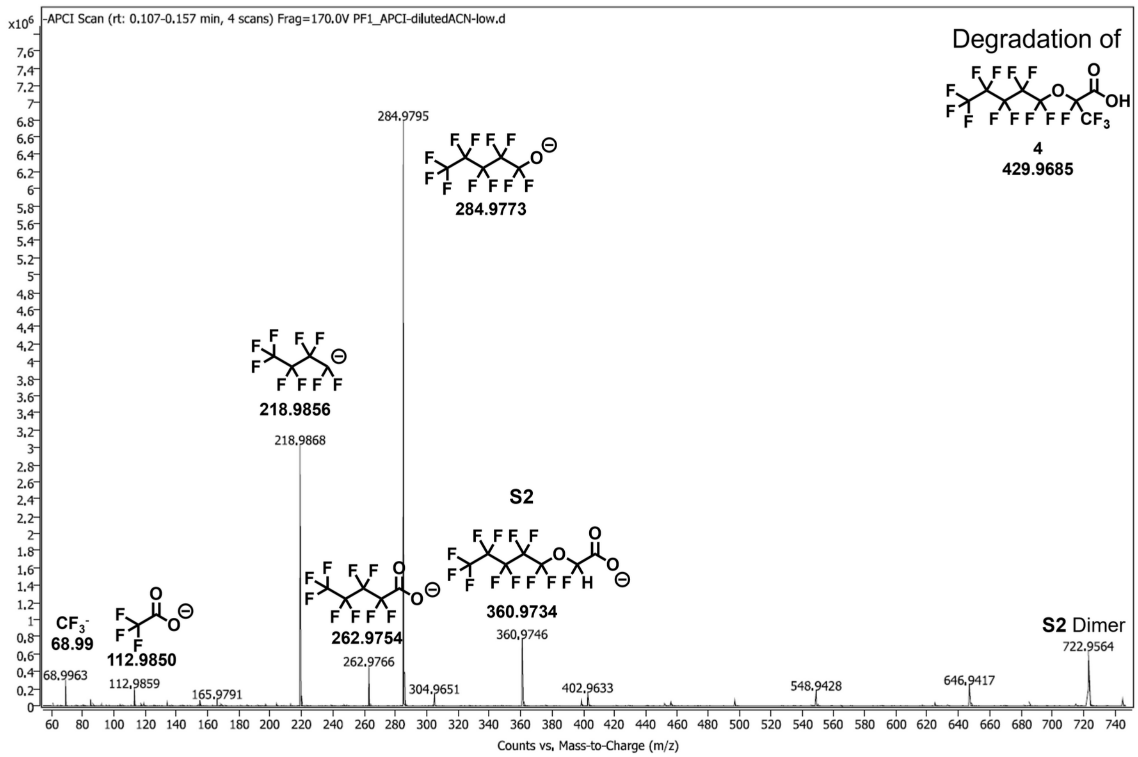

Fig. S43. APCI-MS spectrum of an aliquot of **4** degradation reaction diluted in acetonitrile after 4 hours of heating at 120°C. Molecular species identified from this reaction mixture are consistent with the proposed reaction mechanism, especially the **S2** and **S2** dimer peaks at 360.9746 m/z and 722.9564 m/z.

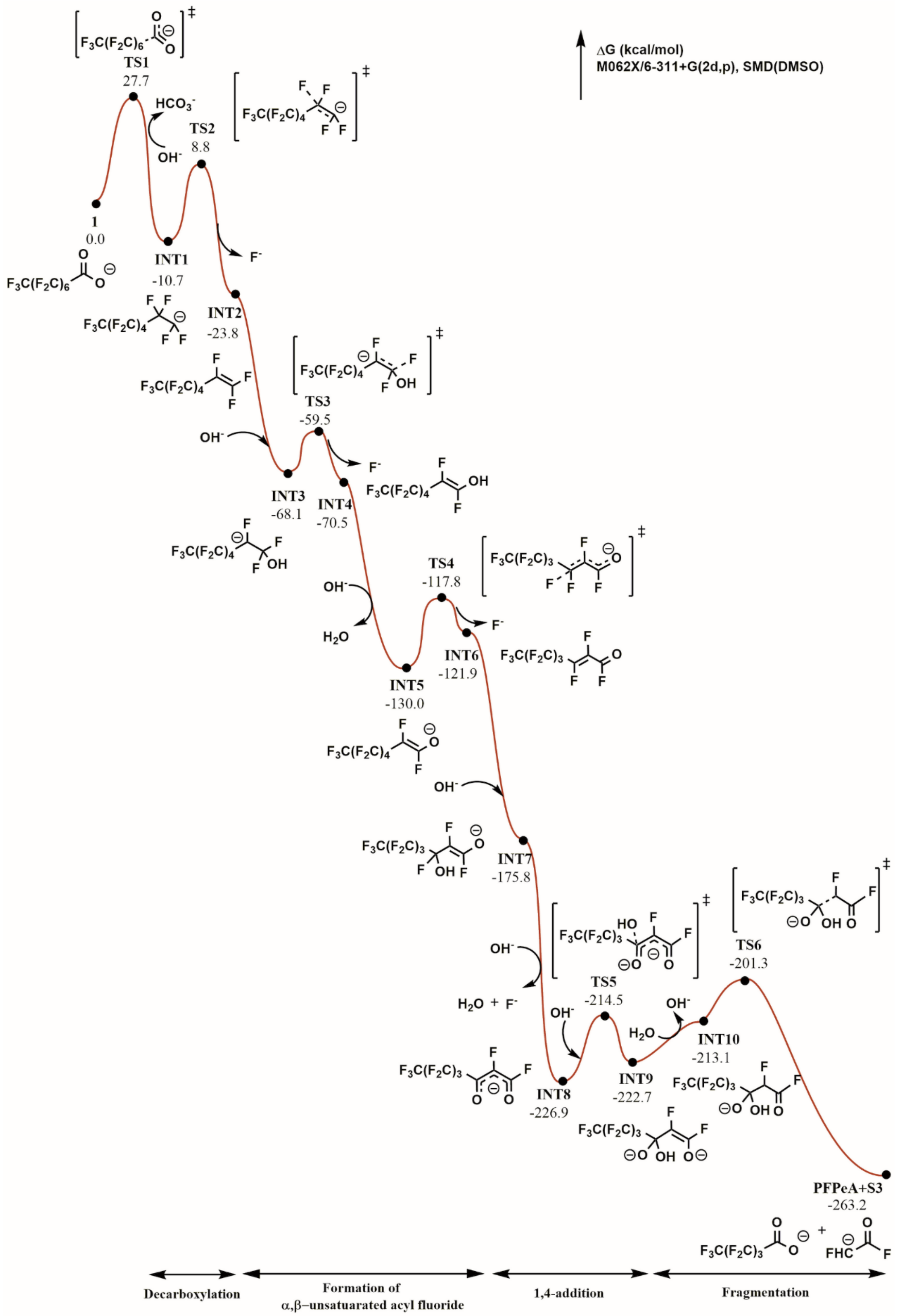

Fig. S44. Gibbs free energy profile for pathways A and D, X = F.

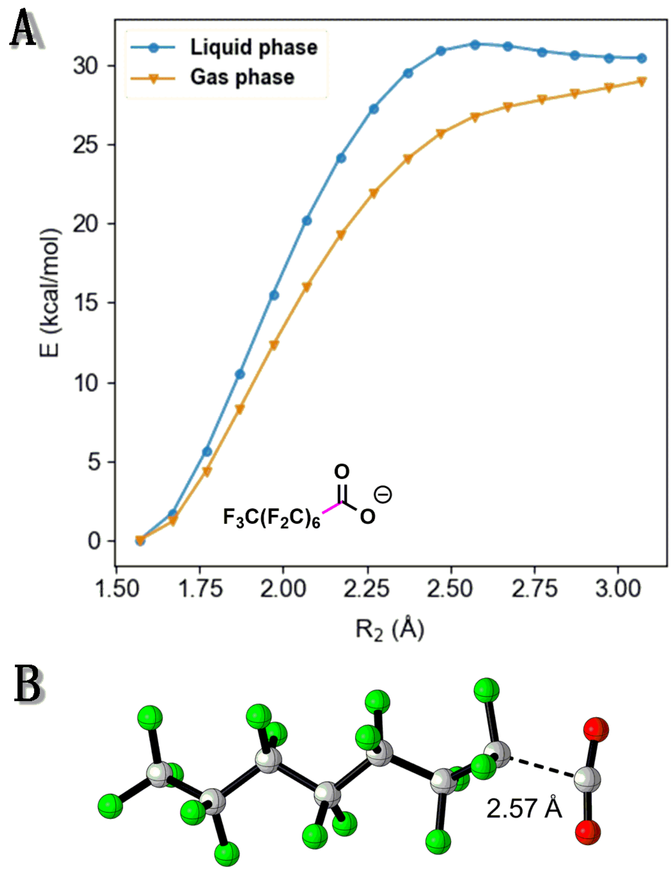

Fig. S45. A) The scanning coordinates of C–C bond length to show solvent effect in decarboxylation. The bond is colored pink. B) 3D structure of TS1.

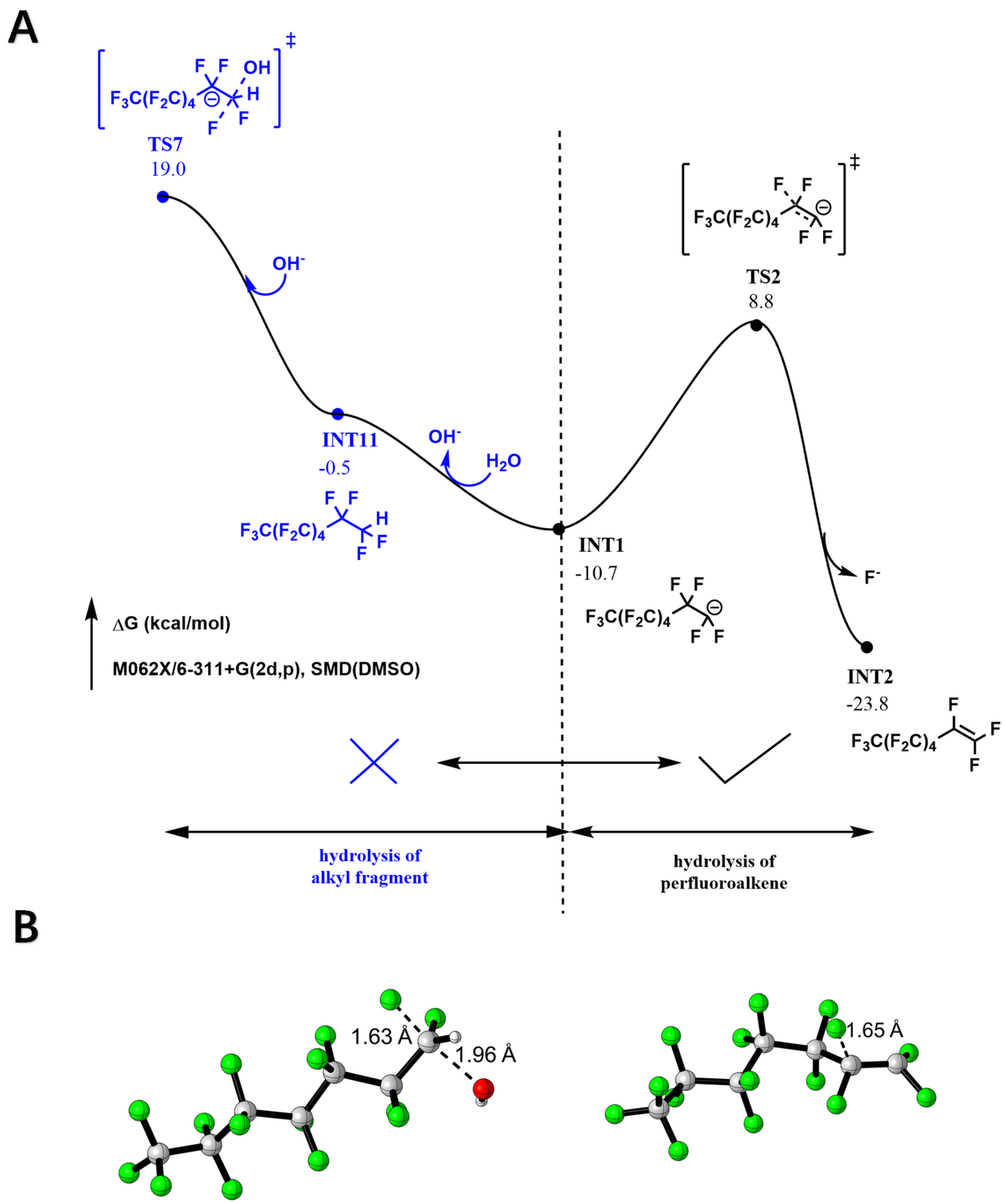

Fig. S46. A) Comparison of β-elimination and protonation of INT1. An S_N2 reaction on a saturated fluoroalkane carbon requires a high energy barrier (29.7 kcal/mol). B) 3D structures of TS7 and TS2.

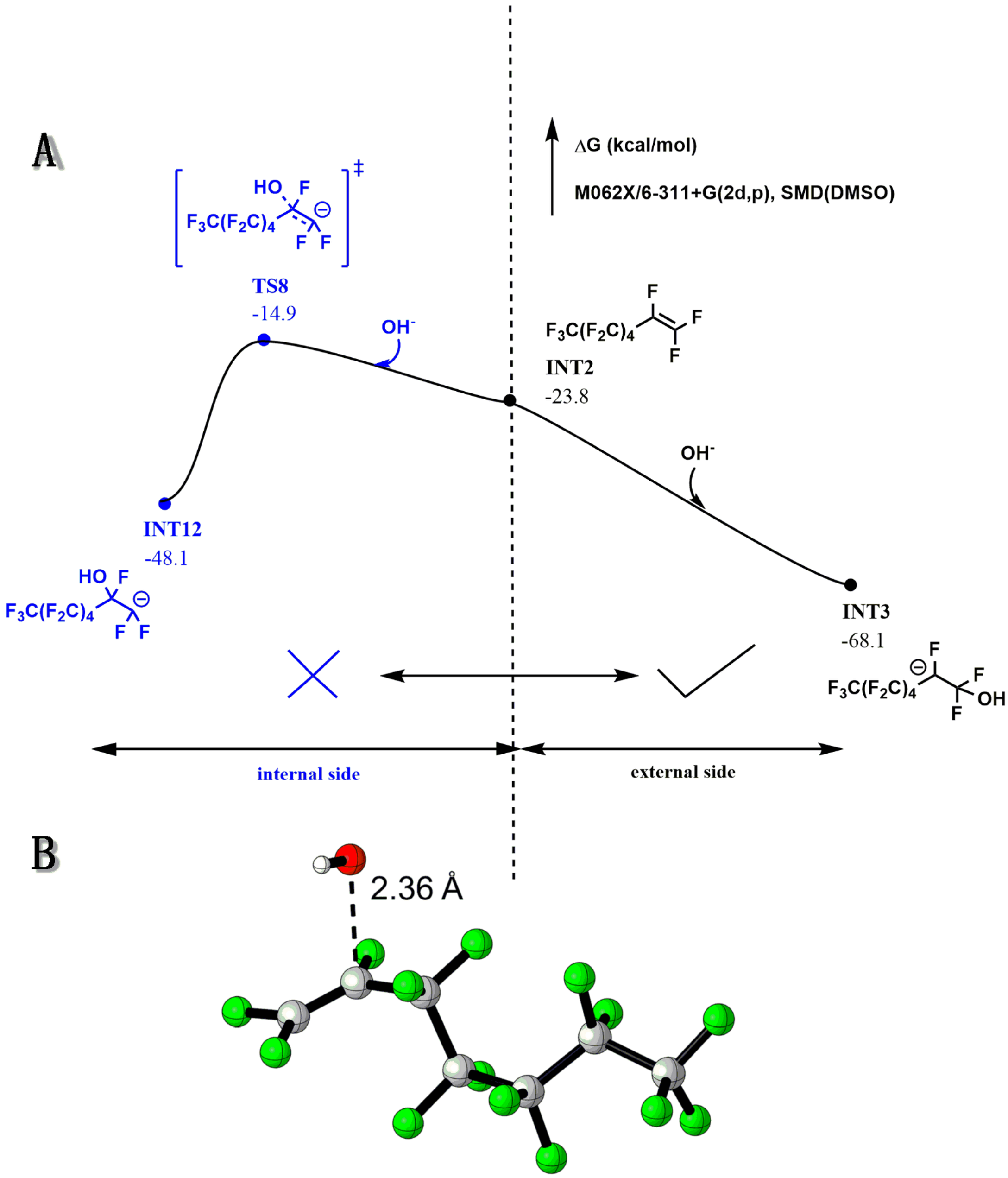

Fig. S47. A) Comparison of hydroxide addition on the internal side and the external side of the alkene. While hydroxide addition on the terminal side has a inflection point, addition on the internal side has no enthalpic barrier. B) 3D structure of TS8.

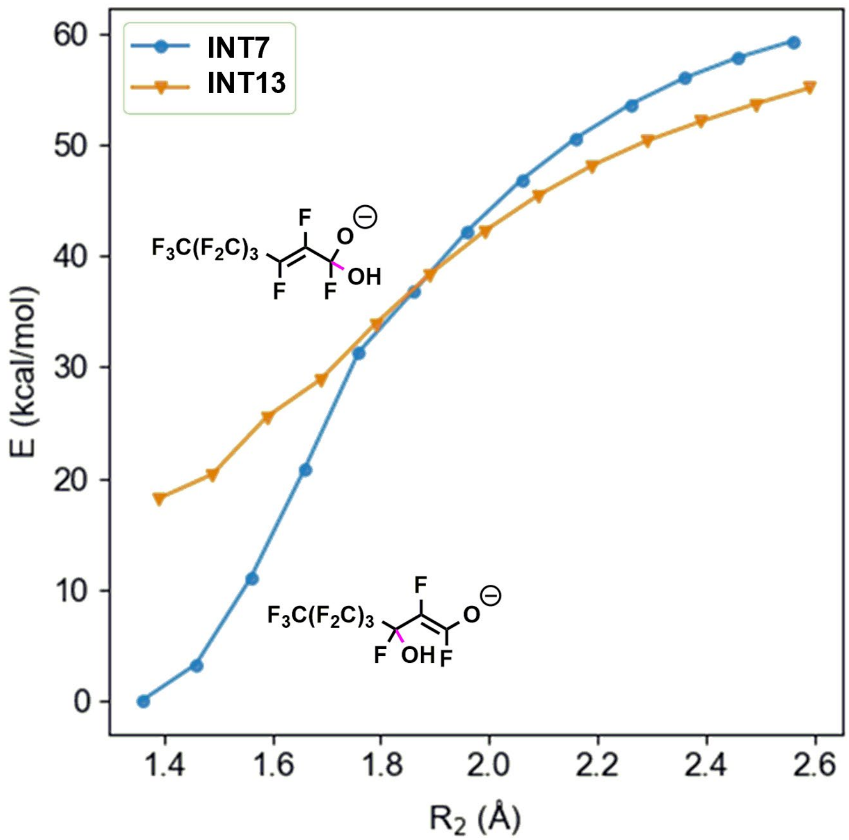

Fig. S48. The scanning coordinates of the carbon–oxygen bonds of INT7 and INT13. When gradually increasing the carbon–oxygen bond length, the energy does not have an inflection point but continuously rises, indicating that 1,2-addition and 1,4-addition both do not have enthalpic barriers.

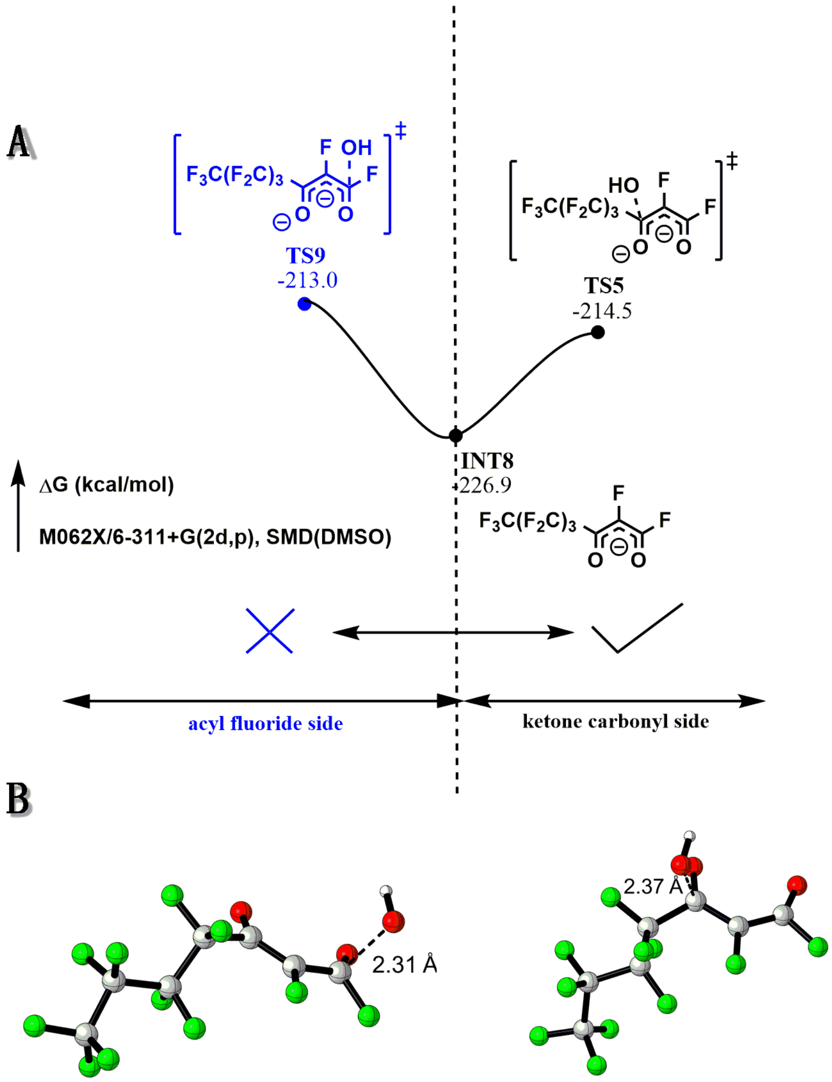

Fig. S49. A) Comparison of hydroxide addition on the acyl fluoride side and the ketone carbonyl side of INT8. B) 3D structures of TS9 and TS5.

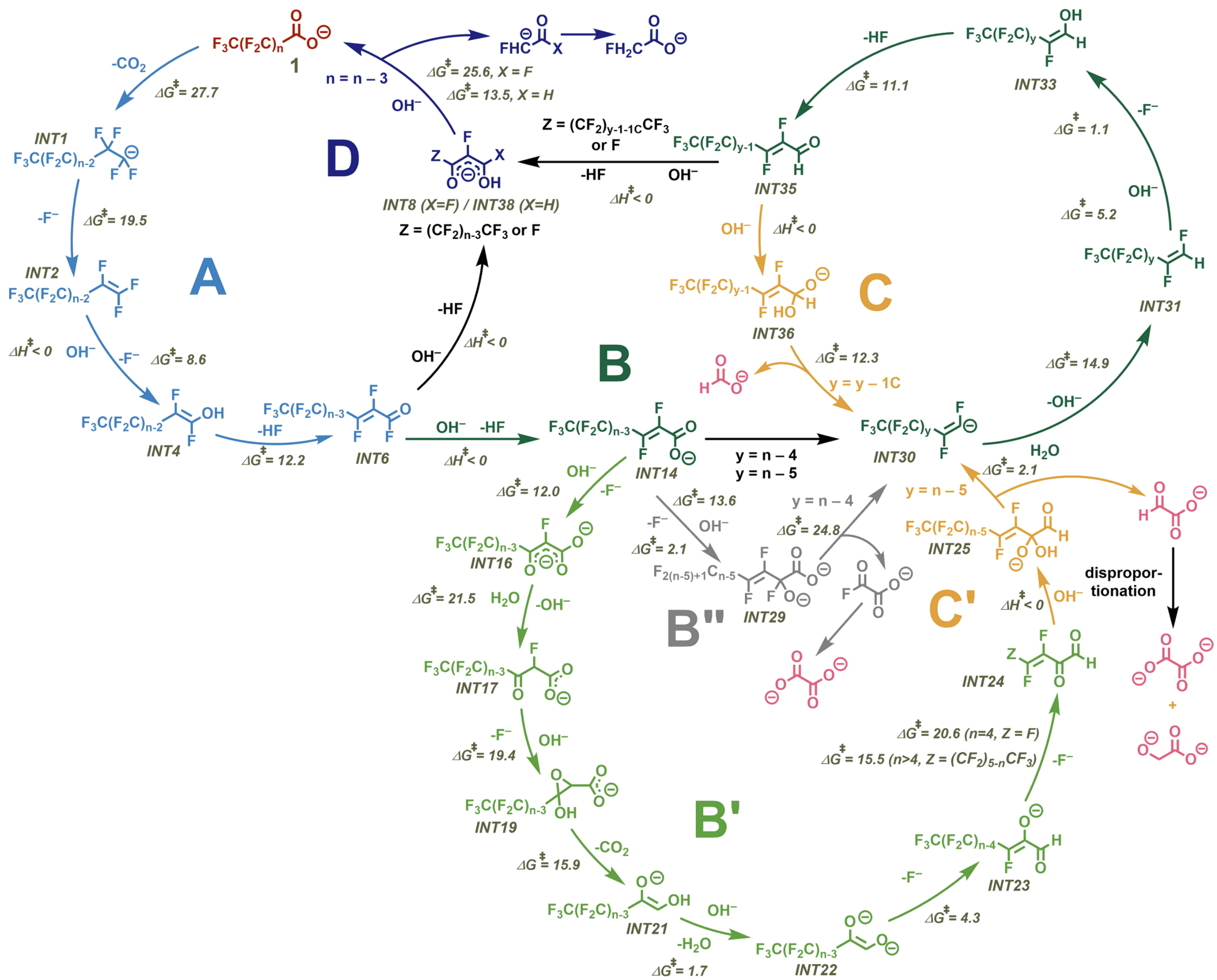

Fig. S50. Proposed pathways for converting INT14 to INT30 and forming carbon byproducts.

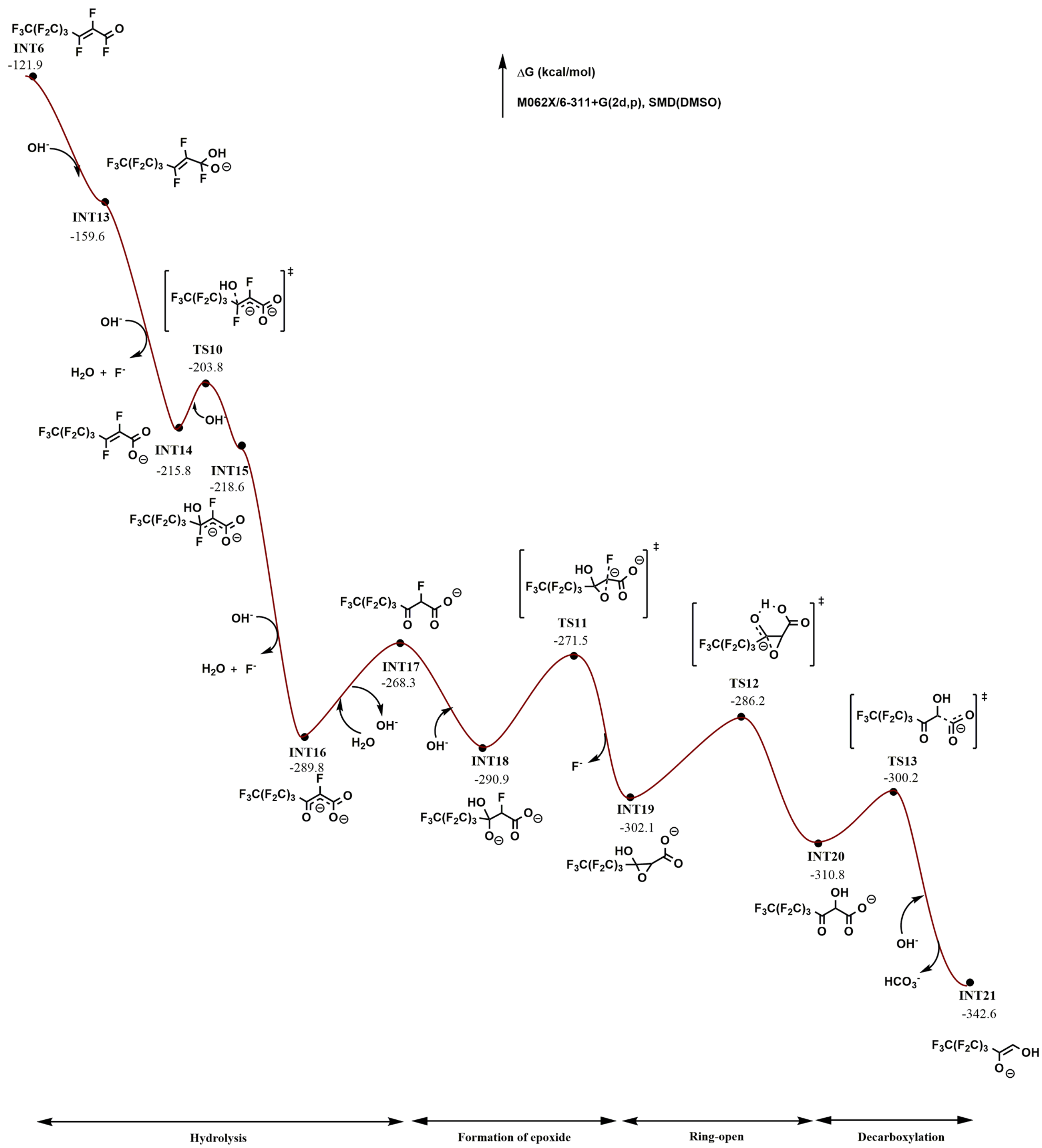

Fig. S51. Gibbs free energy profile for pathway B′ (I), ending with decarboxylation.

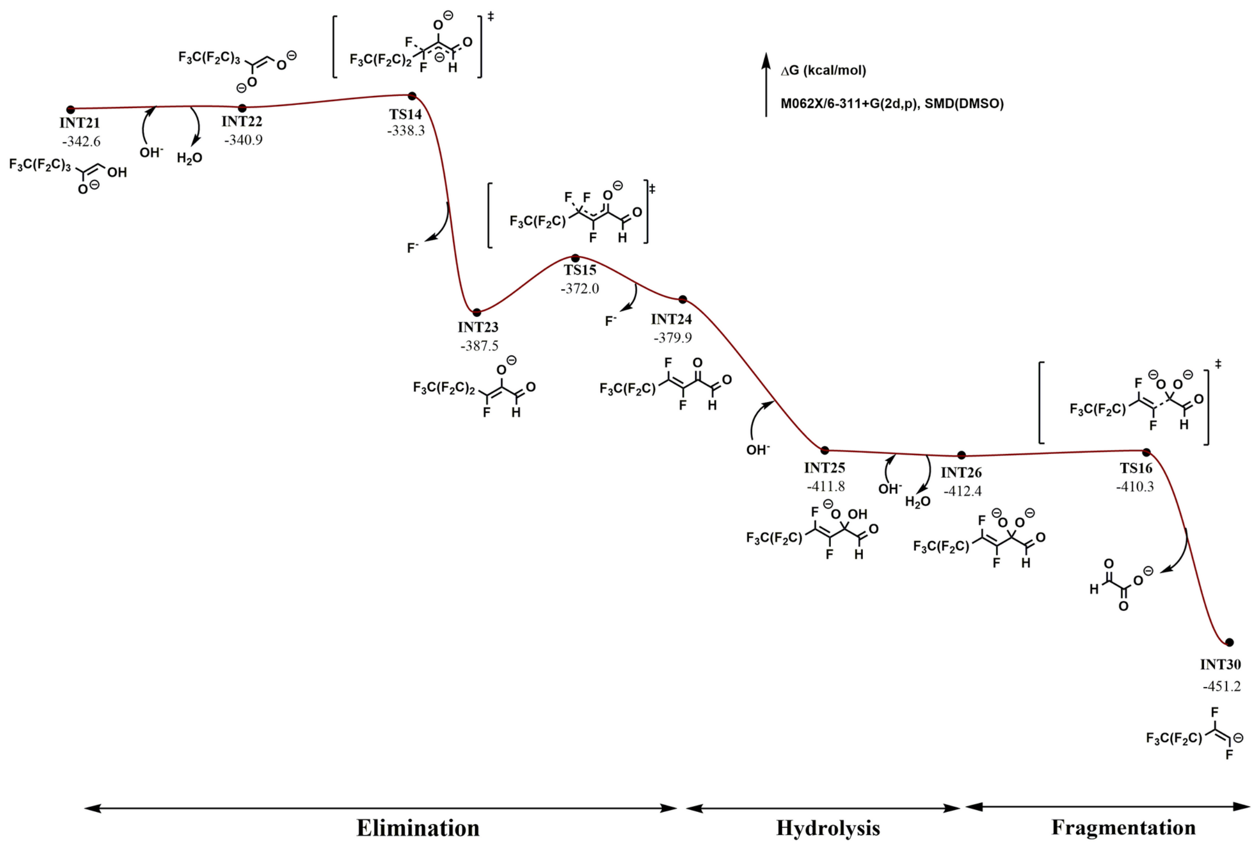

Fig. S52. Gibbs free energy profile for pathways B′ (II) + pathway C′.

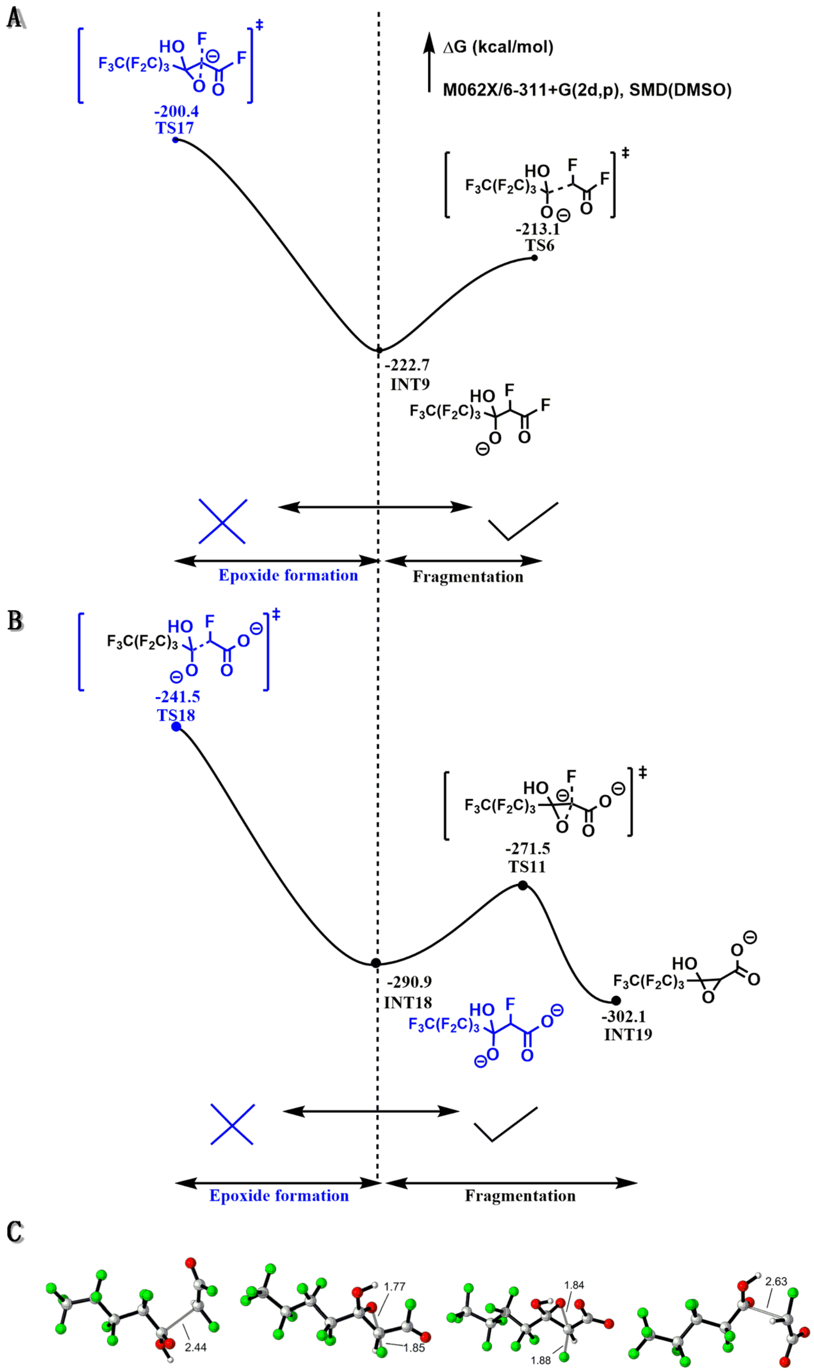

Fig. S53. A) Comparison of epoxide formation and the fragmentation of INT9 (acid fluoride). B) Comparison of epoxide formation and the fragmentation of INT18 (carboxylate). C) 3D structures of TS6, TS17, TS11, TS18.

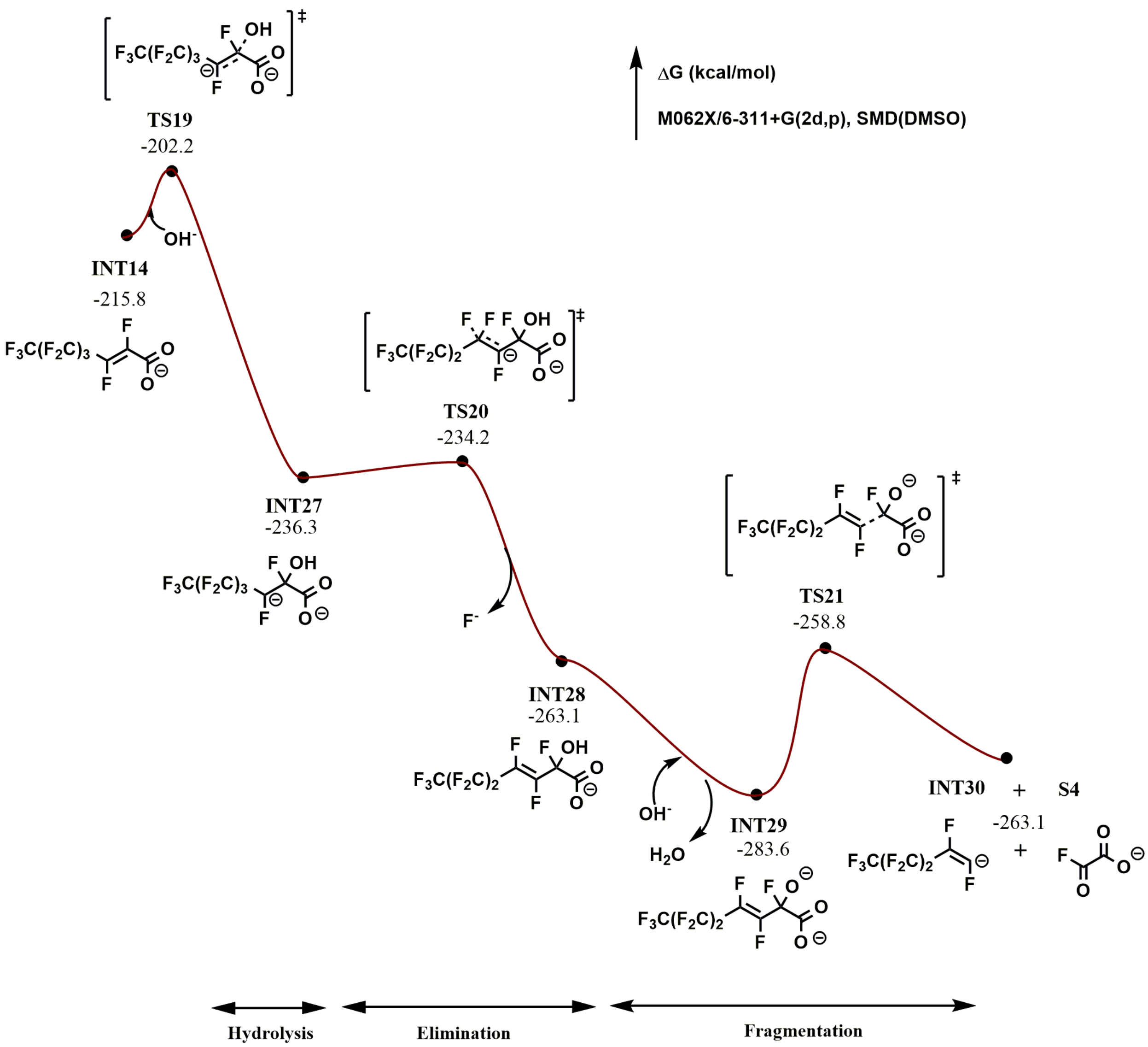

Fig. S54. Gibbs free energy profile for pathway B″.

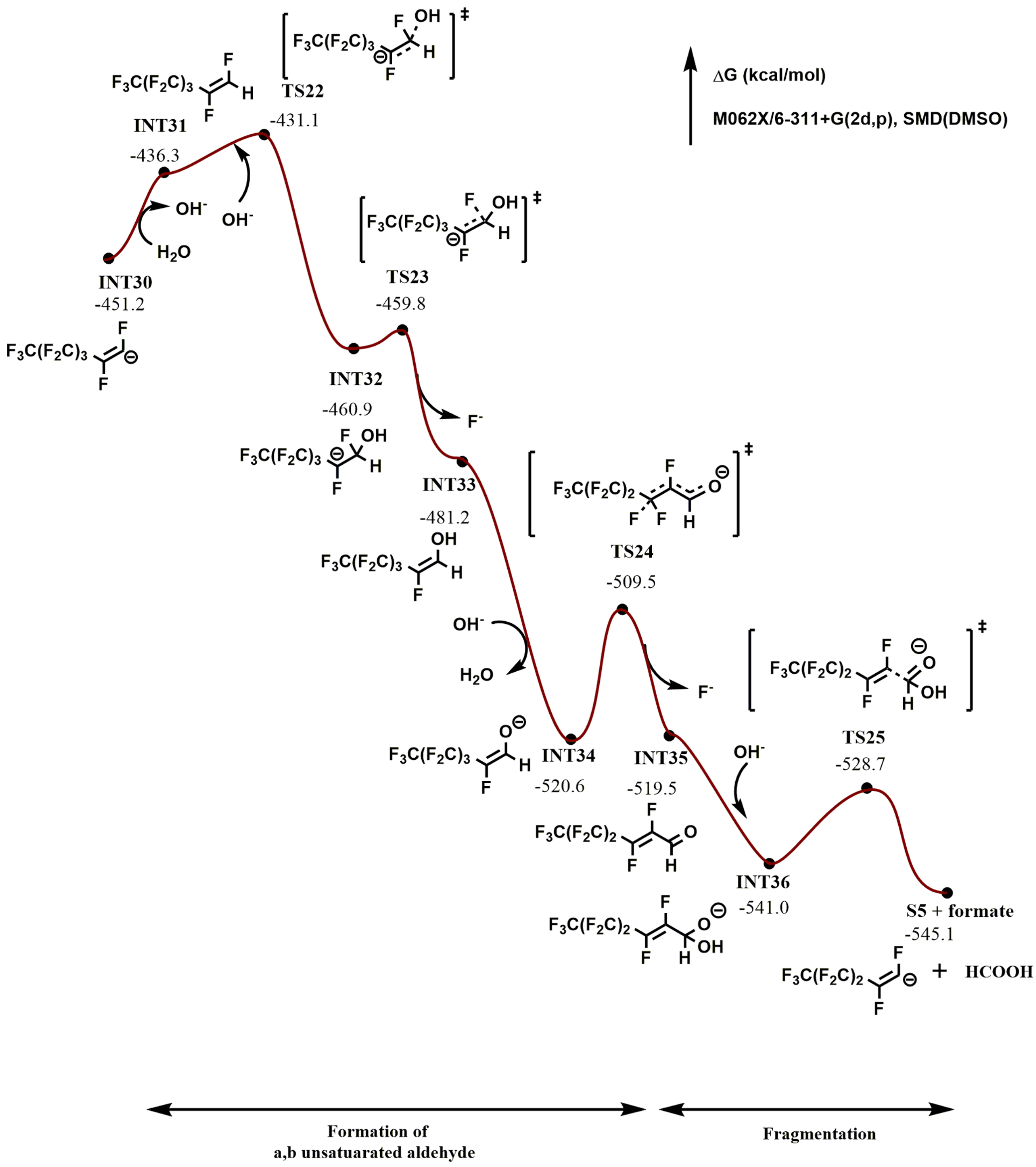

Fig. S55. Gibbs free energy profile for pathway C.

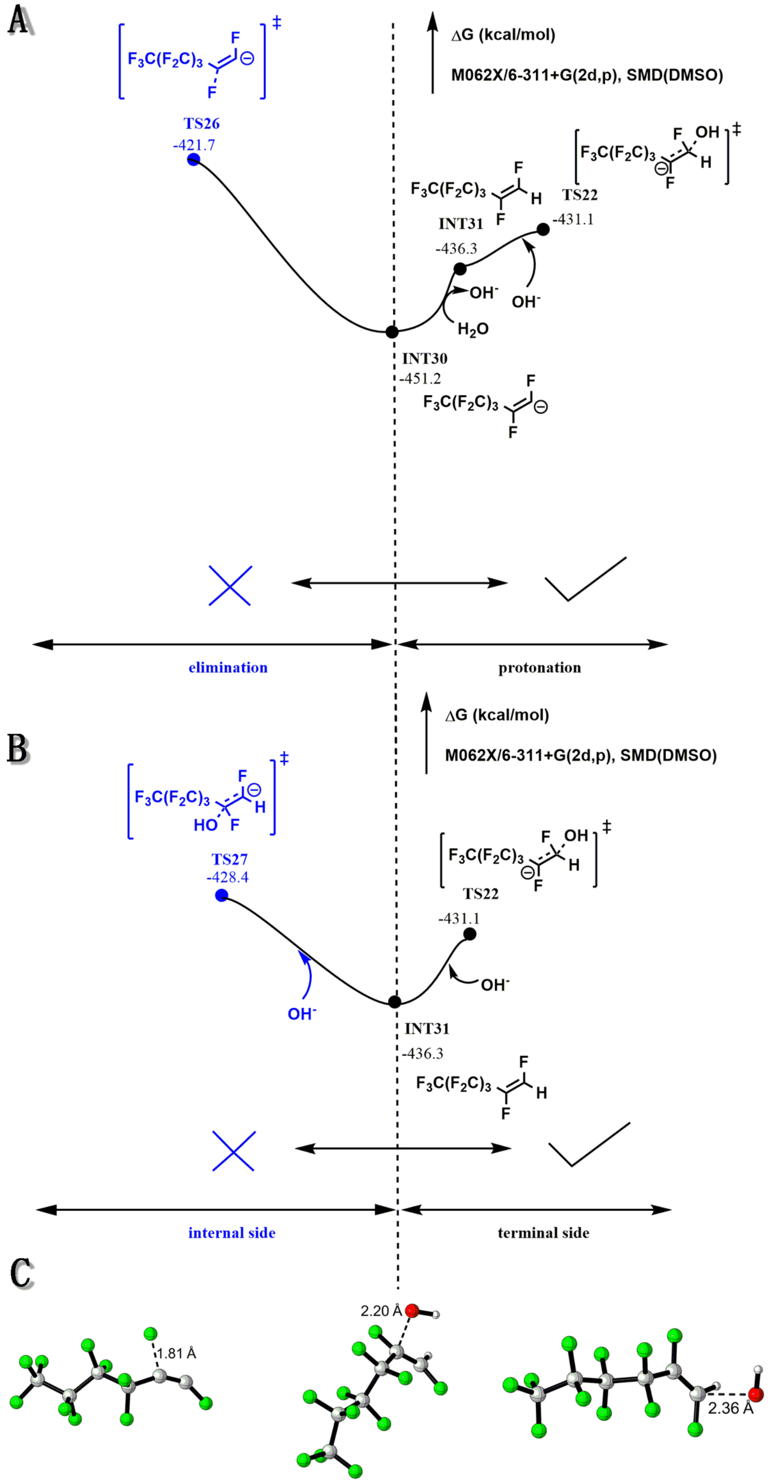

Fig. S56. A) Comparison of β-elimination and protonation of INT30. B) Comparison of hydroxide addition on the internal side and the terminal side. C) 3D structures of TS26, TS27 and TS22.

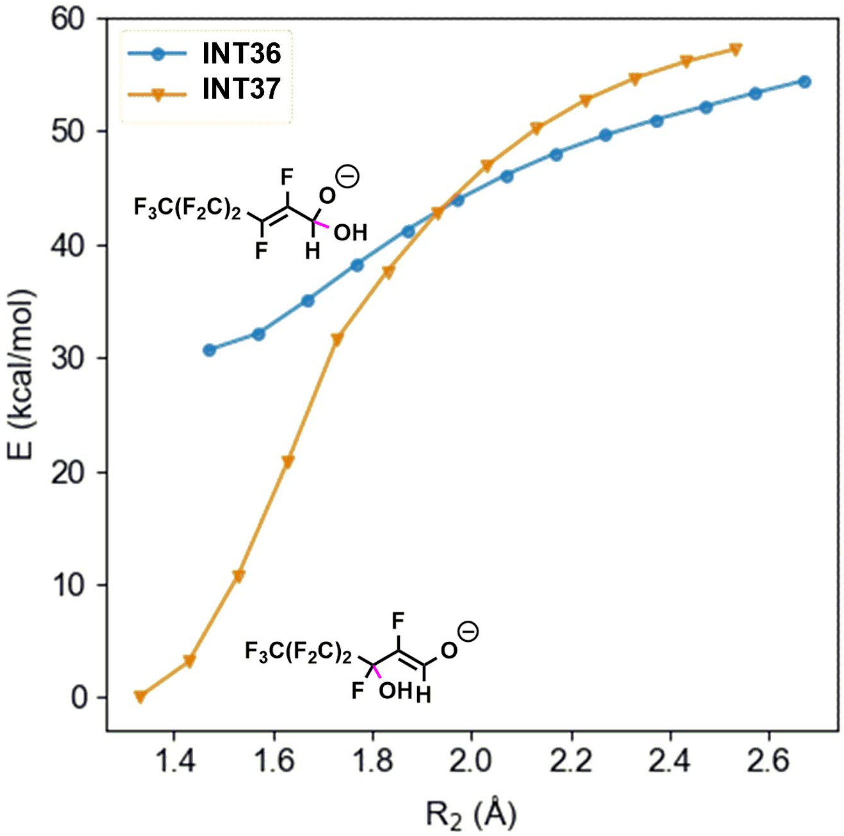

Fig. S57. The scanning coordinates of carbon–oxygen bond of INT36 and INT37, also indicating that 1,2-addition and 1,4-addition both have no enthalpic barrier.

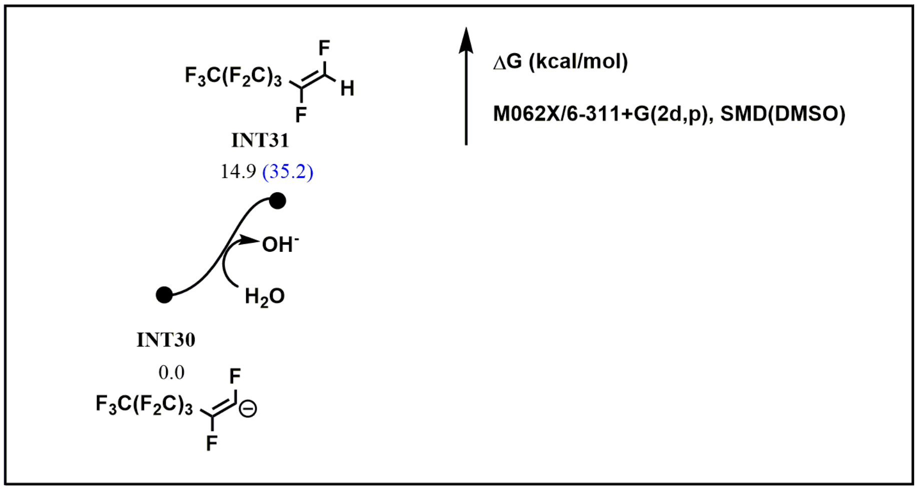

Fig. S58. Comparison of protonation in solvent and in gas phase (energy in the blue parentheses).

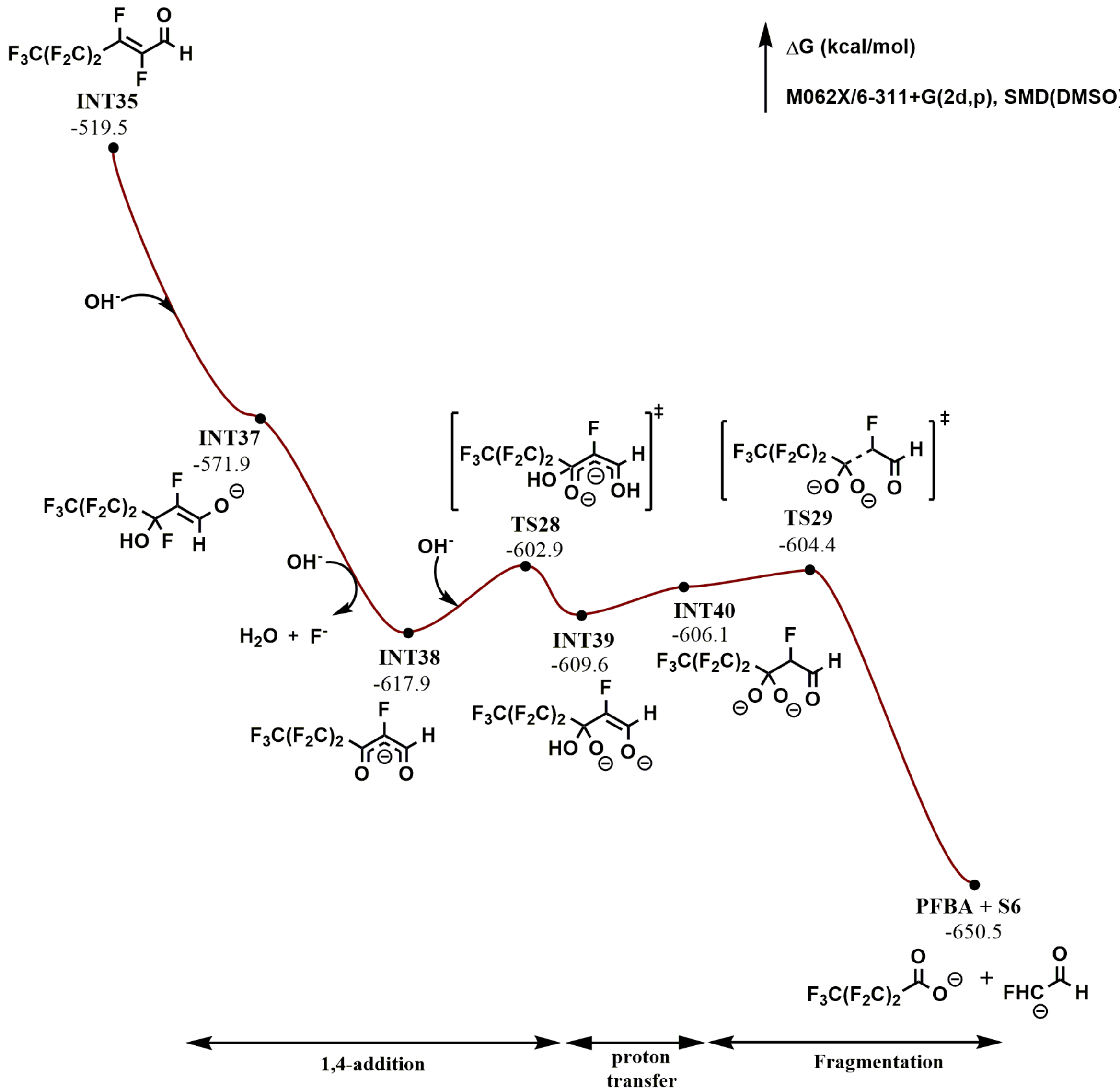

Fig. S59. Gibbs free energy profile for pathway D, X=H.

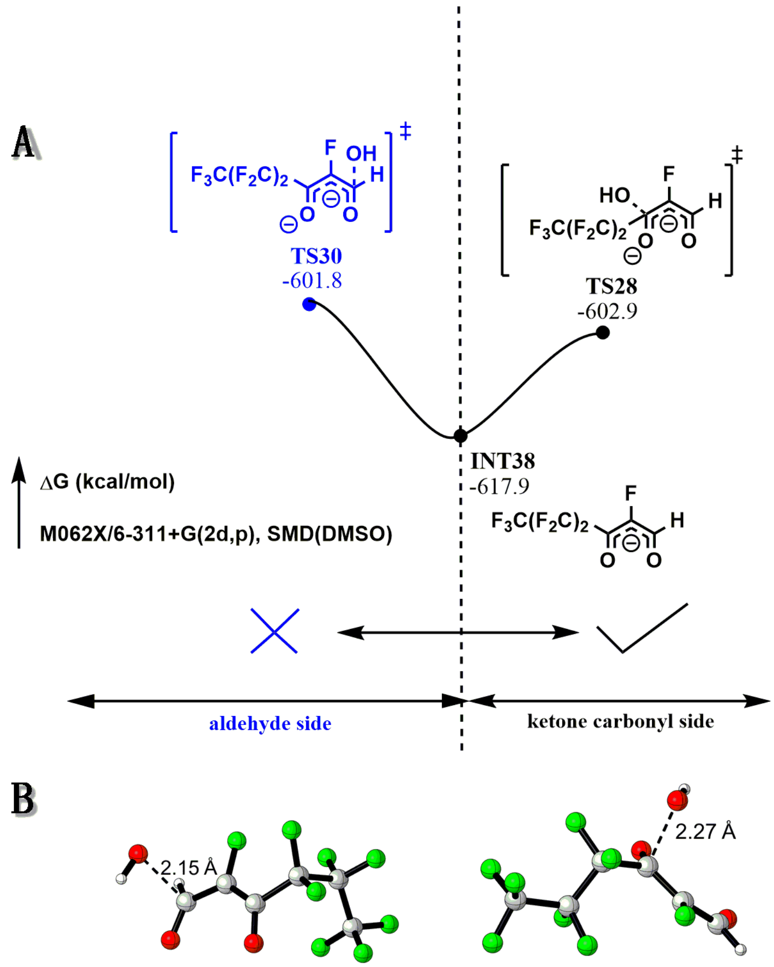

Fig. S60. A) Comparison of hydroxide addition on the aldehyde side and the ketone carbonyl side of INT38. B) 3D structures of TS30 and TS28.

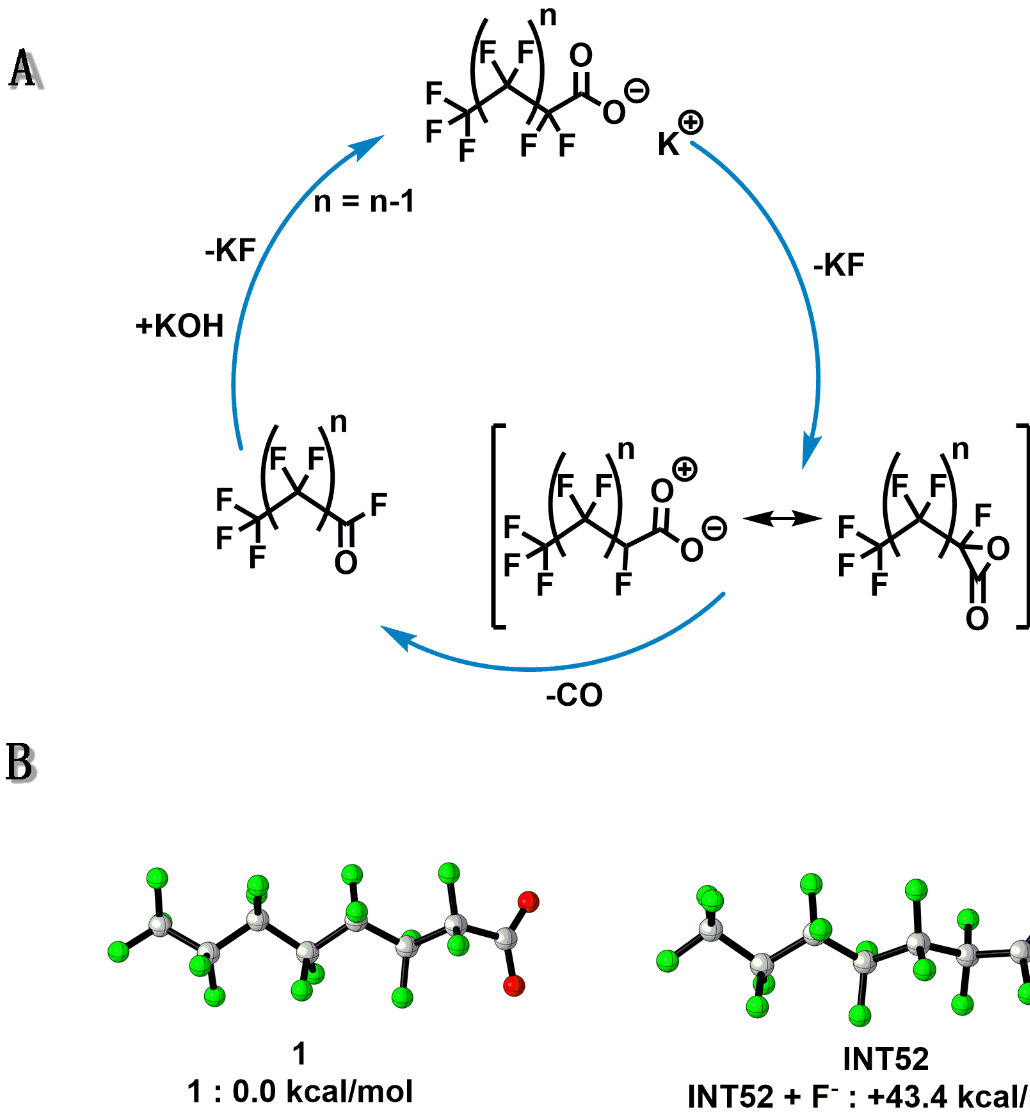

Fig. S61. A) α-lactone mechanism proposed by Pellerite (*33*) and calculated by Ge et al. (*34*). B) The Gibbs free energy change for selected intermediate indicates that this mechanism is not feasible.

A

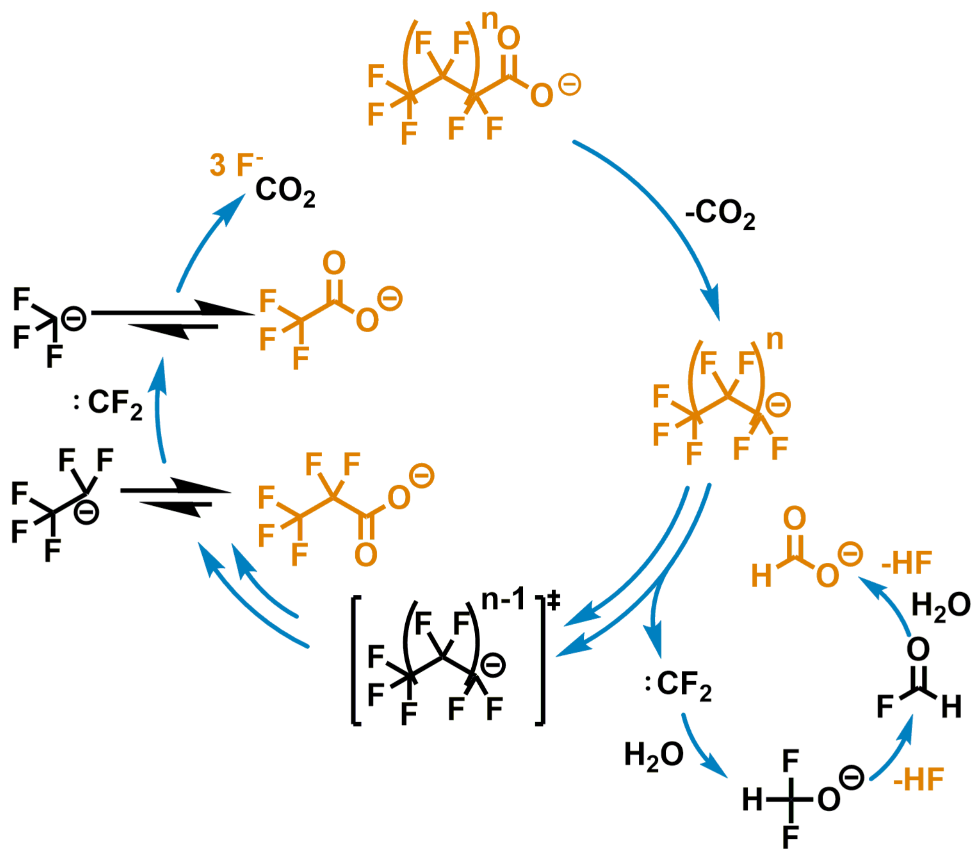

B

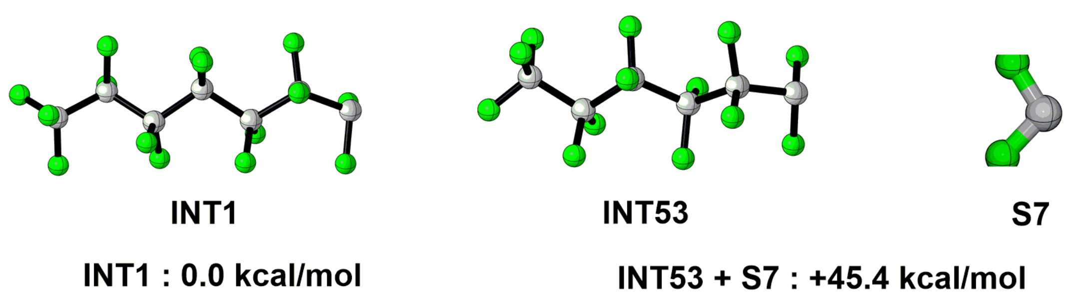

Fig. S62. A) Mechanism proposed previously assuming that difluorocarbene is the key intermediate. B) The Gibbs free energy change for selected intermediate indicates that this mechanism is not feasible.

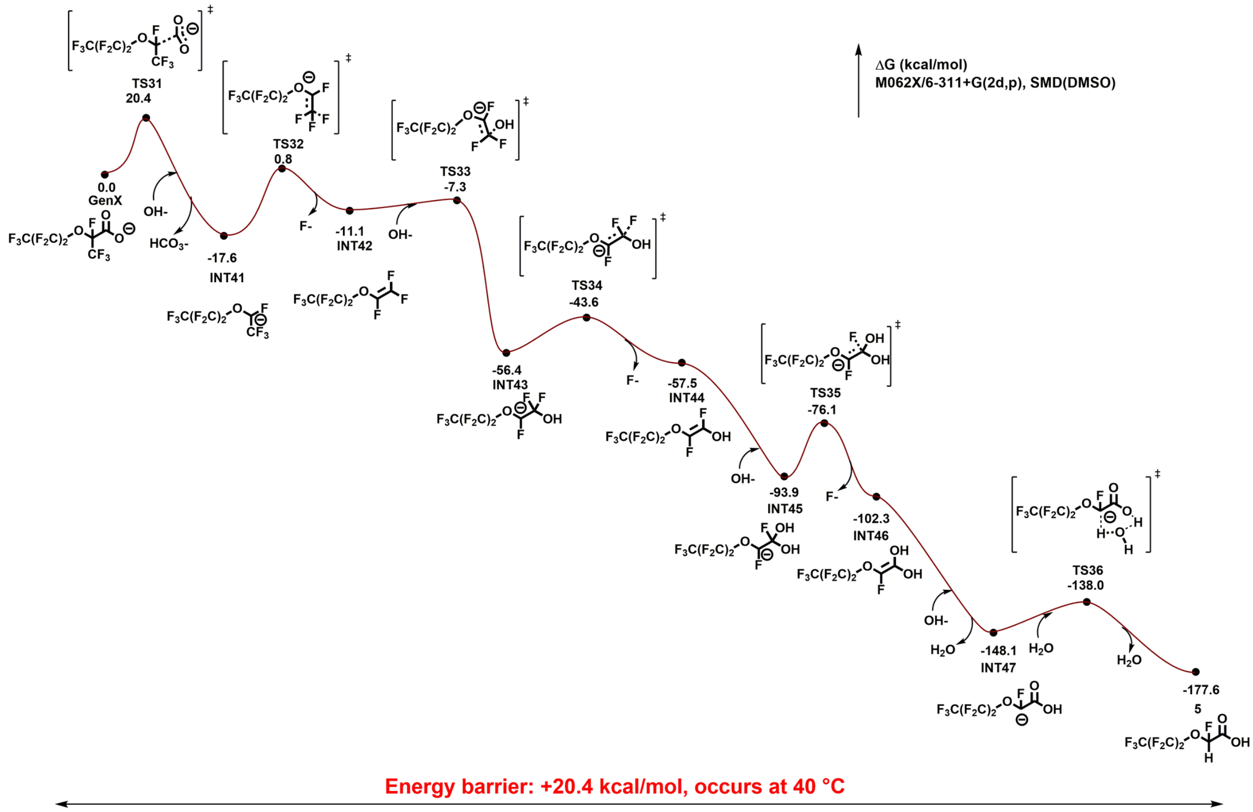

Fig. S63. Gibbs free energy profile for pathways A and E for GenX.

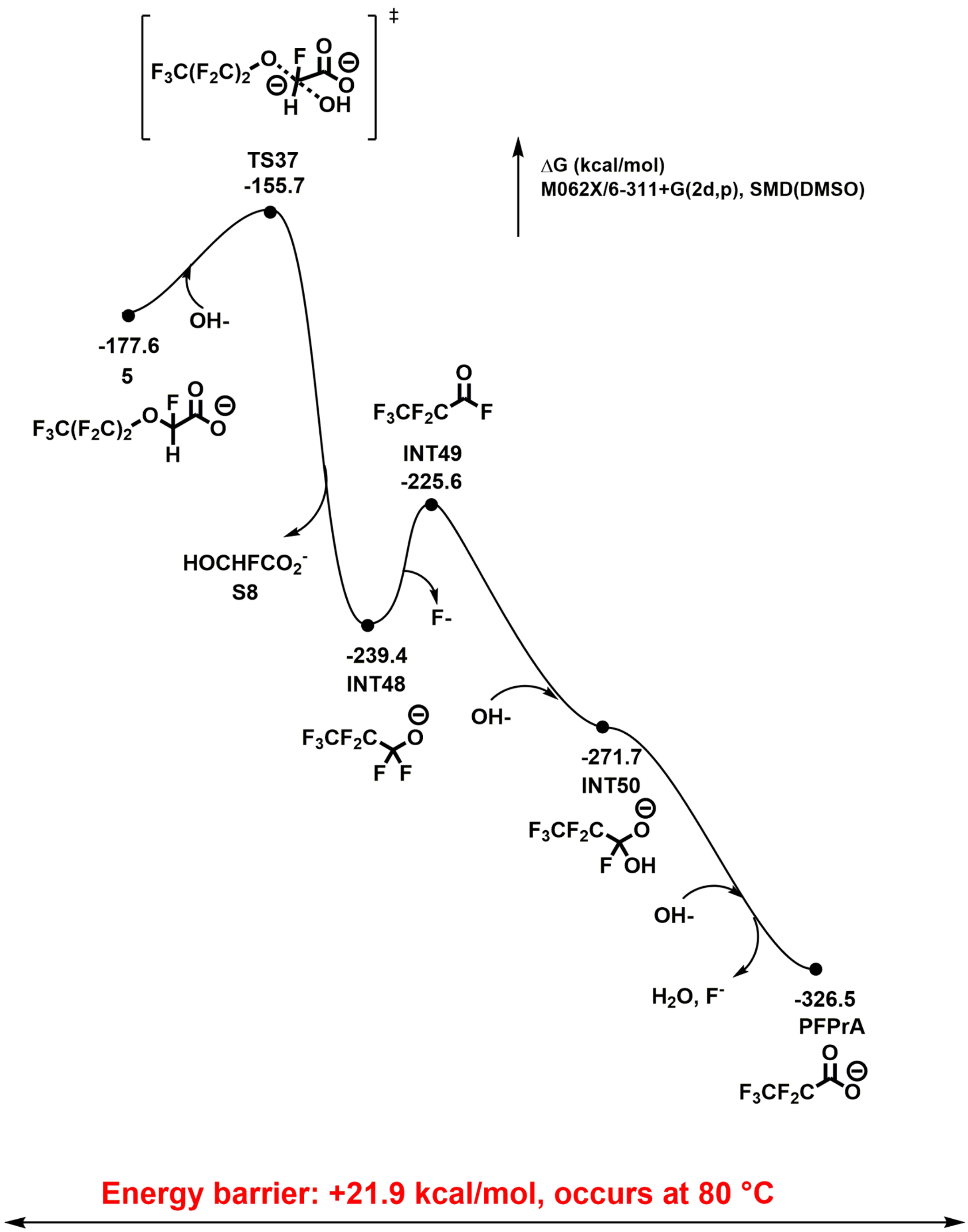

Fig. S64. Gibbs free energy profile for pathway F for GenX.

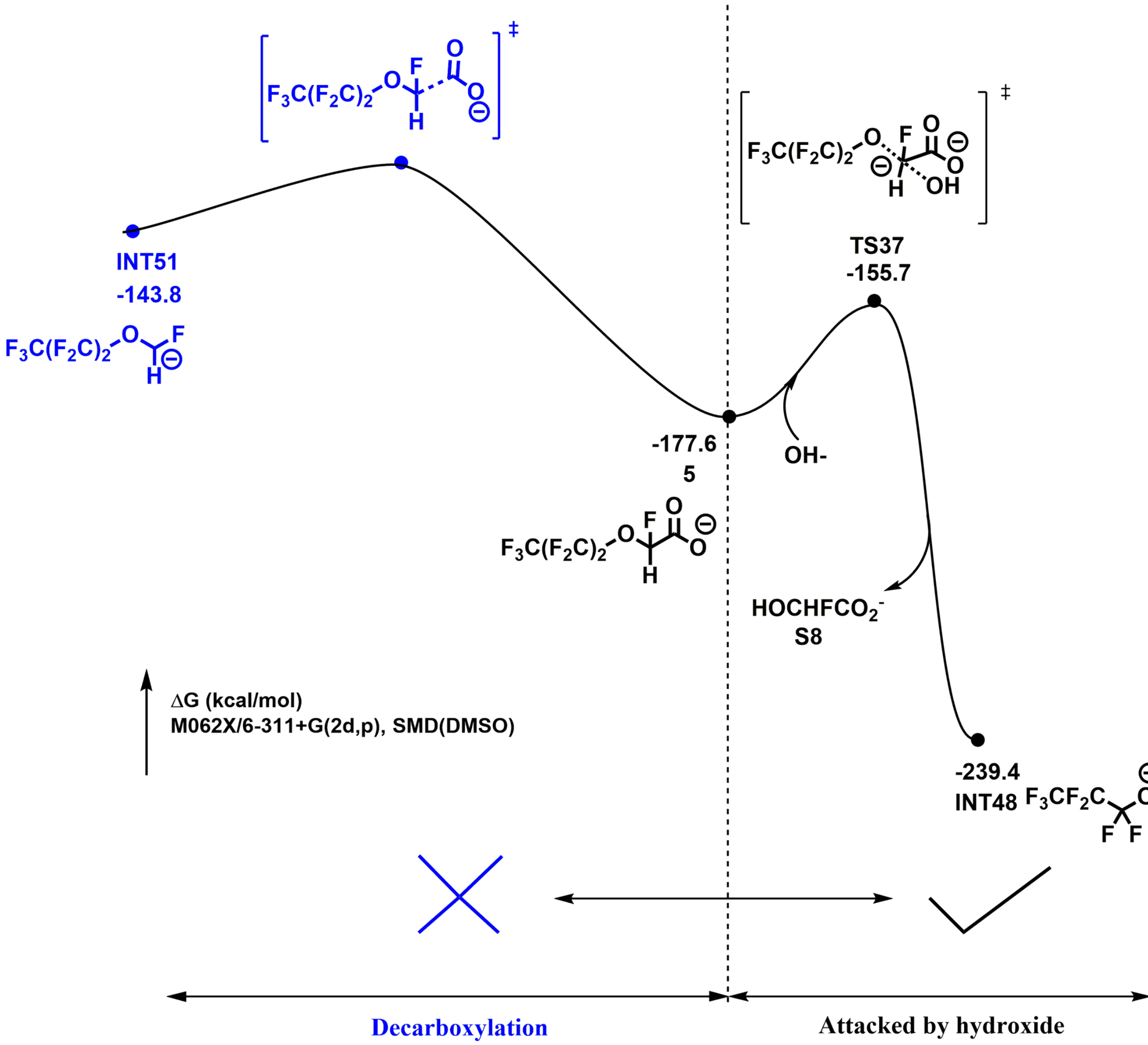

Fig. S65. Comparison of hydroxide attack vs. decarboxylation of **5**. The transition state for the transformation of **5** to INT51 will be higher than the energy of INT51, which is already 33.8 higher than **5**, disfavoring the reaction compared to TS37 (21.9 kcal/mol relative to **5**) and INT48 (-61.8 kcal/mol relative to **5**).

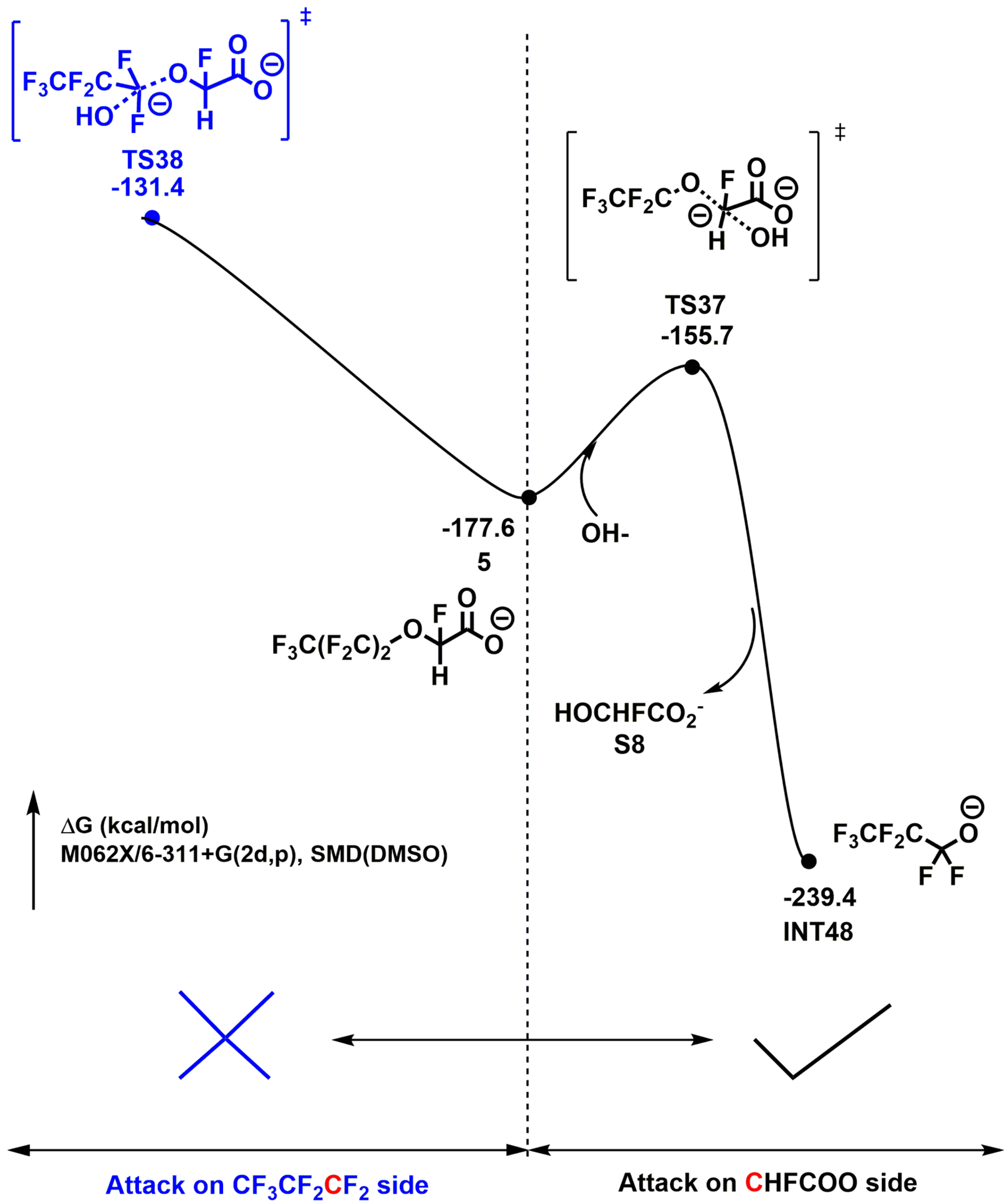

Fig. S66. Comparison of hydroxide attack on different sides of compound **5**.

Table S1. Emerging PFAS Destruction Methods.

Ref. No.	Technique	Matrix/ Reagents	Substrates	Time, (Temp, Press.)	Conc	Result	Specific Drawbacks	Proposed Mechanism	Evidence for Mechanism	See	Related publications	Overall Drawbacks
(*9*)	Sonication	MQ	PFOA, PFOS	120–180 min	5 ppm PFOS, 5 ppm PFOA	> 90% F^-	-	Desulfonylation > alkene > CF_3 radical, difluorocarbene, CF > CO, CO_2, F^-	GC-MS headspace	Figure 3	(*10*)	"Designing an effective ultrasound reactor has proven to be one of the most challenging aspects for the application of sonolysis in water treatment due to challenges in the optimization of operating conditions and parameters such as frequency and power"; matrix components may also reduce efficiency (*20*)
(*11*)	Plasma	NaCl, aqueous	PFOA, PFOS	120 min	8.3 ppm	5 mg/L F^- per 8.3 mg/L orig PFOA (60%); 4.4 mg/L F^- for PFOS (53%)	PFAS adsorbed to the reactor (~20–40%), many short-chain PFAS byproducts formed	DHEH	None	Figure 7	-	-
(*12*)	Electrochemical, Ti/RuO_2	100 mg.L NaCl, 1500 mg/L Na_2SO_4	PFOA, PFOS	6 h	5 ppm	98% F^- for PFOS, 58% F^- for PFOA	Quantifying the removal of PFOA due to electrochemical treatment versus sorption difficult to determine; PFOA sorption in zero-current control = 67%	None	N/A	Section 3.3	-	Energy consumption, the formation of toxic by-products, electrode issues such as mass transfer and fouling, and the lack of cost-effective and scalable electrode materials. (*51*, *52*)
(*21*)	Electrochemical, Ti/SnO_2-Sb-Bi	1.4 g/L $NaClO_4$	PFOA	3 h	50 ppm	63.8% F^-, observation of distribution of smaller PFCAs	High energy consumption; oxidation of other matrix components	DHEH, O_2 generation from two perfluoroalcohol radicals	Mostly proposed, water as O source $[C_4F_9(^{18}O)]$- supported by ^{18}O tests, one MS peak.	-	-	
(*13*)	Electrochemical, BDD	DI water, 0.1 M Na_2SO_4	PFBS, PFHxS, PFOS	43 h	2.9 ppm PFBS, 11 ppm PFHxS, 15 ppm PFOS	45% PFBS, 91% PFHxS, 98% PFOS decrease, overall 66% F^-	Complete oxidation of bromide and chloride at 120 h groundwater treatment and production of toxic byproducts, elevated short-chain concentrations after treatment, inefficient defluorination, optimization needed	PFSA > shorter-chain PFCAs	Literature	-	-	
(*13*)	Electrochemical, BDD	Concentrated groundwater	PFBA, PFPeA, PFHxA, PFHpA, PFOA, PFBS, PFHxS, PFOS and 6:2 FTSA	18 h	0.02-20 ppm	Decrease of PFBS (83%), PFHxS (92%), PFOS (96%) and 6:2 FTSA (60%). PFBA, PFPeA, PFHxA and PFHpA increased. 42% F^-						
(*16*)	UV-sulfite / hydrated electrons	10 mM Na_2SO_3, and 5 mM $NaHCO_3$ (pH 9.5, adjusted by 1 M NaOH)	PFCAs, PFSAs, diPFCAs, FTCAs	48 h	10 ppm (relative to PFOA)	F^- ratios of 98.2–49.1% for PFCAs, 81.4-63.2% for diPFCAs, 0.71–33.4% for telomeric PFCAs, 0.94-57.0% for PFSAs, smaller-chain PFAS generated during degradation	Generation of shorter-chain PFAS, generation of H-substituted PFAS	DHEH, H/F exchange	MS of intermediates, monitored degradation of alternate/proposed intermediates, DFT calculations of BDE of intermediates	-	(*15*, *17*)	Hydrated electron processes can require extreme operating conditions, such as high temperature, high reductant dosage, and high solution pH. Needs testing in complex matrices. (*20*)
(*53*)	Oxidation-reduction-oxidation (basic persulfate oxidation, UV-sulfite reduction)	Aqueous. Ox: $K_2S_2O_8$ at pH ≥ 12, Red: 10 mM of Na_2SO_3 and 5 mM of $NaHCO_3$ at pH 12.	PFCAs, PFSAs, FTCAs, FTSAs	40 min–24 h per step	207-10 ppm (relative to PFOA)	97–103% F^- except for n = 7, 8 fluorotelomers (85–89%), n = 4 PFSA (94%), and n = 4 FTSA (93%)	Complicated treatment train	Detailed mechanism proposal, see paper	Literature, study of SO_4^- radical vs OH radical, characterization of intermediate distribution, stoichiometry of reactants consumed, DFT calculations of BDE of intermediates	-	-	

(*18*)	Persulfate-UV	pH 3.0-3.1, $K_2S_2O_8$ (6.4-50.0 mM), aqueous solution	PFOA	12 h	559 ppm	disappearance of PFOA after 4 h, production of F^- after PFOA disappeared; 73.8% F^- plus shorter-chain PFCAs	Formation of shorter-chains PFCAs	DHEH	Observations and literature	Figure 2	-	"Generally, higher doses of persulfate, high temperature, or creating extreme pH conditions are necessary to achieve an effective degradation of PFOA"; not effective for PFOS (*20*)
(*22*)	UV photolysis	aqueous	PFOA	72 h	559 ppm	34% F^-, shorter PFCAs formed	Low defluorination	DHEH	^{18}O experiments	Table 1 Entry 2	-	PFOA does not absorb at wavelengths >220 nm (*20*)
(*22*)	UV, tungstic heteropolyacid	aqueous, 6.68 mM tungstic polyacid	PFOA	24 h	559 ppm	88% F^-, suppressed shorter-chain PFCA generation compared to direct photolysis	Catalyst needs to be separated from reaction mixture	Proposed catalyst coordination and reoxidation steps, proposed photo-Kolbe decarboxylation cleavage, hydrolysis downstream	UV studies of catalyst under anaerobic conditions, ^{18}O experiments	-	-	-
(*19*)	VUV-Fe	aqueous, $FeCl_3 \cdot 6H_2O$ (20 µM), various additives tested	PFOA	72 h	15 ppm	100% F^-, shorter PFCAs formed	Interference from matrix constituents	Direct photolysis leading to perfluoroalkyl radical, hydrolysis to shorter-chain PFCA; Fe^{3+} complex with PFOA leading to PFOA radical, hydrolysis to shorter-chain PFCA	Literature, none	Figure 1	-	-
(*54*)	Thermal treatment of AC in N_2 gas stream	Activated carbon	PFOA, PFHxA, PFOS	10 min	10 mg PFAS/g	~27–76% F^- at 700 °C, ~80% F^- at 1000 °C. Volatile organic fluorine found at 800–900 °C.	PFAS destroyed on surface of GAC at 700 °C and destroyed in gas phase at 1000 °C but in equilibrium with volatilizing at temperatures between 700–1000 °C, which gives incomplete destruction. Fluorine mass balance difficult to quantify; error is 20–30%.	None	N/A	Figures 2, 3, 4	(*55*)	-
(*56*)	Thermal treatment of GAC	PFAS adsorbed to granulated activated carbon with surface water	7 PFCAs, 3 PFSAs, HFPO-DA	10 °C/min ramp, 30 min hold	not specified	Thermal degradation of PFAS from 150–600 °C for PFOA, 450–600 °C for PFOS; 80–90% F^- for PFOA and PFOS at temperatures ≥700 °C	High temperature	Radical and alkene-based mechanism	Organofluorine species identified by TD−Pyr− GC−MS	Figure 4	-	-
(*23*)	Hydrothermal Alkaline	1-5 M NaOH, aqueous	PFOS	8 h, 350 °C, 2–16.5 MPa	50 ppm	Low concentrations of PFHpA, PFHxA and PFPeA, 80–90% F^-	High temperature, pressure	Nucleophilic hydroxide substitution of sulfonic acid head group, subsequent DHEH	Observation of shorter-chain intermediates, literature	Figure 2	(*57*)	-
This Study	Basic polar aprotic solvent-assisted	8:1 DMSO:H_2O, 2.67 M NaOH	PFCAs	24 h, 120 °C	36,800 ppm	80–100 F^-, TFA, formate formed	Organic solvent	Detailed mechanism proposal, see paper	DFT calculations of activation energies, explanation of byproducts, NMR of intermediates, explanation of chain-length patterns, monitored degradation of intermediates	-	-	-

Summary of emerging PFAS degradation methods and their major drawbacks. DHEH = decarboxylation–hydroxylation–elimination–hydrolysis (*16*).

Table S2. Summary of kinetic fitting parameters for degradation of PFOA at various temperatures.

°C	a	b	c	k	adjusted R^2	trial replicates
80	0.07476	2.90×10^{5}	0.02057	3.45×10^{-6}	0.9466	single run
90	0.06934	8.62×10^{4}	0.01227	1.16×10^{-5}	0.9842	duplicate
100	0.07908	3.82×10^{4}	0.00953	2.62×10^{-5}	0.9813	triplicate
120	0.08268	6.32×10^{3}	0.00449	1.58×10^{-4}	0.9949	triplicate

Kinetic fitting parameters for PFOA degradation at different temperatures (**Figures S25–S28**) as fitted to the equation $y = ae^{-x/b} + c$ in MATLAB using the Curve Fitting application.

Table S3. Defluorination of various PFAS substrates under varying conditions.

Compound	Solvent	Temp (°C)	Time	F IC%[a]
2	DMSO	40	25 min	4%
1	DMSO	40	25 min	n.d.
2	DMSO	120	5 min	11%
1	DMSO	120	5 min	n.d.
2	DMSO	40	48 h	57%
3	DMSO	40	48 h	70%
PFOS	DMSO	120	150 h	0.3%
1	DMAc[b]	120	44 h	31%
1	sulfolane[b]	120	44 h	38%
1	water	120	44 h	0.1%
control[c]	DMSO	120	24 h	0.2%

Defluorination of various PFAS substrates under varying conditions, as measured by fluoride ion concentrations detected by ion chromatography. Perfluoro-1H-heptane (**2**) gives greater fluoride recovery than PFOA at the same times and temperatures, suggesting that decarboxylation is the rate-limiting step in this degradation. Even at low temperatures, **2** and perfluoro-1-heptene (**3**) both give relatively efficient defluorination (>50%). PFOS does not react under these conditions, and PFOA (**1**) does not defluorinate in pure water, only in polar aprotic solvents such as dimethylacetaminde (DMAc) or sulfolane. Control experiments run without PFOA show that the polytetrafluoroethylene reactor does not release fluoride into the reaction. [a] n.d. = not detected. [b] Using standard conditions for DMSO; not optimized for other solvents. 100% degradation of PFOA as all ^{19}F NMR peaks disappeared. [c] Percent calculated relative to a 1 mmol PFOA degradation reaction; average of triplicate reactions.

Table S4. Distribution of carbonaceous byproducts of the PFOA degradation reaction, as measured by quantitative ^{13}C NMR spectroscopy of the isolated reaction precipitate dissolved in D_2O.

Compound	Mol% C relative to PFOA	Mol/Mol PFOA
Formate[a]	31.1 ± 4.0	2.5 ± 0.3
Carbonate	25.7 ± 3.1	2.1 ± 0.3
Oxalate	17.8 ± 3.0	0.7 ± 0.1
Glycolate	15.0 ± 1.4	0.6 ± 0.1[c]
Trifluoroacetate[b]	8.0 ± 1.0	0.32 ± 0.04
Tartronate[c]	4.3 ± 1.1	0.2 ± 0.1[c]
Unidentified	4.9 ± 2.4	0.4 ± 0.2[c]
Total	106.7 ± 8.3	8.5 ± 0.7[d]

Unless noted, all errors reported as standard deviation of triplicate measurements. [a] Calculated by adding the formate in the reaction solvent, as measured by ^{1}H NMR, to the formate in the reaction precipitate, as measured by ^{13}C NMR. [b] Calculated via ^{19}F NMR spectroscopy. [c] Error estimated as 0.1 based on the signal-to-noise of NMR resonances for low-concentration species. Errors for other products are given as the standard deviation of triplicate measurements. [d] Calculated as mols of carbon per mol of PFOA; *i.e.*, accounting for compounds that have multiple carbons integrated in the analysis.

Data S1. XYZ Coordinates of Optimized DFT Structures and Corresponding Energies

PFPeA
E(DMSO)[M06-2X/6-311++G(2d,p), SMD (DMSO)] = -1239.739617 a.u.
G_{corr}(DMSO)[M06-2X/6-311++G(2d,p)] = 0.022082 a.u.
H_{corr}(DMSO)[M06-2X/6-311++G(2d,p)] = 0.07736 a.u.
G = E(DMSO) + G_{corr} = -1239.717535 a.u.
H = E(DMSO) + H_{corr} = -1239.662257 a.u.

C	-2.84528300	-0.33932800	-0.18533300
C	-1.55377900	0.39824300	0.31645700
F	-1.54328100	0.49209200	1.66984500
O	-3.49607300	0.26394200	-1.04186500
O	-3.00368900	-1.43908200	0.36043000
F	-1.45781900	1.66187500	-0.16328500
C	-0.26921600	-0.34000300	-0.10458000
C	1.00501600	0.53627100	-0.05233700
C	2.31519100	-0.28067500	-0.03356500
F	-0.07098200	-1.40637200	0.68731600
F	-0.40887000	-0.77302200	-1.37142200
F	0.99094100	1.29891200	1.05060000
F	1.04349500	1.33001600	-1.12981000
F	2.50194900	-0.84839800	1.14819900
F	2.28377300	-1.22281200	-0.96805300
F	3.33707600	0.52927400	-0.27809800

Formate
E(DMSO)[M06-2X/6-311++G(2d,p), SMD (DMSO)] = -189.762029 a.u.
G_{corr}(DMSO)[M06-2X/6-311++G(2d,p)] = 0.01005 a.u.
H_{corr}(DMSO)[M06-2X/6-311++G(2d,p)] = 0.038226 a.u.
G = E(DMSO) + G_{corr} = -189.751979 a.u.
H = E(DMSO) + H_{corr} = -189.723803 a.u.

C	0.13093100	0.40154300	0.00004400
H	0.11314100	1.49760800	0.00042000
O	1.12633900	-0.26600400	-0.00005000
O	-1.10704000	-0.08963400	-0.00014700
H	-1.05312400	-1.06176500	0.00089000

GenX
E(DMSO)[M06-2X/6-311++G(2d,p), SMD (DMSO)] = -2028.356103 a.u.
G_{corr}(DMSO)[M06-2X/6-311++G(2d,p)] = 0.051716 a.u.
H_{corr}(DMSO)[M06-2X/6-311++G(2d,p)] = 0.126659 a.u.
G = E(DMSO) + G_{corr} = -2028.304387 a.u.
H = E(DMSO) + H_{corr} = -2028.229444 a.u.

C	-4.44504000	0.10771900	-0.28358800
C	-3.14109700	-0.51613800	0.26092700
C	-1.88388600	0.33284700	-0.05068300
C	-0.57724800	-0.49189500	0.06187600
C	0.68547400	0.38509600	0.23210000
F	-4.50247900	1.39310600	0.03902600
F	-4.50683600	-0.01506400	-1.59956600
F	-5.48057000	-0.51918300	0.25314100
F	-3.00816500	-1.73291400	-0.28124500
F	-3.26176600	-0.63704300	1.58589100
F	-1.98057500	0.81600900	-1.29620000
F	-1.84742800	1.35907700	0.80758600
F	-0.45118500	-1.22633500	-1.04767500
F	-0.66606800	-1.31056800	1.11980400
F	0.61880300	1.39789200	-0.64747500
F	0.68221600	0.92261000	1.45818400
O	1.75341600	-0.41586800	0.02571000
C	3.04182000	0.08556100	0.30904600
F	3.23093000	0.02801100	1.65605900
C	3.33429100	1.53433000	-0.25749500
O	3.31654200	2.42905700	0.58914200
O	3.53674400	1.54111200	-1.47685400
C	3.98433000	-0.97672400	-0.27165200
F	5.24753400	-0.57037900	-0.14451800
F	3.86216300	-2.12392800	0.40834700
F	3.74726400	-1.24786900	-1.54549100

1
E(DMSO)[M06-2X/6-311++G(2d,p), SMD (DMSO)] = -1953.114266 a.u.
Gcorr(DMSO)[M06-2X/6-311++G(2d,p)] = 0.04928 a.u.
Hcorr(DMSO)[M06-2X/6-311++G(2d,p)] = 0.121697 a.u.
G = E(DMSO) + Gcorr= -1953.064986 a.u.
H = E(DMSO) + Hcorr= -1952.992569 a.u.

C	4.77319800	-0.14754100	-0.41572100
O	4.99396900	-1.35866900	-0.28532200
O	5.35808600	0.74082100	-1.03988300
C	3.49173700	0.31425800	0.36442500
C	2.21099300	-0.33527800	-0.19594800
C	0.90948200	0.41123100	0.19183200
C	-0.35828100	-0.46657000	0.02986500
C	-1.65660300	0.37668700	-0.05226800
C	-2.92111200	-0.45864700	0.26857600

F	3.57861600	-0.01994200	1.67645900
F	3.30982400	1.65580900	0.31415800
F	2.10506900	-1.59966000	0.24397000
F	2.28513100	-0.35233000	-1.53930200
F	0.98404700	0.80155100	1.47151100
F	0.77205400	1.49476600	-0.58732000
F	-0.45306600	-1.29427300	1.07907300
F	-0.25547400	-1.19109700	-1.09131100
F	-1.58565800	1.38571700	0.82494300
F	-1.76838200	0.88147700	-1.28727300
F	-3.02614600	-0.59122200	1.59351900
F	-2.81202300	-1.67120500	-0.28803000
C	-4.22286600	0.18965800	-0.25218100
F	-5.26027900	-0.42597300	0.29344300
F	-4.25502700	1.47277400	0.08319900
F	-4.30487900	0.08027400	-1.56813100

5
E(DMSO)[M06-2X/6-311++G(2d,p), SMD (DMSO)] = -1691.303754 a.u.
G_{corr}(DMSO)[M06-2X/6-311++G(2d,p)] = 0.052111 a.u.
H_{corr}(DMSO)[M06-2X/6-311++G(2d,p)] = 0.119877 a.u.
G = E(DMSO) + G_{corr} = -1691.251643 a.u.
H = E(DMSO) + H_{corr} = -1691.183877 a.u.

C	3.79738100	-0.15087900	-0.08148100
C	2.44682600	0.59677500	-0.14187700
C	1.23756200	-0.30397900	0.21000100
C	-0.10203200	0.28641500	-0.29647900
C	-1.34436800	-0.30439000	0.40558100
F	3.87583900	-0.85944500	1.03724900
F	3.92794500	-0.96050000	-1.11984900
F	4.78228400	0.73427000	-0.10222400
F	2.30069200	1.08363300	-1.38063100
F	2.49696600	1.61089100	0.72654100
F	1.41547700	-1.50785700	-0.35075000
F	1.19809100	-0.45108800	1.53952600
F	-0.19056400	0.04419800	-1.60868200
F	-0.09606100	1.61298900	-0.09771300
F	-1.20350800	-1.64687500	0.46888800
F	-1.36971600	0.13146100	1.68104800
O	-2.42991200	0.07376500	-0.27711500
C	-3.66695000	-0.48020200	0.16197400
H	-3.60330300	-0.76457600	1.21183400
F	-3.86427500	-1.61984700	-0.57082700
C	-4.76725900	0.58770600	-0.07243200

O	-5.58519100	0.35528900	-0.97191200
O	-4.66766900	1.54962400	0.70818500

6
E(DMSO)[M06-2X/6-311++G(2d,p), SMD (DMSO)] = -1001.947909 a.u.
G_{corr}(DMSO)[M06-2X/6-311++G(2d,p)] = 0.012778 a.u.
H_{corr}(DMSO)[M06-2X/6-311++G(2d,p)] = 0.062475 a.u.
G = E(DMSO) + G_{corr} = -1001.935131 a.u.
H = E(DMSO) + H_{corr} = -1001.885434 a.u.

C	2.24000800	0.06429800	-0.17808200
C	0.83658100	-0.40555800	0.34174700
F	0.79646600	-0.41137000	1.69851400
O	2.79163100	-0.70284100	-0.97085400
O	2.57408400	1.16054900	0.29012700
F	0.52841500	-1.66309200	-0.05805000
C	-0.29768000	0.51570100	-0.14278700
C	-1.70529400	-0.11073000	-0.07743900
F	-0.33175000	1.63232300	0.59753900
F	-0.08060200	0.85792800	-1.42693200
F	-1.90693700	-0.67229000	1.10971900
F	-1.86822600	-1.02774200	-1.02093000
F	-2.62263500	0.83491600	-0.25706100

S3
E(DMSO)[M06-2X/6-311++G(2d,p), SMD (DMSO)] = -351.821033 a.u.
G_{corr}(DMSO)[M06-2X/6-311++G(2d,p)] = 0.000198 a.u.
H_{corr}(DMSO)[M06-2X/6-311++G(2d,p)] = 0.033629 a.u.
G = E(DMSO) + G_{corr} = -351.820835 a.u.
H = E(DMSO) + H_{corr} = -351.787404 a.u.

C	-0.55908200	-0.15439300	0.00010700
C	0.66984400	-0.72503400	0.00079700
O	-1.69780600	-0.61418500	-0.00045400
F	-0.47296400	1.26951500	0.00024900
F	1.81257500	0.06099200	-0.00052400
H	0.86137900	-1.78451700	0.00068200

S4
E(DMSO)[M06-2X/6-311++G(2d,p), SMD (DMSO)] = -401.887993 a.u.
Gcorr(DMSO)[M06-2X/6-311++G(2d,p)] = -0.004819 a.u.
Hcorr(DMSO)[M06-2X/6-311++G(2d,p)] = 0.028553 a.u.
G = E(DMSO) + Gcorr= -401.892812 a.u.

H = E(DMSO) + Hcorr= -401.85944 a.u.

C	0.18741500	-0.84810300	0.00000000
O	1.37337200	-1.19037000	0.00000000
O	-0.86421500	-1.49564100	0.00000000
C	0.00000000	0.71577900	0.00000000
O	0.82212800	1.56185900	0.00000000
F	-1.30830700	1.08746100	0.00000000

S5
E(DMSO)[M06-2X/6-311++G(2d,p), SMD (DMSO)] = -1089.171999 a.u.
G_{corr}(DMSO)[M06-2X/6-311++G(2d,p)] = 0.013571 a.u.
H_{corr}(DMSO)[M06-2X/6-311++G(2d,p)] = 0.065611 a.u.
G = E(DMSO) + G_{corr} = -1089.158428 a.u.
H = E(DMSO) + H_{corr} = -1089.106388 a.u.

C	2.92762700	-0.46464300	-0.38160200
C	1.98371200	0.42757200	-0.07844400
C	0.63302400	0.27225600	0.54277300
C	-0.47067800	-0.02507400	-0.49249000
F	2.52670000	-1.75334400	-0.00581600
F	2.19322300	1.73853600	-0.42822900
F	0.60875900	-0.73154600	1.44639500
F	0.26541700	1.40853900	1.19052700
F	-0.19277200	-1.19371000	-1.09056600
F	-0.46167100	0.94947000	-1.41858500
C	-1.91233100	-0.12442300	0.04025700
F	-2.01182900	-1.06635900	0.96819100
F	-2.31352300	1.03096700	0.55148700
F	-2.72187100	-0.43967800	-0.96706600

S6
E(DMSO)[M06-2X/6-311++G(2d,p), SMD (DMSO)] = -252.545844 a.u.
Gcorr(DMSO)[M06-2X/6-311++G(2d,p)] = 0.009188 a.u.
Hcorr(DMSO)[M06-2X/6-311++G(2d,p)] = 0.040346 a.u.
G = E(DMSO) + Gcorr= -252.536656 a.u.
H = E(DMSO) + Hcorr= -252.505498 a.u.

C	0.63748200	-0.30665700	-0.00002100
C	-0.48555700	0.45585800	0.00000000
O	1.85350600	0.07602900	0.00001000
F	-1.73141200	-0.18215500	0.00000500

H	-0.57475300	1.53297300	-0.00001300
H	0.41785800	-1.39701900	0.00001200

S7
E(DMSO)[M06-2X/6-311++G(2d,p), SMD (DMSO)] = -237.693767 a.u.
G_{corr}(DMSO)[M06-2X/6-311++G(2d,p)] = -0.016377 a.u.
H_{corr}(DMSO)[M06-2X/6-311++G(2d,p)] = 0.010922 a.u.
G = E(DMSO) + G_{corr} = -237.710144 a.u.
H = E(DMSO) + H_{corr} = -237.682845 a.u.

C	0.00000000	0.00000000	0.59047700
F	0.00000000	-1.02383600	-0.19682600
F	0.00000000	1.02383600	-0.19682600

S8
E(DMSO)[M06-2X/6-311++G(2d,p), SMD (DMSO)] = -403.090969 a.u.
G_{corr}(DMSO)[M06-2X/6-311++G(2d,p)] = 0.018354 a.u.
H_{corr}(DMSO)[M06-2X/6-311++G(2d,p)] = 0.053756 a.u.
G = E(DMSO) + G_{corr} = -403.072615 a.u.
H = E(DMSO) + H_{corr} = -403.037213 a.u.

C	-0.64585300	-0.20205800	0.39857500
F	-1.12899900	-1.11853300	-0.56843200
C	0.84299700	0.05474500	0.04981700
O	1.63777500	-0.86051000	0.30158900
O	1.04997300	1.17568600	-0.47033200
H	-0.79035100	-0.70028300	1.35655000
O	-1.37053300	0.94731000	0.32246600
H	-0.76924700	1.55106700	-0.16079500

INT1
E(DMSO)[M06-2X/6-311++G(2d,p), SMD (DMSO)] = -1764.479498 a.u.
Gcorr(DMSO)[M06-2X/6-311++G(2d,p)] = 0.036801 a.u.
Hcorr(DMSO)[M06-2X/6-311++G(2d,p)] = 0.103691 a.u.
G = E(DMSO) + Gcorr= -1764.442697 a.u.
H = E(DMSO) + Hcorr= -1764.375807 a.u.

C	4.20136300	-0.07233900	-0.00445300
C	2.83164800	0.42295900	0.43959700
C	1.56266200	-0.32894200	-0.04082800
C	0.25904600	0.50309200	0.07037800
C	-1.02088600	-0.37158200	0.04869000
C	-2.28678900	0.43862600	-0.32651600
F	4.20180200	0.13803900	-1.40261700

F	4.07114800	-1.48454600	0.08504900
F	2.69167500	1.71959800	0.05781800
F	2.78032500	0.38938100	1.79756900
F	1.69632200	-0.69296300	-1.32586500
F	1.39962300	-1.44348600	0.69838500
F	0.19948000	1.36368300	-0.95798200
F	0.26304700	1.19806300	1.21636300
F	-0.87710200	-1.35619300	-0.84813800
F	-1.19805000	-0.91422100	1.26125500
F	-2.31609200	0.60691200	-1.65184500
F	-2.25123800	1.63740100	0.26884200
C	-3.59905800	-0.26008800	0.09090600
F	-4.61837600	0.34692900	-0.49767100
F	-3.57533800	-1.53125400	-0.28840900
F	-3.76588300	-0.19849100	1.40206200

INT2
E(DMSO)[M06-2X/6-311++G(2d,p), SMD (DMSO)] = -1664.501639 a.u.
Gcorr(DMSO)[M06-2X/6-311++G(2d,p)] = 0.036315 a.u.
Hcorr(DMSO)[M06-2X/6-311++G(2d,p)] = 0.101983 a.u.
G = E(DMSO) + Gcorr= -1664.465324 a.u.
H = E(DMSO) + Hcorr= -1664.399656 a.u.

C	2.79182500	-1.38547500	-0.15575400
C	2.45240100	-0.25186600	0.43257700
C	1.88800700	0.96251700	-0.22925700
C	0.40364500	1.23924400	0.12607100
F	2.56932700	-0.13964300	1.75793600
F	0.33995200	1.62953200	1.40445800
F	-0.03546800	2.23586700	-0.65506900
F	3.25921700	-2.40255900	0.50943700
C	-0.51469100	0.00787700	-0.05549400
F	-0.33791600	-0.80537500	0.99625400
F	-0.16178700	-0.64954300	-1.16842500
C	-2.01171900	0.38408000	-0.16098700
F	-2.29093800	1.35645800	0.71527300
F	-2.25885700	0.82167300	-1.39836100
C	-2.95589200	-0.80551200	0.12330600
F	-2.97440500	-1.08755300	1.41557700
F	-4.18115500	-0.48744800	-0.26365300
F	-2.55174200	-1.87340600	-0.55231200
F	1.98624300	0.87591500	-1.56196100
F	2.69864900	-1.62796800	-1.42990800
F	2.56983000	2.05347400	0.17711400

INT3
E(DMSO)[M06-2X/6-311++G(2d,p), SMD (DMSO)] = -1740.492919 a.u.
Gcorr(DMSO)[M06-2X/6-311++G(2d,p)] = 0.048745 a.u.
Hcorr(DMSO)[M06-2X/6-311++G(2d,p)] = 0.116177 a.u.
G = E(DMSO) + Gcorr= -1740.444174 a.u.
H = E(DMSO) + Hcorr= -1740.376742 a.u.

C	3.52727300	-0.71427400	-0.20976100
C	2.06967600	-0.60524100	0.00297300
C	1.54219700	0.75507400	-0.16253100
C	0.09162000	0.94877700	0.34132700
F	1.85754300	-0.97539300	1.36316300
F	0.05691800	0.95333000	1.68204300
F	-0.33769600	2.15998900	-0.08081100
F	4.30247000	-0.06675200	0.75994100
C	-0.92825700	-0.09503000	-0.16654900
F	-0.79411900	-1.23216900	0.52993200
F	-0.71603300	-0.34865700	-1.46469300
C	-2.39656900	0.38613500	-0.02637800
F	-2.56591400	1.03095800	1.13565700
F	-2.68346300	1.22032900	-1.03198500
C	-3.41809800	-0.77279600	-0.07349600
F	-3.40348400	-1.45887800	1.05836300
F	-4.63308300	-0.27254500	-0.24950200
F	-3.13951100	-1.58930800	-1.08160600
F	1.55702200	1.14383100	-1.46383700
F	3.93091700	-2.02442400	-0.02957000
O	3.91283500	-0.27123000	-1.42531500
H	4.88238600	-0.26461800	-1.45210500
F	2.22264400	1.79508700	0.49747400

INT4
E(DMSO)[M06-2X/6-311++G(2d,p), SMD (DMSO)] = -1640.497449 a.u.
G_{corr}(DMSO)[M06-2X/6-311++G(2d,p)] = 0.047743 a.u.
H_{corr}(DMSO)[M06-2X/6-311++G(2d,p)] = 0.114179 a.u.
G = E(DMSO) + G_{corr} = -1640.449706 a.u.
H = E(DMSO) + H_{corr} = -1640.38327 a.u.

C	2.85944600	-1.34885300	-0.15502800
C	2.44201300	-0.23105600	0.42926800
C	1.87396400	0.97858800	-0.22393300
C	0.38627500	1.24064500	0.12945200
F	2.47974300	-0.13723100	1.76898500

F	0.31163100	1.61993900	1.41129500
F	-0.06193500	2.24174400	-0.64344100
F	3.25806300	-2.35025900	0.61297600
C	-0.52391900	0.00597900	-0.06704000
F	-0.34021800	-0.82302000	0.97151800
F	-0.17427900	-0.63238200	-1.19168900
C	-2.02445300	0.37311700	-0.16083300
F	-2.31043800	1.32715800	0.73340200
F	-2.28020700	0.83162800	-1.38931600
C	-2.95925300	-0.82838400	0.10415800
F	-2.97465900	-1.13273500	1.39150600
F	-4.18761300	-0.51281000	-0.27576200
F	-2.54915400	-1.88238200	-0.58964100
F	1.97355700	0.91194700	-1.55764500
O	2.96269000	-1.56782300	-1.45017900
H	2.84212300	-2.51618500	-1.63477500
F	2.53683300	2.08490700	0.19113900

INT5
E(DMSO)[M06-2X/6-311++G(2d,p), SMD (DMSO)] = -1640.061417 a.u.
G_{corr}(DMSO)[M06-2X/6-311++G(2d,p)] = 0.035336 a.u.
H_{corr}(DMSO)[M06-2X/6-311++G(2d,p)] = 0.100773 a.u.
G = E(DMSO) + G_{corr} = -1640.026081 a.u.
H = E(DMSO) + H_{corr} = -1639.960644 a.u.

C	2.86156400	-1.39937900	-0.32407400
C	2.51872700	-0.25233000	0.35189000
C	1.91802900	0.94832900	-0.21894500
C	0.43741200	1.20964100	0.16452900
F	2.45242400	-0.25473500	1.72901700
F	0.36361500	1.53120700	1.46573500
F	-0.03308700	2.25363400	-0.54970400
F	3.20911300	-2.40409200	0.59355000
C	-0.49104300	-0.00232300	-0.07900800
F	-0.32299800	-0.88490700	0.91847800
F	-0.17325800	-0.59672000	-1.23580400
C	-1.98807500	0.38873300	-0.14047700
F	-2.26011300	1.30454000	0.79849400
F	-2.25505800	0.90602100	-1.34439000
C	-2.93823100	-0.80952600	0.08020600
F	-2.95393500	-1.16606400	1.35468300
F	-4.16521800	-0.46100000	-0.27894300
F	-2.55115900	-1.84256600	-0.65686700
F	1.98220600	0.95701400	-1.56346300

O	2.93798500	-1.68812300	-1.49814500
F	2.55033700	2.10279100	0.21148400

INT6
E(DMSO)[M06-2X/6-311++G(2d,p), SMD (DMSO)] = -1540.049441 a.u.
G_{corr}(DMSO)[M06-2X/6-311++G(2d,p)] = 0.034397 a.u.
H_{corr}(DMSO)[M06-2X/6-311++G(2d,p)] = 0.098281 a.u.
G = E(DMSO) + G_{corr} = -1540.015044 a.u.
H = E(DMSO) + H_{corr} = -1539.95116 a.u.

C	4.00480900	-0.38827400	-0.39493400
C	2.66942000	-0.31640900	0.23667900
C	1.80938000	0.67256200	0.02369800
C	0.43217600	0.76996300	0.64636300
F	2.35681600	-1.31945300	1.04395800
F	0.43465400	0.25407000	1.88055900
F	0.07358700	2.06185400	0.71307600
O	4.48470800	0.38359600	-1.14442700
F	4.64764600	-1.48819500	-0.00208300
C	-0.62170800	0.02405000	-0.20443800
F	-0.42409400	-1.29220600	-0.05025200
F	-0.42197200	0.34393200	-1.49026400
C	-2.08275400	0.37803600	0.16290200
F	-2.20745700	0.47562600	1.49153800
F	-2.39035700	1.55392000	-0.39183300
C	-3.10126600	-0.66905500	-0.33975100
F	-3.03953400	-1.76741900	0.39504700
F	-4.32182900	-0.16392900	-0.25397200
F	-2.84747000	-0.97512200	-1.60559300
F	2.08023300	1.66203100	-0.79992700

INT7
E(DMSO)[M06-2X/6-311++G(2d,p), SMD (DMSO)] = -1616.058051 a.u.
G_{corr}(DMSO)[M06-2X/6-311++G(2d,p)] = 0.048909 a.u.
H_{corr}(DMSO)[M06-2X/6-311++G(2d,p)] = 0.113731 a.u.
G = E(DMSO) + G_{corr} = -1616.009142 a.u.
H = E(DMSO) + H_{corr} = -1615.94432 a.u.

C	3.64735000	-0.76575300	0.33815800
C	2.43300500	-0.55062700	-0.23628300
C	1.83826900	0.78746900	-0.37380200
C	0.41263400	0.94973400	0.22607100
F	1.76861200	-1.56303700	-0.87608100

F	0.50958400	0.88539900	1.56751200
F	-0.05331800	2.17918000	-0.09195400
O	4.41458300	0.03812800	0.88481000
F	4.05143900	-2.07921800	0.29957000
C	-0.67056900	-0.07243300	-0.19122900
F	-0.48787800	-1.21029900	0.49981800
F	-0.59608600	-0.34402800	-1.50002700
C	-2.10954400	0.43160000	0.09249300
F	-2.15635000	1.06735500	1.27048400
F	-2.47634800	1.27898800	-0.87577900
C	-3.15313500	-0.70778300	0.13726900
F	-3.04344300	-1.40256100	1.25876200
F	-4.36930900	-0.18286100	0.08233200
F	-2.99049300	-1.52236000	-0.89734500
F	1.63437400	1.08945700	-1.74006200
O	2.59354100	1.76810100	0.18396500
H	3.42988300	1.35278100	0.51864300

INT8

E(DMSO)[M06-2X/6-311++G(2d,p), SMD (DMSO)] = -1515.607827 a.u.

G_{corr}(DMSO)[M06-2X/6-311++G(2d,p)] = 0.033937 a.u.

H_{corr}(DMSO)[M06-2X/6-311++G(2d,p)] = 0.097523 a.u.

G = E(DMSO) + G_{corr} = -1515.57389 a.u.

H = E(DMSO) + H_{corr} = -1515.510304 a.u.

C	3.95805700	-0.46657700	-0.32059100
C	2.65602400	-0.25512500	0.18137600
C	1.87832600	0.87068800	-0.09976600
C	0.45616400	0.90512600	0.54274300
F	2.14775700	-1.23574100	0.99186300
F	0.45882500	0.52088200	1.83728600
F	-0.00824200	2.17102400	0.50454400
O	4.64975200	0.19516300	-1.03768500
F	4.46636700	-1.67092600	0.13406500
C	-0.57073000	0.04207400	-0.21899600
F	-0.37154700	-1.25396700	0.06601900
F	-0.38928000	0.21895700	-1.53802100
C	-2.04479100	0.39409700	0.10126600
F	-2.18480800	0.65026000	1.40859100
F	-2.39779200	1.48059100	-0.59509000
C	-3.03142600	-0.73643800	-0.26365600
F	-2.94235500	-1.73577600	0.60005800
F	-4.26920000	-0.26202400	-0.23597500
F	-2.77249300	-1.18971900	-1.48388600

O	2.16964300	1.83419700	-0.80473200

INT9
E(DMSO)[M06-2X/6-311++G(2d,p), SMD (DMSO)] = -1591.521889 a.u.
G_{corr}(DMSO)[M06-2X/6-311++G(2d,p)] = 0.046575 a.u.
H_{corr}(DMSO)[M06-2X/6-311++G(2d,p)] = 0.112254 a.u.
G = E(DMSO) + G_{corr} = -1591.475314 a.u.
H = E(DMSO) + H_{corr} = -1591.409635 a.u.

C	-3.49910600	-0.98126500	-0.08961200
C	-3.05978200	0.30120300	-0.07538800
C	-1.70528300	0.90032900	0.28256400
C	-0.56218700	-0.14080600	0.03239500
F	-0.70825000	-0.86140200	-1.11139100
O	-2.97545200	-2.08975900	-0.00571300
O	-1.60777100	1.42784000	1.47489800
O	-1.43219100	1.90002700	-0.77486900
H	-1.15792200	2.65593800	-0.24174300
F	-4.93818200	-1.02175400	-0.26501000
F	-0.49783200	-1.03411200	1.05402000
F	-4.02234100	1.30357600	-0.12479600
C	0.85926400	0.48586500	-0.09306900
C	1.98805700	-0.49665800	0.31067000
C	3.38840400	-0.07823000	-0.19295000
F	1.10247500	0.83244800	-1.37513100
F	1.01958700	1.58087800	0.66196500
F	1.75183500	-1.71966800	-0.18989300
F	2.05848500	-0.57629600	1.64683700
F	3.50746100	-0.28956800	-1.49576000
F	3.62252700	1.20324600	0.05958400
F	4.30701600	-0.80661900	0.43286000

INT10
E(DMSO)[M06-2X/6-311++G(2d,p), SMD (DMSO)] = -1592.038358 a.u.
G_{corr}(DMSO)[M06-2X/6-311++G(2d,p)] = 0.059893 a.u.
H_{corr}(DMSO)[M06-2X/6-311++G(2d,p)] = 0.126051 a.u.
G = E(DMSO) + G_{corr} = -1591.978465 a.u.
H = E(DMSO) + H_{corr} = -1591.912307 a.u.

C	3.48130100	0.99458200	-0.13578200
C	3.00824300	-0.35075600	-0.59820500
C	1.72444400	-0.80230100	0.21959300
C	0.52915900	0.12952300	-0.19205800

F	0.58400000	0.49874700	-1.50129400
O	3.09937700	2.04999800	-0.50420200
O	1.91682200	-0.84283300	1.49071700
O	1.38583200	-2.07010200	-0.39720900
H	1.40928000	-2.67833600	0.35233300
F	4.43040300	0.91400100	0.81209700
F	0.56567700	1.27261200	0.53350000
F	3.98507900	-1.28644500	-0.34073500
H	2.83683000	-0.31502200	-1.67296300
C	-0.87200600	-0.49706100	0.01613700
C	-1.98761700	0.56519800	0.18583100
C	-3.41139300	0.00955200	-0.04160800
F	-1.20317200	-1.24676800	-1.05129200
F	-0.89973000	-1.27543500	1.10606500
F	-1.81155000	1.56523500	-0.69099600
F	-1.94669100	1.06053200	1.42923200
F	-3.63712600	-0.20149200	-1.32963800
F	-3.58036900	-1.12824400	0.62018900
F	-4.29709300	0.89441600	0.39984300

INT11
E(DMSO)[M06-2X/6-311++G(2d,p), SMD (DMSO)] = -1764.996384 a.u.
G_{corr}(DMSO)[M06-2X/6-311++G(2d,p)] = 0.051569 a.u.
H_{corr}(DMSO)[M06-2X/6-311++G(2d,p)] = 0.118723 a.u.
G = E(DMSO) + G_{corr} = -1764.944815 a.u.
H = E(DMSO) + H_{corr} = -1764.877661 a.u.

C	-1.51673500	-0.33739500	-0.03875400
C	-2.76990500	0.43779100	0.43655200
C	-4.09524700	-0.14403600	-0.06858200
F	-1.68237200	-0.70893500	-1.31414400
F	-1.37555900	-1.43508900	0.71784500
F	-4.05171300	-1.48556600	0.08003200
F	-2.67637700	1.71291400	0.02285000
F	-2.78741500	0.41926700	1.77824700
H	-4.93293500	0.27114000	0.49236000
F	-4.23113900	0.13081400	-1.37909000
C	-0.22048400	0.50544200	0.06410700
C	1.05809800	-0.37147700	0.05357600
C	2.32261200	0.43777500	-0.32761100
C	3.63520100	-0.25866200	0.09280800
F	3.61025100	-1.53044400	-0.28394200
F	3.79956100	-0.19390000	1.40378800
F	2.34826500	0.59868500	-1.65318900
F	2.28159500	1.63868900	0.26229500

F	0.90624300	-1.36088100	-0.83571100
F	1.22794300	-0.90333600	1.27012900
F	-0.17172200	1.35260300	-0.97176300
F	-0.24533100	1.20790600	1.20333900
F	4.65351500	0.34751900	-0.49678800

INT12
E(DMSO)[M06-2X/6-311++G(2d,p), SMD (DMSO)] = -1740.461376 a.u.
G_{corr}(DMSO)[M06-2X/6-311++G(2d,p)] = 0.049246 a.u.
H_{corr}(DMSO)[M06-2X/6-311++G(2d,p)] = 0.116617 a.u.
G = E(DMSO) + G_{corr} = -1740.41213 a.u.
H = E(DMSO) + H_{corr} = -1740.344759 a.u.

C	-2.45051000	-1.49293600	0.64239600
C	-2.69791000	-0.17170500	-0.08817000
C	-1.74766200	0.98527000	0.29494300
C	-0.29624200	1.07772500	-0.26549600
F	-2.54816700	-0.28397500	-1.48191300
F	-0.33851700	1.25944700	-1.58948700
F	0.20697000	2.20428300	0.28848600
F	-3.59937000	-2.25089600	0.21048400
C	0.70922000	-0.06462600	0.03385800
F	0.65926400	-0.97040300	-0.94953700
F	0.41114100	-0.63988900	1.20338100
C	2.17112700	0.44500600	0.10819600
F	2.39711300	1.30416900	-0.89532400
F	2.37194100	1.05995300	1.27689400
C	3.21459200	-0.69146500	-0.00943100
F	3.30229800	-1.12158700	-1.25788600
F	4.39886700	-0.22688700	0.36255300
F	2.88385900	-1.70569300	0.77848500
F	-1.66308700	1.08847100	1.63229500
F	-1.43232400	-2.11947400	-0.09756000
F	-2.30406200	2.13518400	-0.15929600
O	-3.95181500	0.29467500	0.18184100
H	-4.51451300	-0.47533000	0.35333000

INT13
E(DMSO)[M06-2X/6-311++G(2d,p), SMD (DMSO)] = -1616.029125 a.u.
G_{corr}(DMSO)[M06-2X/6-311++G(2d,p)] = 0.045918 a.u.
H_{corr}(DMSO)[M06-2X/6-311++G(2d,p)] = 0.112973 a.u.
G = E(DMSO) + G_{corr} = -1615.983207 a.u.
H = E(DMSO) + H_{corr} = -1615.916152 a.u.

C	-2.45073400	-0.12081400	0.31984700
C	-1.58218700	0.77231300	-0.13154800
C	-0.19357100	0.98584300	0.41141000
C	0.84214900	0.02097000	-0.20800200
C	2.23404800	0.05799600	0.46848600
F	-1.83767800	1.57504300	-1.17010700
F	-0.14231100	0.81898400	1.74754800
F	0.19931100	2.24290800	0.13022900
F	0.37814900	-1.23203100	-0.10764700
F	0.97187600	0.32778900	-1.50914400
F	2.17772300	-0.64991500	1.60207600
F	2.58121600	1.31721300	0.76081500
F	-2.05810300	-0.89316200	1.33682100
C	-3.90122700	-0.38898400	-0.06953500
O	-4.72977700	-0.34775100	0.85789400
C	3.35164600	-0.54309500	-0.41158600
F	3.65443000	0.27902900	-1.40413900
F	4.43343900	-0.73208300	0.33003100
F	2.96327600	-1.70798800	-0.91332800
F	-3.69294800	-1.86259000	-0.57469400
O	-4.18535700	0.28386500	-1.24903600
H	-5.13509800	0.45694700	-1.20144100

INT14
E(DMSO)[M06-2X/6-311++G(2d,p), SMD (DMSO)] = -1515.589855 a.u.
G_{corr}(DMSO)[M06-2X/6-311++G(2d,p)] = 0.033678 a.u.
H_{corr}(DMSO)[M06-2X/6-311++G(2d,p)] = 0.097949 a.u.
G = E(DMSO) + G_{corr} = -1515.556177 a.u.
H = E(DMSO) + H_{corr} = -1515.491906 a.u.

C	2.70501900	0.32680800	0.21894000
C	1.86495000	-0.67348700	-0.02175500
C	0.49724100	-0.83722700	0.59441800
C	-0.58218500	-0.05553300	-0.19099800
C	-2.00636300	-0.10933300	0.40479000
F	2.12763200	-1.64702200	-0.89470900
F	0.46933400	-0.41743900	1.87202500
F	0.15925800	-2.14117900	0.57481200
F	-0.21067900	1.23180600	-0.24390900
F	-0.61321700	-0.55246100	-1.43829600
F	-2.01421700	0.55781800	1.56551600
F	-2.36353700	-1.38068500	0.62357300
F	2.28474100	1.25984900	1.08355700
C	4.10381500	0.56548800	-0.37622600
O	4.62862800	1.62794900	-0.01492100

O	4.51261200	-0.32880100	-1.13079700
C	-3.09752800	0.52065400	-0.48954100
F	-3.24903700	-0.17003400	-1.60864300
F	-4.24414700	0.50401200	0.17792800
F	-2.79497800	1.77562600	-0.78652300

INT15
E(DMSO)[M06-2X/6-311++G(2d,p), SMD (DMSO)] = -1591.516658 a.u.
Gcorr(DMSO)[M06-2X/6-311++G(2d,p)] = 0.04802 a.u.
Hcorr(DMSO)[M06-2X/6-311++G(2d,p)] = 0.11318 a.u.
G = E(DMSO) + Gcorr= -1591.468638 a.u.
H = E(DMSO) + Hcorr= -1591.403478 a.u.

C	3.83428900	-0.87650500	-0.34675100
C	2.37243400	-0.74130000	-0.07462200
C	1.86724300	0.66121100	-0.07691400
C	0.40616100	0.80054100	0.44620700
F	2.06121400	-1.22400600	1.25499200
F	0.33695700	0.64685800	1.77997300
F	-0.00386400	2.08003100	0.19179900
O	4.50635500	-1.67151400	0.36734900
C	-0.66280600	-0.12503700	-0.17894500
F	-0.59898600	-1.34222000	0.38242900
F	-0.48107800	-0.24818300	-1.50100200
C	-2.10807400	0.40754600	0.02168900
F	-2.25937100	0.91868500	1.25138300
F	-2.35540500	1.36678000	-0.87937000
C	-3.18962500	-0.68033000	-0.15892900
F	-3.20859500	-1.50792400	0.87450400
F	-4.37775500	-0.09590400	-0.25090400
F	-2.96822500	-1.37395700	-1.26804500
F	1.77606200	1.16297600	-1.37565000
O	2.62492100	1.57608700	0.65434400
H	2.24285500	2.46222500	0.56061900
O	4.28757700	-0.22797500	-1.33319400

INT16
E(DMSO)[M06-2X/6-311++G(2d,p), SMD (DMSO)] = -1491.099371 a.u.
Gcorr(DMSO)[M06-2X/6-311++G(2d,p)] = 0.033874 a.u.
Hcorr(DMSO)[M06-2X/6-311++G(2d,p)] = 0.097175 a.u.
G = E(DMSO) + Gcorr= -1491.065497 a.u.
H = E(DMSO) + Hcorr= -1491.002196 a.u.

C	4.07695500	-0.62105900	-0.28988800
C	2.70061500	-0.25745800	0.16763400
C	1.93467000	0.85074100	-0.10257100
C	0.51044600	0.87069600	0.54916600
F	2.12065100	-1.21294100	0.99838000
F	0.47568300	0.50195200	1.85605700
F	0.02231200	2.13759800	0.51425700
O	4.53608100	-1.70783500	0.14945400
C	-0.53099500	0.01450600	-0.20283200
F	-0.38077800	-1.28446400	0.10718100
F	-0.34303300	0.15205600	-1.52764700
C	-2.00353700	0.40204700	0.08673300
F	-2.16715700	0.68936300	1.38599400
F	-2.33176900	1.47875500	-0.63930100
C	-3.00944300	-0.71519600	-0.26643500
F	-2.95893200	-1.69609000	0.62227900
F	-4.23831900	-0.21351500	-0.26811800
F	-2.74778700	-1.20598500	-1.47172600
O	2.16714600	1.86021100	-0.81321900
O	4.65551000	0.17434500	-1.06711500

INT17
E(DMSO)[M06-2X/6-311++G(2d,p), SMD (DMSO)] = -1491.597622 a.u.
Gcorr(DMSO)[M06-2X/6-311++G(2d,p)] = 0.047996 a.u.
Hcorr(DMSO)[M06-2X/6-311++G(2d,p)] = 0.111136 a.u.
G = E(DMSO) + Gcorr= -1491.549626 a.u.
H = E(DMSO) + Hcorr= -1491.486486 a.u.

C	3.11728700	-1.24329800	0.08415600
C	3.17682300	0.31914000	0.12049000
C	1.86249500	0.84142400	-0.38478800
C	0.64345900	0.82330600	0.57506500
F	4.18035100	0.82985100	-0.66832700
F	0.99691500	0.61377700	1.84892200
F	0.11533500	2.07268400	0.52115700
O	4.11174100	-1.82808200	-0.34342200
C	-0.47758900	-0.20000300	0.17674800
F	-0.60014100	-1.13317200	1.12431900
F	-0.17720900	-0.78482900	-0.99101800
C	-1.86811900	0.45574300	0.00538000
F	-2.20076300	1.10402300	1.13117700
F	-1.83199900	1.31717000	-1.01961400
C	-3.01727300	-0.53726200	-0.28479800
F	-3.21792200	-1.34695500	0.74360200

F	-4.12630000	0.16436600	-0.49067800
F	-2.76762000	-1.25933500	-1.36663300
O	1.69389900	1.30412100	-1.47601000
O	2.03128500	-1.67479800	0.51931700
H	3.34627600	0.63755900	1.15122900

INT18
E(DMSO)[M06-2X/6-311++G(2d,p), SMD (DMSO)] = -1567.555407 a.u.
Gcorr(DMSO)[M06-2X/6-311++G(2d,p)] = 0.061602 a.u.
Hcorr(DMSO)[M06-2X/6-311++G(2d,p)] = 0.126622 a.u.
G = E(DMSO) + Gcorr= -1567.493805 a.u.
H = E(DMSO) + Hcorr= -1567.428785 a.u.

C	3.81439100	-0.94764600	-0.15240000
C	2.31482300	-0.69690100	0.13811500
C	1.84972100	0.68699800	-0.37006200
C	0.38532700	0.97656300	0.13412300
F	0.29152400	1.17627700	1.47721200
F	-0.06329000	2.12621300	-0.44212400
O	4.10325600	-2.00787400	-0.73241000
C	-0.67336400	-0.10495100	-0.18127700
F	-0.55741700	-1.10934900	0.71592400
F	-0.51324300	-0.63213600	-1.40258600
C	-2.13366600	0.41441500	-0.11357800
F	-2.29829200	1.26628900	0.90829400
F	-2.42550900	1.05109500	-1.25644900
C	-3.17790200	-0.70901800	0.06641700
F	-3.15375500	-1.18184500	1.30403300
F	-4.38926200	-0.21906500	-0.17045000
F	-2.94874000	-1.70320700	-0.78215100
O	1.91384500	0.74600400	-1.67192100
O	4.60865300	-0.06783900	0.27264600
O	2.59068000	1.69746100	0.35261000
H	3.48880600	1.31107100	0.41157700
F	2.14543400	-0.82823100	1.53835500
H	1.71669400	-1.48421700	-0.31751200

INT19
E(DMSO)[M06-2X/6-311++G(2d,p), SMD (DMSO)] = -1467.574059 a.u.
Gcorr(DMSO)[M06-2X/6-311++G(2d,p)] = 0.060697 a.u.
Hcorr(DMSO)[M06-2X/6-311++G(2d,p)] = 0.122871 a.u.
G = E(DMSO) + Gcorr= -1467.513362 a.u.
H = E(DMSO) + Hcorr= -1467.451188 a.u.

C	-4.39158000	-0.01878300	-0.02004200
C	-3.03645800	0.64647400	-0.26192000
C	-1.83745500	-0.18326200	-0.04718200
C	-0.54325300	0.47127700	0.38401800
F	-0.50852300	0.58127800	1.72790500
O	-5.36051100	0.73143200	0.10984000
O	-2.23872400	0.12412500	-1.34987700
O	-1.91660400	-1.46256200	0.37357700
H	-2.92601900	-1.64612600	0.28527700
F	-0.44744100	1.71315900	-0.13369000
H	-2.99997700	1.72462200	-0.15929000
C	0.71061900	-0.31905000	-0.05651800
C	2.00095200	0.53592500	-0.05911600
C	3.29372100	-0.30888100	-0.04534600
F	0.89725600	-1.36054300	0.76769900
F	0.52051100	-0.78361500	-1.30033800
F	2.02213400	1.33005900	1.02040100
F	2.02346900	1.29479900	-1.16032500
F	3.49696900	-0.83849600	1.15065300
F	3.21440400	-1.28185600	-0.94452900
F	4.32414000	0.46922100	-0.34504900
O	-4.37660600	-1.28508800	0.04972300

INT20
E(DMSO)[M06-2X/6-311++G(2d,p), SMD (DMSO)] = -1467.587186 a.u.
Gcorr(DMSO)[M06-2X/6-311++G(2d,p)] = 0.059994 a.u.
Hcorr(DMSO)[M06-2X/6-311++G(2d,p)] = 0.12368 a.u.
G = E(DMSO) + Gcorr= -1467.527192 a.u.
H = E(DMSO) + Hcorr= -1467.463506 a.u.

C	3.07308400	1.31353300	0.06015200
C	3.13751600	-0.23789700	0.38194200
C	1.93955000	-0.86213600	-0.27754300
C	0.58833600	-0.86428400	0.48459700
F	0.64590600	-0.22955200	1.66580000
O	4.06225000	1.71560200	-0.57940100
O	4.31710100	-0.78627000	-0.10788700
O	1.93734400	-1.38904700	-1.35557300
F	0.26903400	-2.15476000	0.74008100
H	3.05658500	-0.35238300	1.46627700
C	-0.56365500	-0.26529700	-0.35870400
C	-1.77721600	0.16220200	0.49862400
C	-3.07280900	0.35083100	-0.32163600
F	-0.13003700	0.80231800	-1.03617900

F	-0.98109200	-1.18766700	-1.24278300
F	-1.50482900	1.32280700	1.10223600
F	-2.02045000	-0.77253200	1.42917900
F	-2.82990700	1.07342300	-1.40726500
F	-3.57452300	-0.81983000	-0.68301000
F	-3.96864600	0.98347200	0.42342400
O	2.07227200	1.91441500	0.46328200
H	4.73373000	-0.02605300	-0.55759000

INT21
E(DMSO)[M06-2X/6-311++G(2d,p), SMD (DMSO)] = -1278.987059 a.u.
Gcorr(DMSO)[M06-2X/6-311++G(2d,p)] = 0.048508 a.u.
Hcorr(DMSO)[M06-2X/6-311++G(2d,p)] = 0.10651 a.u.
G = E(DMSO) + Gcorr= -1278.938551 a.u.
H = E(DMSO) + Hcorr= -1278.880549 a.u.

C	3.29679600	-0.61603300	0.63189400
C	2.54643000	0.12407900	-0.21727900
C	1.21746200	0.62619000	0.29362800
F	1.14903600	0.64286400	1.65272400
F	0.97665900	1.90197500	-0.12474200
C	0.00739800	-0.21442900	-0.17304500
F	-0.01757600	-1.36086700	0.53669800
F	0.12849300	-0.53408600	-1.46916000
C	-1.36244100	0.48873000	-0.00513300
F	-1.40690500	1.17209900	1.14732400
F	-1.53942700	1.34437400	-1.02100600
C	-2.56100600	-0.48346300	-0.00638500
F	-2.61500900	-1.16605400	1.12761200
F	-3.68529900	0.21004900	-0.13414500
F	-2.46602600	-1.33349400	-1.02117500
O	2.86604200	0.39116600	-1.43682600
H	3.06887100	-0.86177000	1.65684800
O	4.48885200	-1.11380300	0.15207000
H	4.50863800	-0.79932400	-0.76804100

INT22
E(DMSO)[M06-2X/6-311++G(2d,p), SMD (DMSO)] = -1278.452041 a.u.
Gcorr(DMSO)[M06-2X/6-311++G(2d,p)] = 0.034676 a.u.
Hcorr(DMSO)[M06-2X/6-311++G(2d,p)] = 0.09191 a.u.
G = E(DMSO) + Gcorr= -1278.417365 a.u.
H = E(DMSO) + Hcorr= -1278.360131 a.u.

C	-3.47200100	0.71588600	-0.34947000
C	-2.63850400	-0.39147100	-0.33749100
C	-1.37728800	-0.35013200	0.45943800
F	-1.37019800	0.52615500	1.50664900
F	-1.08699100	-1.58351900	1.03234100
C	-0.09353300	-0.00449800	-0.34368100
F	-0.06833500	1.32950100	-0.57047800
F	-0.08748400	-0.61244600	-1.54201200
C	1.24562500	-0.38150700	0.33944700
F	1.20179600	-0.13898300	1.65894000
F	1.48448100	-1.68938900	0.15305900
C	2.46807800	0.38286100	-0.21132900
F	2.46431800	1.64346700	0.19918100
F	3.58322000	-0.19316100	0.22733600
F	2.47692800	0.36065000	-1.53885200
O	-2.79462400	-1.51054000	-1.04549700
H	-4.34094200	0.51627500	-1.02267500
O	-3.43449000	1.87009200	0.23871200

INT23
E(DMSO)[M06-2X/6-311++G(2d,p), SMD (DMSO)] = -1178.525239 a.u.
Gcorr(DMSO)[M06-2X/6-311++G(2d,p)] = 0.031733 a.u.
Hcorr(DMSO)[M06-2X/6-311++G(2d,p)] = 0.089049 a.u.
G = E(DMSO) + Gcorr= -1178.493506 a.u.
H = E(DMSO) + Hcorr= -1178.43619 a.u.

C	-3.79077200	-0.02941600	0.25801200
C	-2.42290900	-0.65695500	0.02963400
C	-1.42795700	0.14533100	-0.46716400
F	-1.65365700	1.48253600	-0.70183000
C	-0.02043600	-0.20822400	-0.70884400
F	0.46123100	0.43659400	-1.81883800
F	0.14054400	-1.53342100	-0.90840900
C	0.93910800	0.18200000	0.44128300
F	0.74406000	1.47612400	0.75345000
F	0.63997900	-0.56757600	1.51522800
C	2.44809700	0.01362300	0.18292800
F	2.87402800	0.86949900	-0.73622800
F	3.11382800	0.25173500	1.31107800
F	2.72953000	-1.22086500	-0.21444500
O	-2.38547100	-1.87871100	0.33370400
H	-4.61336300	-0.72870500	0.01362500
O	-4.01244600	1.04107700	0.76269900

INT24
E(DMSO)[M06-2X/6-311++G(2d,p), SMD (DMSO)] = -1078.514592 a.u.
Gcorr(DMSO)[M06-2X/6-311++G(2d,p)] = 0.031303 a.u.
Hcorr(DMSO)[M06-2X/6-311++G(2d,p)] = 0.086442 a.u.
G = E(DMSO) + Gcorr= -1078.483289 a.u.
H = E(DMSO) + Hcorr= -1078.42815 a.u.

C	-3.60886800	0.59723200	-0.15617100
C	-2.55426600	-0.50593700	-0.02749800
C	-1.17792000	-0.10845400	0.38064000
F	-1.08161500	1.03217000	1.05837500
C	-0.07952100	-0.80558400	0.11532900
F	-0.12082900	-1.92242000	-0.58703500
C	1.32241600	-0.40559100	0.51655200
F	1.32840100	0.19606600	1.71474700
F	2.09292800	-1.50193400	0.57822200
C	1.98091500	0.56153800	-0.48373600
F	1.28756100	1.69060100	-0.54322500
F	3.21862300	0.83579000	-0.09968700
F	2.01499200	0.00854000	-1.68925600
O	-2.85214700	-1.63480600	-0.30889000
H	-4.64614600	0.23953900	-0.06005900
O	-3.31172100	1.72379600	-0.42859600

INT25
E(DMSO)[M06-2X/6-311++G(2d,p), SMD (DMSO)] = -1154.485333 a.u.
Gcorr(DMSO)[M06-2X/6-311++G(2d,p)] = 0.043074 a.u.
Hcorr(DMSO)[M06-2X/6-311++G(2d,p)] = 0.101363 a.u.
G = E(DMSO) + Gcorr= -1154.442259 a.u.
H = E(DMSO) + Hcorr= -1154.38397 a.u.

C	-3.16714100	0.84937700	-0.01711700
C	-2.40427600	-0.44176800	0.31226200
C	-0.98563300	-0.39667500	-0.28877200
F	-0.65545300	-1.35176900	-1.16505600
C	-0.04925400	0.47975700	0.03988400
F	-0.29276800	1.43552300	0.94831000
C	1.36505000	0.50825400	-0.45628600
F	1.45830100	0.10829200	-1.73872000
F	1.85514400	1.76247300	-0.37122400
C	2.31541700	-0.38771400	0.35369700
F	1.94693900	-1.65883200	0.24730100
F	3.56241100	-0.26980700	-0.08909000

F	2.28566600	-0.03749300	1.63538900
O	-2.40556000	-0.62804300	1.60849500
H	-4.16960000	0.84167600	0.45559300
O	-2.76804200	1.80261500	-0.63553500
O	-3.11999100	-1.46513500	-0.42290000
H	-3.36880300	-2.08002400	0.27971900

INT26
E(DMSO)[M06-2X/6-311++G(2d,p), SMD (DMSO)] = -1153.957796 a.u.
Gcorr(DMSO)[M06-2X/6-311++G(2d,p)] = 0.033008 a.u.
Hcorr(DMSO)[M06-2X/6-311++G(2d,p)] = 0.087809 a.u.
G = E(DMSO) + Gcorr= -1153.924788 a.u.
H = E(DMSO) + Hcorr= -1153.869987 a.u.

C	-3.14643200	0.81602800	0.22506300
C	-2.46337900	-0.54939300	0.27118500
C	-1.02492500	-0.43718100	-0.31853800
F	-0.64428700	-1.48333600	-1.07481700
C	-0.08362300	0.47442300	-0.09113300
F	-0.31766700	1.51042300	0.74779000
C	1.33949400	0.44780900	-0.53588500
F	1.49321200	-0.12891900	-1.74645400
F	1.83271500	1.70824400	-0.61567900
C	2.27350800	-0.30922000	0.42123900
F	1.93310300	-1.59218000	0.47735400
F	3.54001100	-0.22994600	0.01839300
F	2.19062000	0.20836300	1.64405000
O	-2.30819100	-0.98047600	1.54036300
H	-4.06690200	0.79156200	0.85296500
O	-2.88557800	1.80644300	-0.42971600
O	-3.25002100	-1.24849100	-0.57818100

INT27
E(DMSO)[M06-2X/6-311++G(2d,p), SMD (DMSO)] = -1591.544297 a.u.
Gcorr(DMSO)[M06-2X/6-311++G(2d,p)] = 0.047579 a.u.
Hcorr(DMSO)[M06-2X/6-311++G(2d,p)] = 0.11277 a.u.
G = E(DMSO) + Gcorr= -1591.496718 a.u.
H = E(DMSO) + Hcorr= -1591.431527 a.u.

C	-4.16901800	0.53002200	0.00554600
C	-2.86342700	-0.30610500	0.28145800
C	-1.59549500	0.49333300	0.11952000
C	-0.39749600	-0.35389400	-0.01816200

F	-2.95170600	-0.69546600	1.64800800
F	-0.36135500	-1.28976800	0.96902500
F	-0.24789000	-1.07129000	-1.21391800
O	-4.32144600	1.59191000	0.61788900
C	0.93509900	0.42862700	0.08749100
F	1.12303300	0.80990200	1.36856800
F	0.89113400	1.53945600	-0.66903900
C	2.19552400	-0.35891800	-0.34998200
F	2.12627000	-1.63625500	0.05399300
F	2.29706400	-0.33386300	-1.68652600
C	3.51180100	0.21962300	0.21362000
F	3.63611000	-0.04937600	1.50509800
F	4.53857900	-0.32775900	-0.42704900
F	3.55523400	1.53488500	0.03840100
F	-1.72969000	1.15929600	-1.15198400
O	-2.94009400	-1.47061200	-0.45707500
H	-3.83934800	-1.40697600	-0.84557600
O	-4.95766300	-0.02967300	-0.79863600

INT28
E(DMSO)[M06-2X/6-311++G(2d,p), SMD (DMSO)] = -1491.588193 a.u.
Gcorr(DMSO)[M06-2X/6-311++G(2d,p)] = 0.046879 a.u.
Hcorr(DMSO)[M06-2X/6-311++G(2d,p)] = 0.110902 a.u.
G = E(DMSO) + Gcorr= -1491.541314 a.u.
H = E(DMSO) + Hcorr= -1491.477291 a.u.

C	3.88036100	-0.31423500	0.58217600
C	2.82325000	0.03112100	-0.53684500
C	1.42146000	-0.13014900	-0.02556300
C	0.43294000	0.74589800	0.05331100
F	3.00408100	1.36660800	-0.87697300
F	0.54173100	1.99342600	-0.40502100
O	3.70075800	0.21608900	1.67993900
C	-0.93721200	0.46267100	0.61577500
F	-1.46673600	1.61056900	1.07820100
F	-0.88158900	-0.41828100	1.62786600
C	-1.89159900	-0.10239300	-0.45561600
F	-1.93229500	0.76440100	-1.47853100
F	-1.39571400	-1.26976600	-0.88839000
C	-3.34249000	-0.35936000	-0.00546200
F	-3.92266500	0.76506100	0.38586000
F	-4.02288100	-0.85271100	-1.03345800
F	-3.37691500	-1.23676700	0.98643800
F	1.20997600	-1.37444300	0.40959100
O	3.02004500	-0.75737600	-1.62546800

H	3.88055200	-1.18855700	-1.42163200
O	4.77747800	-1.07691800	0.17112100

INT29
E(DMSO)[M06-2X/6-311++G(2d,p), SMD (DMSO)] = -1491.08802 a.u.
Gcorr(DMSO)[M06-2X/6-311++G(2d,p)] = 0.032457 a.u.
Hcorr(DMSO)[M06-2X/6-311++G(2d,p)] = 0.096837 a.u.
G = E(DMSO) + Gcorr= -1491.055563 a.u.
H = E(DMSO) + Hcorr= -1490.991183 a.u.

C	3.95028000	-0.51309400	0.31135500
C	2.87091000	0.11907300	-0.63611500
C	1.47203700	-0.17315500	-0.06912700
C	0.48130800	0.59247100	0.37229800
F	3.04232200	1.63124500	-0.23526000
F	0.58037600	1.92844700	0.49670500
O	3.51875400	-0.88419500	1.42912400
C	-0.89381300	0.12017900	0.75007300
F	-1.41662600	0.95419900	1.67730700
F	-0.88248100	-1.12029800	1.27384500
C	-1.86191900	0.10851600	-0.45043600
F	-1.87004500	1.33467900	-0.99838000
F	-1.40760900	-0.77074600	-1.35519400
C	-3.32581600	-0.26507700	-0.15064100
F	-3.87978100	0.60667800	0.67931400
F	-4.01002500	-0.25465900	-1.29018300
F	-3.40547200	-1.47867100	0.37647200
F	1.18668300	-1.48052600	-0.19865500
O	2.91866300	-0.04177800	-1.88160600
O	5.11333300	-0.58485200	-0.12228900

INT30
E(DMSO)[M06-2X/6-311++G(2d,p), SMD (DMSO)] = -1326.96338 a.u.
G_{corr}(DMSO)[M06-2X/6-311++G(2d,p)] = 0.022378 a.u.
H_{corr}(DMSO)[M06-2X/6-311++G(2d,p)] = 0.080251 a.u.
G = E(DMSO) + G_{corr} = -1326.941002 a.u.
H = E(DMSO) + H_{corr} = -1326.883129 a.u.

C	-3.47176500	0.74020000	-0.51052300
C	-2.60354900	-0.25360200	-0.31438500
C	-1.34945800	-0.34381400	0.48991800
C	-0.08346500	0.01459200	-0.32123200
C	1.25065800	-0.39262300	0.34775400

F	-2.80126700	-1.42900600	-0.99688700
F	-1.15679600	-1.60941400	0.95531700
F	-1.38210000	0.47618500	1.55954400
F	-0.14146100	-0.60195000	-1.51316700
F	-0.07602400	1.34202600	-0.53190000
F	1.45289200	-1.70182000	0.15415300
F	1.20335000	-0.15196600	1.66476000
F	-3.09910200	1.87979000	0.21170900
C	2.47490500	0.35763100	-0.21929600
F	3.58377000	-0.23441400	0.20247800
F	2.45315800	0.33270200	-1.54592600
F	2.48536200	1.61627800	0.19176200

INT31
E(DMSO)[M06-2X/6-311++G(2d,p), SMD (DMSO)] = -1327.4713 a.u.
G_{corr}(DMSO)[M06-2X/6-311++G(2d,p)] = 0.035704 a.u.
H_{corr}(DMSO)[M06-2X/6-311++G(2d,p)] = 0.094259 a.u.
G = E(DMSO) + G_{corr} = -1327.435596 a.u.
H = E(DMSO) + H_{corr} = -1327.377041 a.u.

C	-3.30856900	0.76929600	-0.47225000
C	-2.55846500	-0.30643600	-0.33208800
C	-1.32015600	-0.43751500	0.51244400
C	-0.05651000	-0.01923700	-0.27519600
C	1.27927700	-0.14274100	0.48879400
F	-2.85260300	-1.41748400	-1.01471800
F	-1.17934700	-1.71790300	0.89734700
F	-1.40856000	0.33566800	1.60721200
F	0.00376500	-0.78600500	-1.37504200
F	-0.21391700	1.26235500	-0.63862100
F	1.44367600	-1.40620900	0.89846300
F	1.25029400	0.66997500	1.55188900
F	-3.01521300	1.89668500	0.16959800
H	-4.18737200	0.81050400	-1.10273400
C	2.53117700	0.23125800	-0.33760900
F	3.59544700	0.10352600	0.44395900
F	2.66837900	-0.57681500	-1.37751900
F	2.46217200	1.48306700	-0.76277200

INT32
E(DMSO)[M06-2X/6-311++G(2d,p), SMD (DMSO)] = -1403.431621 a.u.
G_{corr}(DMSO)[M06-2X/6-311++G(2d,p)] = 0.048638 a.u.
H_{corr}(DMSO)[M06-2X/6-311++G(2d,p)] = 0.109148 a.u.
G = E(DMSO) + G_{corr} = -1403.382983 a.u.

H = E(DMSO) + H_{corr} = -1403.322473 a.u.

C	3.23094800	-0.17918300	-0.45600100
C	2.36769500	0.80003500	0.21252300
C	1.08532500	0.33852100	0.76426400
C	-0.17469600	0.41359200	-0.15051300
C	-1.35320600	-0.47392700	0.32100700
F	2.05683900	1.83180100	-0.73397300
F	0.69048000	1.08448900	1.87364700
F	1.17120600	-0.94237300	1.21531300
F	-0.61928600	1.68607300	-0.21488700
F	0.12311000	0.01803000	-1.39738200
F	-1.50715200	-0.40616800	1.65096200
F	-1.10543400	-1.74710500	-0.01928600
F	2.55796800	-1.06136900	-1.41280400
H	3.93494100	0.35039400	-1.10209100
O	3.85449200	-1.02984300	0.43306900
H	4.42331700	-1.62160400	-0.07584600
C	-2.70980500	-0.08687200	-0.30799100
F	-3.58857900	-1.05441300	-0.07310600
F	-2.59201800	0.07040400	-1.62026900
F	-3.17288600	1.03584900	0.22218900

INT33
E(DMSO)[M06-2X/6-311++G(2d,p), SMD (DMSO)] = -1303.465409 a.u.
G_{corr}(DMSO)[M06-2X/6-311++G(2d,p)] = 0.048309 a.u.
H_{corr}(DMSO)[M06-2X/6-311++G(2d,p)] = 0.10697 a.u.
G = E(DMSO) + G_{corr} = -1303.4171 a.u.
H = E(DMSO) + H_{corr} = -1303.358439 a.u.

C	-3.40871400	-0.65293200	-0.39597500
C	-2.53699300	0.34132200	-0.29137500
C	-1.27936100	0.38674600	0.51217200
C	-0.03129400	0.00458900	-0.31659300
C	1.31392300	0.37320800	0.35221800
F	-2.72723200	1.46647400	-1.01184800
F	-1.34931900	-0.45193400	1.55847400
F	-1.07282600	1.63952200	0.98270100
F	-0.06547800	-1.31898300	-0.53751100
F	-0.09106200	0.63557900	-1.49913900
F	1.25931200	0.11659100	1.66538500
F	1.54238200	1.67902000	0.17334400
H	-4.26866700	-0.51585900	-1.04424100
O	-3.27544900	-1.81968500	0.25437800

H	-4.02904200	-2.38668700	0.04402400
C	2.51652400	-0.40021000	-0.23048400
F	2.48428200	-0.35876100	-1.55640400
F	2.49676900	-1.66299400	0.16613400
F	3.64059200	0.16034100	0.19057800

INT34
E(DMSO)[M06-2X/6-311++G(2d,p), SMD (DMSO)] = -1302.996352 a.u.
G_{corr}(DMSO)[M06-2X/6-311++G(2d,p)] = 0.034948 a.u.
H_{corr}(DMSO)[M06-2X/6-311++G(2d,p)] = 0.092916 a.u.
G = E(DMSO) + G_{corr} = -1302.961404 a.u.
H = E(DMSO) + H_{corr} = -1302.903436 a.u.

C	-3.48302800	-0.73685300	-0.35404800
C	-2.58296400	0.29816900	-0.22843400
C	-1.32557300	0.34561300	0.51433100
C	-0.05677500	0.00747700	-0.31178700
C	1.29139800	0.36593000	0.35740600
F	-2.72913600	1.39515600	-1.06605100
F	-1.33915900	-0.51386400	1.55660700
F	-1.07728000	1.60540700	1.01884000
F	-0.06276500	-1.31290300	-0.57655400
F	-0.10526000	0.66658500	-1.48327700
F	1.25202600	0.09272500	1.66930200
F	1.52657200	1.67528200	0.19719300
H	-4.28016000	-0.48121700	-1.08416300
O	-3.51576300	-1.84468500	0.22785400
C	2.49632700	-0.39489300	-0.23559600
F	2.46592500	-0.34148800	-1.56175300
F	3.62187700	0.16552400	0.18817100
F	2.48830500	-1.66286300	0.14753300

INT35
E(DMSO)[M06-2X/6-311++G(2d,p), SMD (DMSO)] = -1202.995254 a.u.
G_{corr}(DMSO)[M06-2X/6-311++G(2d,p)] = 0.033674 a.u.
H_{corr}(DMSO)[M06-2X/6-311++G(2d,p)] = 0.090349 a.u.
G = E(DMSO) + G_{corr} = -1202.96158 a.u.
H = E(DMSO) + H_{corr} = -1202.904905 a.u.

C	-3.71295900	-0.41482400	0.38207300
C	-2.30535500	-0.56888300	-0.07131200
C	-1.42550000	0.40661800	-0.26240500
C	0.00661000	0.22778200	-0.71423000

C	0.94886200	-0.01483100	0.48337200
F	-1.94384800	-1.83419500	-0.28379700
F	-1.73769300	1.66942800	-0.02882200
F	0.11790300	-0.81062500	-1.55465500
F	0.40535100	1.34295400	-1.34708100
F	0.60694100	-1.17816700	1.05209400
F	0.76838600	0.97797800	1.36587400
H	-4.24939400	-1.37257100	0.47379900
O	-4.21719700	0.64701400	0.62494500
C	2.45312900	-0.07738100	0.15261900
F	2.69582600	-1.02202800	-0.74323200
F	2.87796000	1.08718000	-0.31250400
F	3.12009000	-0.36079600	1.26389400

INT36
E(DMSO)[M06-2X/6-311++G(2d,p), SMD (DMSO)] = -1278.950611 a.u.
G_{corr}(DMSO)[M06-2X/6-311++G(2d,p)] = 0.04664 a.u.
H_{corr}(DMSO)[M06-2X/6-311++G(2d,p)] = 0.105728 a.u.
G = E(DMSO) + G_{corr} = -1278.903971 a.u.
H = E(DMSO) + H_{corr} = -1278.844883 a.u.

C	-3.48659200	-0.14403000	0.58515000
C	-2.05037400	-0.37155300	0.09002000
C	-1.11431800	0.50067000	-0.26249800
C	0.28168000	0.16408600	-0.71242200
C	1.26133900	0.04565000	0.47353300
F	-1.70526100	-1.67286500	0.04225200
F	-1.29964600	1.82637500	-0.20949700
F	0.32720300	-0.99374000	-1.39619900
F	0.74012600	1.14354600	-1.52253300
F	0.89210500	-1.00361700	1.22192200
F	1.16872400	1.16317200	1.21240000
H	-3.56529800	-0.82406700	1.46723500
O	-3.82564600	1.09449100	0.76500500
O	-4.30121300	-0.85080900	-0.42027300
H	-4.61435600	-0.11845700	-0.96665800
C	2.74907200	-0.14479300	0.12045200
F	2.92167900	-1.22040400	-0.63476500
F	3.22306200	0.91506500	-0.51762500
F	3.43753000	-0.30276600	1.24584000

INT37
E(DMSO)[M06-2X/6-311++G(2d,p), SMD (DMSO)] = -1278.999481 a.u.
G_{corr}(DMSO)[M06-2X/6-311++G(2d,p)] = 0.046262 a.u.

H_{corr}(DMSO)[M06-2X/6-311++G(2d,p)] = 0.103647 a.u.
G = E(DMSO) + G_{corr} = -1278.953219 a.u.
H = E(DMSO) + H_{corr} = -1278.895834 a.u.

C	3.38311700	0.90695200	-0.38062200
C	2.11874800	0.83336200	0.08547800
C	1.43628100	-0.45980800	0.31714800
C	0.00936900	-0.57368500	-0.31216900
C	-1.18327600	-0.03874800	0.51943400
F	1.40650600	1.97619900	0.33493400
F	1.13988700	-0.61794200	1.71997200
F	0.00157600	0.06360800	-1.50711100
F	-0.27212400	-1.86810400	-0.55658400
F	-0.88022300	1.09633100	1.15962500
F	-1.53750800	-0.96149200	1.42696400
H	3.80567200	1.90518500	-0.53919600
O	4.11099300	-0.13595900	-0.64946300
O	2.18858900	-1.47879400	-0.10352700
H	3.15837500	-1.05137600	-0.37695200
C	-2.43622000	0.25632500	-0.33493400
F	-3.47948600	0.43628900	0.46771000
F	-2.27044200	1.35736900	-1.05434000
F	-2.70027600	-0.75805500	-1.14960800

INT38
E(DMSO)[M06-2X/6-311++G(2d,p), SMD (DMSO)] = -1178.543293 a.u.
G_{corr}(DMSO)[M06-2X/6-311++G(2d,p)] = 0.033347 a.u.
H_{corr}(DMSO)[M06-2X/6-311++G(2d,p)] = 0.089702 a.u.
G = E(DMSO) + G_{corr} = -1178.509946 a.u.
H = E(DMSO) + H_{corr} = -1178.453591 a.u.

C	-3.66129800	-0.57836500	0.26114100
C	-2.30493500	-0.48179700	-0.13625900
C	-1.48688900	0.64841900	-0.14286100
C	-0.01537500	0.46064100	-0.62982400
C	0.90728600	-0.09181400	0.47122700
F	-1.76778500	-1.68361500	-0.55937300
F	0.08888400	-0.34511100	-1.71129000
F	0.48249900	1.66221500	-0.98769100
F	0.53117500	-1.33903700	0.79023600
F	0.78785000	0.68611100	1.56055900
H	-4.05257600	-1.61104900	0.15905500
O	-4.39266300	0.31528200	0.67977900

O	-1.78242900	1.79328500	0.20687600
C	2.40942900	-0.15415200	0.13047800
F	2.62037700	-0.89463500	-0.94934100
F	2.90755900	1.05722900	-0.07086500
F	3.05655300	-0.70705400	1.15268700

INT39
E(DMSO)[M06-2X/6-311++G(2d,p), SMD (DMSO)] = -1254.450677 a.u.
G_{corr}(DMSO)[M06-2X/6-311++G(2d,p)] = 0.046842 a.u.
H_{corr}(DMSO)[M06-2X/6-311++G(2d,p)] = 0.104407 a.u.
G = E(DMSO) + G_{corr} = -1254.403835 a.u.
H = E(DMSO) + H_{corr} = -1254.34627 a.u.

C	-3.60472400	0.20469600	-0.31570100
C	-2.26286100	0.11700700	-0.55118000
C	-1.13388700	-0.71751300	-0.00605600
C	-0.09929200	0.26748100	0.76418600
C	1.20180500	0.70014200	0.05867100
F	-1.77125100	1.12676800	-1.41133900
F	-0.69434200	1.44366600	1.13009100
F	0.31340300	-0.29004200	1.93284000
F	0.93484400	1.35813800	-1.07630100
F	1.82633700	1.58993400	0.87528100
H	-4.03316800	1.03943000	-0.92086000
O	-4.40896600	-0.45899100	0.41411900
O	-1.44925200	-1.72750000	0.73321000
O	-0.29903800	-1.12504500	-1.17772100
H	-0.24291000	-2.07464400	-1.01635300
C	2.24590600	-0.42700200	-0.24917300
F	3.44517800	-0.06928500	0.22493600
F	1.93979700	-1.58574400	0.31962900
F	2.38963800	-0.61136400	-1.55337500

INT40
E(DMSO)[M06-2X/6-311++G(2d,p), SMD (DMSO)] = -1254.44469 a.u.
G_{corr}(DMSO)[M06-2X/6-311++G(2d,p)] = 0.045437 a.u.
H_{corr}(DMSO)[M06-2X/6-311++G(2d,p)] = 0.10404 a.u.
G = E(DMSO) + G_{corr} = -1254.399253 a.u.
H = E(DMSO) + H_{corr} = -1254.34065 a.u.

C	-3.47237900	-0.76819300	0.18740600
C	-2.15173700	-0.55488300	-0.47439400
C	-1.47766400	0.72081500	0.21940100

C	0.06222600	0.69941300	-0.29405000
C	1.12831800	-0.03062400	0.55787600
F	-1.43279200	-1.75887200	-0.26905300
F	0.20256300	0.20119000	-1.57655600
F	0.54060600	1.97584300	-0.36784900
F	0.72886100	-1.22041900	1.03209900
F	1.48899600	0.73952400	1.60524900
H	-3.41041500	-1.33381400	1.13432700
O	-4.53788000	-0.38306500	-0.22984500
O	-1.44382700	0.57386600	1.54789600
O	-2.06421500	1.77510000	-0.33605900
H	-2.24518300	-0.42283300	-1.55058200
C	2.44210500	-0.33513000	-0.19958300
F	2.28489500	-1.32838700	-1.06945800
F	2.89831600	0.73043100	-0.85117200
F	3.38164100	-0.71252600	0.67233900

INT41
E(DMSO)[M06-2X/6-311++G(2d,p), SMD (DMSO)] = -1839.732628 a.u.
G_{corr}(DMSO)[M06-2X/6-311++G(2d,p)] = 0.039458 a.u.
H_{corr}(DMSO)[M06-2X/6-311++G(2d,p)] = 0.10878 a.u.
G = E(DMSO) + G_{corr} = -1839.69317 a.u.
H = E(DMSO) + H_{corr} = -1839.623848 a.u.

C	-4.02391400	-0.36619900	-0.10673400
C	-2.73116200	0.20918900	0.51308300
C	-1.48464300	0.00459000	-0.38299400
C	-0.16059400	0.12977000	0.41085200
C	1.07731200	0.40503200	-0.47282000
F	-4.12355500	0.00379200	-1.37677700
F	-4.02755600	-1.68768300	-0.03658000
F	-5.06893300	0.09943600	0.56085000
F	-2.54126700	-0.38823900	1.69635500
F	-2.91452700	1.51859000	0.70730000
F	-1.54507100	-1.21697000	-0.93243800
F	-1.52214200	0.91663700	-1.36209500
F	0.02387500	-1.01599600	1.07877900
F	-0.28227300	1.13132600	1.29787600
F	0.99834600	-0.41559300	-1.54983600
F	0.98036600	1.66406400	-0.95231100
O	2.16705200	0.21067300	0.26021900
C	3.40284000	0.53199500	-0.43922400
F	3.86334700	1.68585900	0.25162000
C	4.32659600	-0.53868600	0.06359000
F	5.58630100	-0.31234400	-0.34985000

F	4.41211500	-0.67473800	1.41270200
F	3.96374900	-1.74586600	-0.40073600

INT42
E(DMSO)[M06-2X/6-311++G(2d,p), SMD (DMSO)] = -1739.723881 a.u.
G_{corr}(DMSO)[M06-2X/6-311++G(2d,p)] = 0.039301 a.u.
H_{corr}(DMSO)[M06-2X/6-311++G(2d,p)] = 0.107161 a.u.
G = E(DMSO) + G_{corr} = -1739.68458 a.u.
H = E(DMSO) + H_{corr} = -1739.61672 a.u.

C	3.79938800	0.13085900	-0.25179500
C	2.48718100	-0.49056800	0.27556200
C	1.22154800	0.22190400	-0.26101000
C	-0.03010400	-0.08038200	0.60177400
C	-1.35431500	0.20231500	-0.13915000
F	3.72098200	0.30493400	-1.56460000
F	4.02891700	1.29636100	0.33020000
F	4.80423400	-0.68775700	0.01654100
F	2.50290500	-0.42537900	1.61264400
F	2.45387300	-1.77059200	-0.10298500
F	1.42911700	1.54450100	-0.26150200
F	1.00820800	-0.18059300	-1.51891900
F	0.01811100	0.68201600	1.69672800
F	-0.02137200	-1.37005000	0.96150700
F	-1.28992700	1.40095200	-0.72961200
F	-1.54745000	-0.70981800	-1.09285200
O	-2.36018100	0.15486900	0.79000800
C	-3.59704400	0.44953600	0.31277300
F	-3.93042400	1.72884600	0.37281400
C	-4.43939100	-0.46460800	-0.11861500
F	-4.15136700	-1.73783500	-0.18310800
F	-5.65271200	-0.19261700	-0.51877800

INT43
E(DMSO)[M06-2X/6-311++G(2d,p), SMD (DMSO)] = -1815.715991 a.u.
G_{corr}(DMSO)[M06-2X/6-311++G(2d,p)] = 0.051117 a.u.
H_{corr}(DMSO)[M06-2X/6-311++G(2d,p)] = 0.121299 a.u.
G = E(DMSO) + G_{corr} = -1815.664874 a.u.
H = E(DMSO) + H_{corr} = -1815.594692 a.u.

C	-4.02018400	-0.36665900	-0.10709300
C	-2.72612500	0.20164600	0.51673900
C	-1.48238600	0.01048900	-0.38612400
C	-0.15583000	0.12476700	0.40507800

C	1.07867200	0.41538000	-0.47908100
F	-4.12242400	0.01836100	-1.37242900
F	-4.02324200	-1.68888500	-0.05272500
F	-5.06395900	0.09070300	0.56801400
F	-2.53152000	-0.41187600	1.69103500
F	-2.90983800	1.50802800	0.72968600
F	-1.54404600	-1.20297100	-0.95292900
F	-1.52258200	0.93660400	-1.35176000
F	0.03346100	-1.03111900	1.05429500
F	-0.27480000	1.11171000	1.30866000
F	0.99362500	-0.38371600	-1.57108400
F	0.98214600	1.68371000	-0.93226700
O	2.17268100	0.20528200	0.24178900
C	3.42406600	0.53309500	-0.45652800
F	3.85440400	1.68868200	0.25793600
C	4.33360000	-0.54853800	0.09657500
F	5.61274800	-0.29826300	-0.28892000
F	4.00565500	-1.73451600	-0.51240600
O	4.37213100	-0.74682700	1.44218100
H	3.52398700	-0.46679700	1.81489000

INT44
E(DMSO)[M06-2X/6-311++G(2d,p), SMD (DMSO)] = -1715.718778 a.u.
G_{corr}(DMSO)[M06-2X/6-311++G(2d,p)] = 0.050346 a.u.
H_{corr}(DMSO)[M06-2X/6-311++G(2d,p)] = 0.119337 a.u.
G = E(DMSO) + G_{corr} = -1715.668432 a.u.
H = E(DMSO) + H_{corr} = -1715.599441 a.u.

C	-3.76904300	0.40779900	0.17837300
C	-2.53593100	-0.42270200	-0.24184500
C	-1.19977400	0.18635200	0.24792000
C	0.01797000	-0.36809300	-0.53345600
C	1.35443600	-0.17463000	0.21357200
F	-3.68388400	0.72677700	1.46322600
F	-3.85049700	1.51511000	-0.54085100
F	-4.86234100	-0.31222300	-0.01756400
F	-2.52441600	-0.50476200	-1.57798900
F	-2.66512600	-1.64775800	0.27334500
F	-1.23808400	1.51509800	0.08854400
F	-1.05915900	-0.08802200	1.54985900
F	0.08958100	0.26478100	-1.70747000
F	-0.15077600	-1.67871900	-0.74823000
F	1.42425900	1.08178600	0.68037300
F	1.41843400	-0.99771800	1.26005900
O	2.36434900	-0.41826000	-0.67645400

C	3.61488600	-0.45453600	-0.12513400
F	3.99357500	-1.65328000	0.30897400
C	4.42175200	0.59232700	-0.10502700
F	5.64216900	0.46667800	0.37803800
O	4.19317200	1.83065900	-0.52140800
H	3.31044600	1.91197500	-0.91635600

INT45
E(DMSO)[M06-2X/6-311++G(2d,p), SMD (DMSO)] = -1791.697331 a.u.
G_{corr}(DMSO)[M06-2X/6-311++G(2d,p)] = 0.062912 a.u.
H_{corr}(DMSO)[M06-2X/6-311++G(2d,p)] = 0.134013 a.u.
G = E(DMSO) + G_{corr} = -1791.634419 a.u.
H = E(DMSO) + H_{corr} = -1791.563318 a.u.

C	-4.03339000	-0.34353900	-0.09695600
C	-2.73181900	0.21887000	0.51640100
C	-1.49103500	-0.00272800	-0.38368100
C	-0.16203100	0.11073900	0.40368400
C	1.07678300	0.36818300	-0.48430700
F	-4.13481800	0.02552400	-1.36717700
F	-4.05125400	-1.66487800	-0.02478600
F	-5.07051300	0.13428400	0.57445000
F	-2.54500600	-0.37704200	1.70091900
F	-2.89998600	1.53090100	0.70750800
F	-1.56822700	-1.22585100	-0.92806400
F	-1.52414800	0.90568100	-1.36646800
F	0.01036200	-1.03429500	1.07653100
F	-0.27049400	1.11735300	1.28737700
F	0.97987900	-0.45933500	-1.55894200
F	0.98465700	1.62537200	-0.97492600
O	2.16496300	0.16671000	0.24220300
C	3.40258300	0.47397000	-0.46257200
F	3.82517200	1.68489600	0.18517000
C	4.37883900	-0.55519800	0.06969900
F	4.26734800	-0.72490500	1.46163000
O	5.68127200	-0.18819600	-0.17124100
H	5.75307800	0.75879800	0.01469300
O	4.14325000	-1.79813900	-0.45388600
H	3.66472000	-1.66292000	-1.28390500

INT46
E(DMSO)[M06-2X/6-311++G(2d,p), SMD (DMSO)] = -1691.712462 a.u.
G_{corr}(DMSO)[M06-2X/6-311++G(2d,p)] = 0.062661 a.u.
H_{corr}(DMSO)[M06-2X/6-311++G(2d,p)] = 0.1321 a.u.

$G = E(DMSO) + G_{corr} = -1691.649801$ a.u.
$H = E(DMSO) + H_{corr} = -1691.580362$ a.u.

C	-3.77387500	0.41451300	0.18292700
C	-2.54372200	-0.41710300	-0.24333300
C	-1.20493400	0.18445400	0.24871900
C	0.01082200	-0.36656300	-0.53788100
C	1.34928000	-0.18335200	0.20828300
F	-3.68783200	0.72474000	1.46992600
F	-3.85263700	1.52690300	-0.52884900
F	-4.86982500	-0.30068800	-0.01730700
F	-2.53559600	-0.49196800	-1.57999600
F	-2.67723400	-1.64481200	0.26518200
F	-1.24195800	1.51490100	0.10011500
F	-1.06626900	-0.09985100	1.54903400
F	0.07791600	0.27431700	-1.70829400
F	-0.16602400	-1.67556400	-0.76384500
F	1.41072400	1.06149600	0.70090600
F	1.40310200	-1.02479400	1.24805100
O	2.35267000	-0.42524200	-0.67999000
C	3.60511500	-0.43794800	-0.13508900
F	4.00405100	-1.64938000	0.28861600
C	4.43767100	0.59425400	-0.11525200
O	5.68293400	0.54504000	0.38310000
H	5.83475900	-0.29820000	0.83765800
O	4.10156200	1.77480400	-0.64176700
H	4.60001800	2.47416600	-0.19049300

INT47
E(DMSO)[M06-2X/6-311++G(2d,p), SMD (DMSO)] = -1691.254953 a.u.
G_{corr}(DMSO)[M06-2X/6-311++G(2d,p)] = 0.05056 a.u.
H_{corr}(DMSO)[M06-2X/6-311++G(2d,p)] = 0.118592 a.u.
$G = E(DMSO) + G_{corr} = -1691.204393$ a.u.
$H = E(DMSO) + H_{corr} = -1691.136361$ a.u.

C	3.77541300	0.32838700	-0.12975000
C	2.48548000	-0.28098300	0.46284000
C	1.21633200	0.06619600	-0.35374800
C	-0.08378900	-0.13076000	0.46494400
C	-1.35515900	-0.27013500	-0.40146000
F	3.82136300	0.11560800	-1.43842900
F	3.82582600	1.63025000	0.10168400
F	4.82534100	-0.24669600	0.43745400

F	2.35594800	0.17114300	1.71667200
F	2.63270900	-1.60914000	0.48869000
F	1.29123000	1.34629100	-0.74519600
F	1.19726300	-0.71338200	-1.44199200
F	-0.21746500	0.92478500	1.27751500
F	0.04314100	-1.23857000	1.21477200
F	-1.29577600	0.67538100	-1.37053300
F	-1.30081700	-1.46062800	-1.03869200
O	-2.41645700	-0.15135700	0.39023100
C	-3.66620200	-0.37961800	-0.27164800
F	-4.06371100	-1.66518900	0.11409800
C	-4.65345000	0.58853600	0.10603300
O	-5.85655900	0.38684000	0.19869000
O	-4.15486900	1.84893800	0.22986300
H	-4.92413400	2.42621600	0.34206500

INT48

E(DMSO)[M06-2X/6-311++G(2d,p), SMD (DMSO)] = -1364.208256 a.u.

G_{corr}(DMSO)[M06-2X/6-311++G(2d,p)] = 0.022959 a.u.

H_{corr}(DMSO)[M06-2X/6-311++G(2d,p)] = 0.079972 a.u.

G = E(DMSO) + G_{corr} = -1364.185297 a.u.

H = E(DMSO) + H_{corr} = -1364.128284 a.u.

C	-2.53042600	-0.26463400	0.07187500
C	-1.22385100	0.50964300	-0.21082600
C	0.05411100	-0.33545900	0.02199600
C	1.32433900	0.52800800	0.20000700
C	2.70507500	-0.16409500	-0.00665800
F	-2.49172600	-1.46278700	-0.49699200
F	-2.71762900	-0.40929800	1.37474300
F	-3.55464100	0.41303900	-0.42916900
F	-1.21847700	1.58923000	0.58386600
F	-1.25837900	0.90946800	-1.48779200
F	-0.13799700	-1.07603400	1.12834300
F	0.17740600	-1.16283800	-1.02446100
F	1.27509600	1.02699000	1.45247100
F	1.23059000	1.57411700	-0.65551700
F	2.49021600	-1.48193100	0.55556100
F	2.70524700	-0.48916700	-1.40679500
O	3.69089400	0.43526300	0.39916200

INT49

E(DMSO)[M06-2X/6-311++G(2d,p), SMD (DMSO)] = -1264.18692 a.u.

G_{corr}(DMSO)[M06-2X/6-311++G(2d,p)] = 0.021739 a.u.

H_{corr}(DMSO)[M06-2X/6-311++G(2d,p)] = 0.077517 a.u.
G = E(DMSO) + G_{corr} = -1264.165181 a.u.
H = E(DMSO) + H_{corr} = -1264.109403 a.u.

C	-2.34178700	-0.30707500	-0.02465800
C	-1.05494400	0.54737400	-0.02744700
C	0.23212200	-0.30353700	-0.15679300
C	1.49775600	0.44655400	0.31826800
C	2.77848200	-0.22473800	-0.20947400
F	-2.29281400	-1.19616900	-1.00848100
F	-2.47825800	-0.94021800	1.12878100
F	-3.38747300	0.48298800	-0.20700700
F	-1.01546600	1.25035800	1.11054700
F	-1.11831300	1.38997400	-1.06110500
F	0.10292400	-1.42542600	0.56081500
F	0.40157900	-0.62833800	-1.44582100
F	1.52251100	0.46538600	1.65576000
F	1.45306500	1.69674800	-0.14756500
F	2.96632800	-1.38730600	0.39580100
O	3.49293700	0.20956900	-1.02936200

INT50
E(DMSO)[M06-2X/6-311++G(2d,p), SMD (DMSO)] = -1791.697331 a.u.
G_{corr}(DMSO)[M06-2X/6-311++G(2d,p)] = 0.062912 a.u.
H_{corr}(DMSO)[M06-2X/6-311++G(2d,p)] = 0.134013 a.u.
G = E(DMSO) + G_{corr} = -1791.634419 a.u.
H = E(DMSO) + H_{corr} = -1791.563318 a.u.

C	-2.54150700	-0.26658600	0.05831300
C	-1.22853100	0.51108700	-0.18224300
C	0.04535600	-0.34922700	0.01484400
C	1.32226100	0.49940100	0.22466300
C	2.70656200	-0.18512400	-0.00816800
F	-2.51535700	-1.43283500	-0.57410900
F	-2.73333100	-0.47923100	1.35145000
F	-3.56006900	0.44639500	-0.40594300
F	-1.22434600	1.55176200	0.66365200
F	-1.25958400	0.97179400	-1.43935500
F	-0.15698900	-1.12966700	1.09272800
F	0.15394100	-1.13992000	-1.06140900
F	1.27093300	0.93673100	1.50511100
F	1.21587600	1.59344400	-0.56831600
F	2.65284300	-0.38315800	-1.49049700
O	3.69283100	0.48826700	0.35047000

O	2.57604200	-1.48878500	0.49742000
H	3.42891200	-1.67099000	0.91262400

INT51
E(DMSO)[M06-2X/6-311++G(2d,p), SMD (DMSO)] = -1502.648099 a.u.
G_{corr}(DMSO)[M06-2X/6-311++G(2d,p)] = 0.039227 a.u.
H_{corr}(DMSO)[M06-2X/6-311++G(2d,p)] = 0.10129 a.u.
G = E(DMSO) + G_{corr} = -1502.608872 a.u.
H = E(DMSO) + H_{corr} = -1502.546809 a.u.

C	3.92154100	-0.07225400	-0.44997100
C	2.69189400	-0.16657100	0.47967800
C	1.34517400	-0.01817200	-0.27069400
C	0.17883500	0.35861300	0.67779400
C	-1.22400500	0.05699600	0.09878000
F	3.75032200	-0.84431400	-1.51508400
F	4.11439400	1.17642600	-0.84325300
F	4.99418200	-0.48155500	0.21117800
F	2.80468400	0.79566000	1.40448400
F	2.72222300	-1.35934900	1.08181700
F	1.47165300	0.94139200	-1.19917100
F	1.08541800	-1.17686100	-0.88850600
F	0.27392100	1.66917900	0.93402600
F	0.32153300	-0.31772000	1.82990100
F	-1.23188400	0.47755700	-1.18551400
F	-1.36539800	-1.29053100	0.05899400
O	-2.12623700	0.64603700	0.88785700
C	-3.51351400	0.87554900	0.52566800
F	-3.47210400	1.76617800	-0.57925400
C	-4.11926300	-0.36723000	-0.06245900
F	-4.04466000	-1.39835200	0.79326400
F	-5.42719500	-0.14906200	-0.31089400
F	-3.62754400	-0.82752600	-1.24705700

INT52
E(DMSO)[M06-2X/6-311++G(2d,p), SMD (DMSO)] = -1853.044898 a.u.
G_{corr}(DMSO)[M06-2X/6-311++G(2d,p)] = 0.047232 a.u.
H_{corr}(DMSO)[M06-2X/6-311++G(2d,p)] = 0.11804 a.u.
G = E(DMSO) + G_{corr} =$_{corr}$ = -1852.997666 a.u.
H = E(DMSO) + H_{corr} = -1852.926858 a.u.

C	-2.94947900	-0.83186100	-0.50895000
C	-1.79047700	0.00799900	-0.23720500
C	-0.82230800	-0.10847600	0.72505300

C	0.35932300	0.89796200	0.64962200
C	1.46716500	0.52158800	-0.35002800
F	-1.66427500	1.02111400	-1.17423700
F	0.00777000	2.17295100	0.33295800
F	0.96670700	0.97848000	1.85752200
F	2.50533300	1.37105300	-0.19589800
F	1.01442200	0.65100400	-1.60738600
H	-3.30167100	-0.71166200	-1.54613900
O	-3.26409700	-1.82909600	0.14974900
O	-0.70171500	-0.95439100	1.65018100
C	2.03829900	-0.90181600	-0.22358300
F	2.46299600	-1.14456400	1.00779900
F	1.13978600	-1.81069200	-0.56732700
F	3.07759100	-1.01571500	-1.05205100
O	-4.44585200	0.66875800	-0.14247100
H	-4.81311800	0.10443800	0.54460400

INT53
E(DMSO)[M06-2X/6-311++G(2d,p), SMD (DMSO)] = -1526.687926 a.u.
G_{corr}(DMSO)[M06-2X/6-311++G(2d,p)] = 0.027651 a.u.
H_{corr}(DMSO)[M06-2X/6-311++G(2d,p)] = 0.088876 a.u.
G = E(DMSO) + G_{corr} = -1526.660275 a.u.
H = E(DMSO) + H_{corr} = -1526.59905 a.u.

C	3.56550300	0.08156600	-0.06897200
C	2.17429400	0.54491800	0.34152400
C	0.94646600	-0.33857400	0.00044300
C	-0.40734500	0.41502100	0.05472000
C	-1.62280900	-0.53525000	0.18643200
F	3.53535500	-1.30917900	0.22082900
F	3.52585900	0.09111800	-1.48204400
F	2.15199400	0.69005200	1.69311000
F	1.94276600	1.76744200	-0.20477200
F	0.87842900	-1.36174400	0.87403900
F	1.06922300	-0.84837800	-1.23548900
F	-0.42293000	1.24713200	1.10579600
F	-0.55250900	1.13766200	-1.06700400
F	-1.72959300	-0.93413300	1.45838600
F	-1.44995100	-1.60860100	-0.59626700
C	-2.96155500	0.12419500	-0.21193500
F	-3.96057000	-0.64743200	0.19208200
F	-3.07633700	1.31352400	0.36507800
F	-3.04143800	0.26795200	-1.52521800

TS1
E(DMSO)[M06-2X/6-311++G(2d,p), SMD (DMSO)] = -1953.064359 a.u.
Gcorr(DMSO)[M06-2X/6-311++G(2d,p)] = 0.043547 a.u.
Hcorr(DMSO)[M06-2X/6-311++G(2d,p)] = 0.117816 a.u.
G = E(DMSO) + Gcorr= -1953.020812 a.u.
H = E(DMSO) + Hcorr= -1952.946543 a.u.

C	5.26639900	-1.02744200	-0.44095600
O	5.24462100	-1.69568800	0.51083500
O	5.47305900	-0.55548200	-1.48326400
C	3.49279300	0.71512700	0.22183100
C	2.21531900	-0.11407300	0.23781200
C	0.86447100	0.57927700	-0.07360200
C	-0.37831900	-0.21760500	0.39840000
C	-1.68647200	0.22667800	-0.30408500
C	-2.95322900	-0.20579400	0.47556500
F	3.35660700	1.58800400	1.32213500
F	3.31170500	1.58012400	-0.87998900
F	2.08789900	-0.70222100	1.45469700
F	2.33866300	-1.10585800	-0.68603500
F	0.81918400	1.78220100	0.52123700
F	0.75319000	0.75985000	-1.40370200
F	-0.53213200	-0.04607800	1.72069800
F	-0.19852500	-1.52194000	0.14852100
F	-1.70290100	1.56112000	-0.41781800
F	-1.72831000	-0.31176400	-1.53029000
F	-3.14819700	0.64246100	1.48955400
F	-2.78593400	-1.44186100	0.96239200
C	-4.23005200	-0.20709100	-0.39301100
F	-5.28830000	-0.31602000	0.39604200
F	-4.31495300	0.92642900	-1.07727600
F	-4.22209700	-1.22612600	-1.23708800

TS2
E(DMSO)[M06-2X/6-311++G(2d,p), SMD (DMSO)] = -1764.447022 a.u.
Gcorr(DMSO)[M06-2X/6-311++G(2d,p)] = 0.035404 a.u.
Hcorr(DMSO)[M06-2X/6-311++G(2d,p)] = 0.102308 a.u.
G = E(DMSO) + Gcorr= -1764.411618 a.u.
H = E(DMSO) + Hcorr= -1764.344714 a.u.

C	-0.82274300	-0.11163400	-0.09904300
C	0.20325900	0.97896100	0.28582200
C	-2.27461700	0.43749000	-0.14228400

C	1.69236100	0.74541200	-0.11555000
F	0.10397200	1.22314900	1.59278700
F	-0.16788100	2.10641300	-0.36532800
F	-0.53776700	-0.58812700	-1.31830600
F	-0.78239700	-1.10891800	0.79064400
C	-3.33731400	-0.68073500	-0.04264500
F	-2.46707000	1.08065600	-1.29783900
F	-2.47917500	1.28649000	0.87256100
C	2.36530000	-0.57268300	0.22257600
F	1.74282900	0.91116900	-1.45961000
F	2.35679200	1.77581600	0.44318900
F	-4.51684600	-0.19033300	-0.39407000
F	-3.02580300	-1.67998200	-0.85816000
F	-3.42051600	-1.13914500	1.19597300
C	3.72300800	-0.64996500	0.05187500
F	1.63311100	-1.64256100	-0.19744300
F	1.86944200	-0.67662000	1.79144300
F	4.25417600	-1.83329100	-0.36778200
F	4.40429500	0.37738400	-0.53522500

TS3
E(DMSO)[M06-2X/6-311++G(2d,p), SMD (DMSO)] = -1740.477606 a.u.
Gcorr(DMSO)[M06-2X/6-311++G(2d,p)] = 0.047194 a.u.
Hcorr(DMSO)[M06-2X/6-311++G(2d,p)] = 0.115023 a.u.
G = E(DMSO) + Gcorr= -1740.430412 a.u.
H = E(DMSO) + Hcorr= -1740.362583 a.u.

C	2.95074000	1.04895900	0.04882200
C	2.40012100	-0.08645300	-0.49282000
C	1.68908300	-1.16609300	0.18537100
C	0.17858400	-1.32834400	-0.13748800
F	2.15632900	-0.07631700	-1.84936300
F	0.03468300	-1.71038700	-1.41554300
F	-0.33170700	-2.30059800	0.64817800
F	1.84046500	2.35805900	0.36846600
C	-0.66310000	-0.05466200	0.08586500
F	-0.43511700	0.80034700	-0.92069400
F	-0.30968800	0.52018600	1.24150900
C	-2.18500300	-0.34239600	0.15370500
F	-2.52449100	-1.26042500	-0.76085600
F	-2.48651500	-0.80931100	1.37007000
C	-3.04822400	0.91411800	-0.09645000
F	-3.03801500	1.24126200	-1.37889600
F	-4.29741500	0.66144600	0.26732400
F	-2.58990200	1.93395300	0.61766200

F	1.79836700	-1.08890100	1.52698300
F	3.35215100	0.95382800	1.33264500
O	3.77924500	1.76012300	-0.73070800
H	3.57955800	2.69379000	-0.56408500
F	2.19233100	-2.41042700	-0.16662800

TS4
E(DMSO)[M06-2X/6-311++G(2d,p), SMD (DMSO)] = -1640.040513 a.u.
G_{corr}(DMSO)[M06-2X/6-311++G(2d,p)] = 0.033828 a.u.
H_{corr}(DMSO)[M06-2X/6-311++G(2d,p)] = 0.099765 a.u.
G = E(DMSO) + G_{corr} = -1640.006685 a.u.
H = E(DMSO) + H_{corr} = -1639.940748 a.u.

C	3.64600700	-0.98767500	-0.32728100
C	2.43813000	-0.46540400	0.27784500
C	1.74322400	0.57128200	-0.21546300
C	0.36278000	0.95668300	0.28505400
F	2.06730800	-1.00740800	1.45156200
F	0.31331600	1.01500100	1.61903500
F	-0.01761800	2.13333800	-0.23435600
F	4.13970200	-2.00954700	0.40452000
C	-0.68408900	-0.08625100	-0.18618200
F	-0.51700400	-1.21656500	0.51590300
F	-0.46603800	-0.35292300	-1.48351800
C	-2.15070700	0.38731200	-0.03979900
F	-2.31006200	1.04701400	1.11412400
F	-2.44564400	1.20711200	-1.05411800
C	-3.16577300	-0.77781000	-0.06478500
F	-3.12910200	-1.45550200	1.07137000
F	-4.38542500	-0.28732100	-0.22847300
F	-2.89206400	-1.59846600	-1.07107100
F	1.99936000	1.02716100	-1.42132800
O	4.19361500	-0.64306600	-1.31978800
F	2.45589800	2.33763100	0.66990100

TS5
E(DMSO)[M06-2X/6-311++G(2d,p), SMD (DMSO)] = -1591.504072 a.u.
G_{corr}(DMSO)[M06-2X/6-311++G(2d,p)] = 0.041853 a.u.
H_{corr}(DMSO)[M06-2X/6-311++G(2d,p)] = 0.10965 a.u.
G = E(DMSO) + G_{corr} = -1591.462219 a.u.
H = E(DMSO) + H_{corr} = -1591.394422 a.u.

C	-3.55065200	-1.10358500	0.30517800
C	-2.48993100	-0.38360700	-0.22727100

C	-1.77385500	0.63902700	0.45404900
C	-0.38817600	1.01800200	-0.13633400
F	-2.16891200	-0.62442700	-1.54439400
F	-0.31388900	1.17719500	-1.46901600
F	0.08197200	2.14154100	0.44759000
O	-4.08911600	-1.12153900	1.38551100
O	-1.97033700	0.99501200	1.61300700
O	-2.52225300	2.52336000	-0.77685800
H	-2.96972700	2.70695200	0.05448800
F	-4.05851600	-2.00612900	-0.65370200
C	0.64681000	-0.08927500	0.20360200
F	0.46704700	-1.13365900	-0.62919100
F	0.47111000	-0.53151000	1.46036700
C	2.12270700	0.36782600	0.09398500
F	2.29796400	1.16771800	-0.96662800
F	2.45577900	1.04277500	1.20273000
C	3.11929400	-0.80271800	-0.04785500
F	3.05178300	-1.33692700	-1.25823800
F	4.35268300	-0.35107300	0.14357300
F	2.86366800	-1.74057500	0.85581000

TS6
E(DMSO)[M06-2X/6-311++G(2d,p), SMD (DMSO)] = -1592.015604 a.u.
G_{corr}(DMSO)[M06-2X/6-311++G(2d,p)] = 0.055916 a.u.
H_{corr}(DMSO)[M06-2X/6-311++G(2d,p)] = 0.123535 a.u.
G = E(DMSO) + G_{corr} = -1591.959688 a.u.
H = E(DMSO) + H_{corr} = -1591.892069 a.u.

C	3.40535100	1.23498700	-0.23538400
C	3.40730700	-0.05592400	-0.72468400
C	1.50356000	-1.24088100	0.24159400
C	0.51788900	-0.11697800	-0.11523600
F	0.63707000	0.30533400	-1.38221800
O	2.94376000	2.26581800	-0.68160000
O	1.86683700	-1.42423000	1.37334200
O	1.51394400	-2.17159800	-0.72726600
H	2.02788600	-2.92717500	-0.39756300
F	3.97520400	1.30734800	1.04542900
F	0.70580000	0.91668600	0.71883100
F	4.22524400	-0.98939600	-0.11283100
H	3.24336500	-0.25501900	-1.77184000
C	-0.94784800	-0.59266700	0.06105800
C	-1.95711300	0.57327500	0.19856400
C	-3.41449900	0.15476200	-0.09286100
F	-1.29513800	-1.34155000	-0.99785800

F	-1.04515000	-1.35072300	1.16342100
F	-1.63937000	1.55900800	-0.65053100
F	-1.91169600	1.04324500	1.45001200
F	-3.59597000	-0.04130400	-1.38956900
F	-3.70808400	-0.96106000	0.56284100
F	-4.23185100	1.11717300	0.30972600

TS7
E(DMSO)[M06-2X/6-311++G(2d,p), SMD (DMSO)] = -1840.883225 a.u.
G_{corr}(DMSO)[M06-2X/6-311++G(2d,p)] = 0.061362 a.u.
H_{corr}(DMSO)[M06-2X/6-311++G(2d,p)] = 0.130947 a.u.
G = E(DMSO) + G_{corr} = -1840.821863 a.u.
H = E(DMSO) + H_{corr} = -1840.752278 a.u.

C	1.28199700	0.48196900	0.01129600
C	2.58136500	-0.32209600	0.31363700
C	3.92466500	0.38297900	0.07219300
F	1.37138600	1.08705300	-1.18172000
F	1.03810300	1.38793000	0.97003800
F	3.37062800	1.91229700	0.13843500
F	2.44304900	-1.41330100	-0.47543700
F	2.50322500	-0.68946200	1.60445100
H	4.62225200	0.56517200	0.86682400
O	4.84357300	-1.33028200	0.33403700
H	4.68477200	-1.93440600	-0.39793200
F	4.29097300	0.43970500	-1.21383900
C	0.02369200	-0.43697200	-0.06251000
C	-1.29589700	0.35697000	0.12927300
C	-2.52948800	-0.41018900	-0.41034900
C	-3.86593700	0.10977300	0.16414000
F	-3.90870900	1.43348400	0.08591500
F	-4.00904900	-0.25787900	1.42701700
F	-2.57711600	-0.27632900	-1.73915200
F	-2.42687000	-1.70887200	-0.10140500
F	-1.21823900	1.52480700	-0.52191500
F	-1.47797400	0.59831700	1.43440400
F	-0.02872300	-1.03289600	-1.26365000
F	0.07464800	-1.38167200	0.88545800
F	-4.86510900	-0.39686000	-0.54273900

TS8
E(DMSO)[M06-2X/6-311++G(2d,p), SMD (DMSO)] = -1740.404938 a.u.
G_{corr}(DMSO)[M06-2X/6-311++G(2d,p)] = 0.045724 a.u.
H_{corr}(DMSO)[M06-2X/6-311++G(2d,p)] = 0.114398 a.u.

$G = E(DMSO) + G_{corr} = -1740.359214$ a.u.
$H = E(DMSO) + H_{corr} = -1740.29054$ a.u.

C	3.49146300	0.57346600	0.02872900
C	2.67941700	-0.44709100	-0.24436400
C	1.25319800	-0.45129200	0.24428400
C	0.39226200	0.66576700	-0.39373900
F	2.85291500	-1.07150100	-1.42627100
F	0.93431000	1.86369500	-0.11975300
F	0.38861400	0.49526800	-1.72558700
F	4.72536500	0.66661400	-0.47134800
C	-1.08179600	0.78630800	0.08049800
F	-1.63455600	1.75944000	-0.66771500
F	-1.08722200	1.18572100	1.35820900
C	-1.98020400	-0.46608800	-0.03437700
F	-1.75526100	-1.09942500	-1.19092900
F	-1.71326000	-1.28585200	0.98765100
C	-3.48995200	-0.12948600	0.02256100
F	-3.89108000	0.42406500	-1.11058000
F	-4.16995900	-1.25121600	0.21103800
F	-3.74210400	0.69994800	1.02622000
F	1.17270100	-0.28721700	1.57521100
F	3.34209600	1.37941600	1.08198900
F	0.64857200	-1.60304400	-0.10419200
O	3.12033800	-2.14494300	0.82837000
H	2.81079600	-2.91318000	0.33600500

TS9
E(DMSO)[M06-2X/6-311++G(2d,p), SMD (DMSO)] = -1591.501492 a.u.
G_{corr}(DMSO)[M06-2X/6-311++G(2d,p)] = 0.04165 a.u.
H_{corr}(DMSO)[M06-2X/6-311++G(2d,p)] = 0.109539 a.u.
$G = E(DMSO) + G_{corr} = -1591.459842$ a.u.
$H = E(DMSO) + H_{corr} = -1591.391953$ a.u.

C	3.70177600	-0.49399300	-0.55162500
C	2.39737500	-0.22024900	-0.00750200
C	1.60707800	0.85679900	-0.33651100
C	0.22807100	0.93509200	0.38576300
F	1.96079600	-1.11274800	0.93918500
F	0.28613200	0.65151100	1.70927400
F	-0.25460900	2.19624000	0.28705200
O	4.31137700	0.11591000	-1.38224200
O	1.81649800	1.77142500	-1.15994700
O	4.80120100	0.00853400	1.41509400

H	4.95931700	0.90302900	1.09772300
F	4.04061300	-1.82603000	-0.34987800
C	-0.84250000	0.01998100	-0.24436600
F	-0.63109400	-1.25215200	0.13285000
F	-0.74385200	0.08295500	-1.58316400
C	-2.29749300	0.39948100	0.12594600
F	-2.37495600	0.73792500	1.42035700
F	-2.68405200	1.44289100	-0.61888600
C	-3.31059900	-0.74052200	-0.11491800
F	-3.18101300	-1.68954600	0.79956700
F	-4.54161800	-0.25088700	-0.04225800
F	-3.13125600	-1.27010700	-1.31873200

TS10
E(DMSO)[M06-2X/6-311++G(2d,p), SMD (DMSO)] = -1591.488496 a.u.
Gcorr(DMSO)[M06-2X/6-311++G(2d,p)] = 0.043511 a.u.
Hcorr(DMSO)[M06-2X/6-311++G(2d,p)] = 0.11051 a.u.
G = E(DMSO) + Gcorr= -1591.444985 a.u.
H = E(DMSO) + Hcorr= -1591.377986 a.u.

C	-3.71864800	-1.15747200	0.25941900
C	-2.46871100	-0.50653000	-0.26961400
C	-1.80838600	0.57653400	0.17981500
C	-0.41834100	0.93219300	-0.30653100
F	-2.03089000	-0.98910600	-1.48034100
F	-0.31819300	1.00167100	-1.64184600
F	-0.00149200	2.10760000	0.22107800
O	-4.20161500	-2.05446000	-0.46682400
C	0.63823500	-0.10050000	0.17087600
F	0.51296500	-1.23767700	-0.53258800
F	0.42672100	-0.38239000	1.46848600
C	2.10379700	0.38759000	0.04487300
F	2.27993600	1.06045700	-1.10042200
F	2.38985200	1.19933300	1.07082100
C	3.13312100	-0.76411200	0.06884400
F	3.11540300	-1.43858300	-1.07048300
F	4.34782300	-0.25871900	0.23975200
F	2.87044700	-1.59441800	1.07043600
F	-1.98164900	0.99929700	1.44155200
O	-2.53581400	2.36858000	-0.64389300
H	-2.23149100	3.09603400	-0.09010500
O	-4.14172300	-0.75280100	1.36396700

TS11
E(DMSO)[M06-2X/6-311++G(2d,p), SMD (DMSO)] = -1567.522204 a.u.

Gcorr(DMSO)[M06-2X/6-311++G(2d,p)] = 0.059366 a.u.
Hcorr(DMSO)[M06-2X/6-311++G(2d,p)] = 0.124625 a.u.
G = E(DMSO) + Gcorr= -1567.462838 a.u.
H = E(DMSO) + Hcorr= -1567.397579 a.u.

C	4.22569300	0.32017900	-0.22307700
C	2.90580200	-0.44245700	-0.34021500
C	1.67955800	0.31765300	-0.08100400
C	0.38758800	-0.48845800	0.08236800
F	0.36367100	-1.17490000	1.24826700
O	5.17483100	-0.10445400	-0.89485300
O	1.90833200	0.73853600	-1.34635500
O	1.68865500	1.25978700	0.93843100
H	2.65994100	1.49712800	0.97975300
F	0.28122500	-1.40425800	-0.91264700
F	3.32917800	-1.59581000	1.07887700
H	2.84500800	-1.29116400	-0.99821000
C	-0.90094100	0.36892200	0.05862400
C	-2.16879900	-0.44413600	-0.30333200
C	-3.48632000	0.25730900	0.09199200
F	-1.10256300	0.91414300	1.27199100
F	-0.79623000	1.36100600	-0.83600200
F	-2.15158000	-1.63333900	0.31629900
F	-2.20398400	-0.64284400	-1.62726100
F	-3.66505300	0.22533000	1.40392500
F	-3.47949100	1.52018900	-0.31556200
F	-4.50242200	-0.37154200	-0.48547900
O	4.22628100	1.31590600	0.55585800

TS12
E(DMSO)[M06-2X/6-311++G(2d,p), SMD (DMSO)] = -1467.546213 a.u.
Gcorr(DMSO)[M06-2X/6-311++G(2d,p)] = 0.058277 a.u.
Hcorr(DMSO)[M06-2X/6-311++G(2d,p)] = 0.121759 a.u.
G = E(DMSO) + Gcorr= -1467.487936 a.u.
H = E(DMSO) + Hcorr= -1467.424454 a.u.

C	4.03422600	0.67851000	0.29366600
C	2.88094900	-0.27492900	0.57177900
C	1.84012600	-0.19532900	-0.48619500
C	0.50093600	-0.86060800	-0.13570600
F	0.44689300	-1.33115300	1.12824200
O	5.13709500	0.36494500	-0.05062600
O	3.03266900	-1.58118300	0.22710800
O	1.96514800	0.23512600	-1.62027700

H	2.80627100	2.07789300	0.73591000
F	0.22386300	-1.87849300	-0.97642400
H	2.53219000	-0.06946200	1.60004300
C	-0.64727000	0.16789200	-0.26470900
C	-1.95276200	-0.26712400	0.44464100
C	-3.20085300	0.49825400	-0.04611500
F	-0.25078800	1.32866400	0.29005800
F	-0.92217300	0.38661100	-1.55887500
F	-1.83673000	-0.04459900	1.75921700
F	-2.17177700	-1.57326200	0.24079800
F	-2.95472900	1.80218100	-0.07350900
F	-3.55640700	0.09745400	-1.25667000
F	-4.20671000	0.26903500	0.78686500
O	3.73839400	1.98156300	0.48661500

TS13
E(DMSO)[M06-2X/6-311++G(2d,p), SMD (DMSO)] = -1467.56727 a.u.
Gcorr(DMSO)[M06-2X/6-311++G(2d,p)] = 0.056975 a.u.
Hcorr(DMSO)[M06-2X/6-311++G(2d,p)] = 0.121283 a.u.
G = E(DMSO) + Gcorr= -1467.510295 a.u.
H = E(DMSO) + Hcorr= -1467.445987 a.u.

C	2.52598700	1.67582300	0.05899500
C	3.12114900	-0.37397700	0.47441900
C	2.04689400	-0.88614100	-0.23441700
C	0.69269800	-0.96990500	0.45158700
F	0.69959800	-0.44745100	1.69924300
O	3.00646300	1.86922200	-1.00447500
O	4.35334000	-0.49059700	-0.11907100
O	2.10209300	-1.27810900	-1.42520300
F	0.32736300	-2.27406500	0.57680600
H	3.13968200	-0.25382000	1.54633500
C	-0.43784000	-0.27701200	-0.34831600
C	-1.68481400	0.04886600	0.50795100
C	-2.95125000	0.32760000	-0.33140900
F	0.01131800	0.87722600	-0.86432600
F	-0.82660000	-1.07043700	-1.36030400
F	-1.44287800	1.13764600	1.24644500
F	-1.96190100	-0.98038800	1.32234000
F	-2.67474500	1.17480100	-1.31474300
F	-3.43203400	-0.79357900	-0.84673300
F	-3.88064200	0.86586900	0.44722700
O	1.96818800	2.06240400	1.03234300
H	4.16740300	-0.72764600	-1.04155900

TS14
E(DMSO)[M06-2X/6-311++G(2d,p), SMD (DMSO)] = -1278.445993 a.u.
Gcorr(DMSO)[M06-2X/6-311++G(2d,p)] = 0.032731 a.u.
Hcorr(DMSO)[M06-2X/6-311++G(2d,p)] = 0.090135 a.u.
G = E(DMSO) + Gcorr= -1278.413262 a.u.
H = E(DMSO) + Hcorr= -1278.355858 a.u.

C	3.71878500	-0.08205700	-0.51281900
C	2.57336400	0.60433100	-0.03788500
C	1.39548700	-0.14900800	0.22252500
F	1.35403600	-1.41953700	-0.23782400
F	1.11082700	-0.44193300	1.80348200
C	0.02453800	0.47915300	-0.05722200
F	-0.11075800	0.58381600	-1.41329800
F	-0.11700900	1.71216600	0.44698000
C	-1.22904000	-0.30479300	0.44477500
F	-1.06340200	-1.63428400	0.44207000
F	-1.53204000	0.08001800	1.69450500
C	-2.48963500	-0.02777200	-0.40605200
F	-2.42149800	-0.63602300	-1.58246600
F	-3.55887900	-0.49349200	0.23489900
F	-2.65419200	1.27585400	-0.60002100
O	2.58236800	1.92136100	0.18431200
H	4.52233000	0.66020700	-0.73355600
O	3.97424700	-1.29868800	-0.71947500

TS15
E(DMSO)[M06-2X/6-311++G(2d,p), SMD (DMSO)] = -1178.498823 a.u.
Gcorr(DMSO)[M06-2X/6-311++G(2d,p)] = 0.030046 a.u.
Hcorr(DMSO)[M06-2X/6-311++G(2d,p)] = 0.0876 a.u.
G = E(DMSO) + Gcorr= -1178.468777 a.u.
H = E(DMSO) + Hcorr= -1178.411223 a.u.

C	-3.94585700	-0.07634500	-0.26423500
C	-2.58783700	0.63111900	-0.31667500
C	-1.37580800	-0.15049200	-0.15712700
F	-1.50369800	-1.49451100	-0.09745100
C	-0.13500400	0.34221400	-0.02020300
F	0.24435800	0.64739600	2.03172400
F	0.11945100	1.61504300	-0.24334900
C	1.07302600	-0.57274300	-0.09889600
F	1.09602500	-1.50733200	0.85441900
F	1.02088400	-1.23828700	-1.28700900
C	2.44330000	0.14220900	-0.12647900

F	3.38862700	-0.79351100	-0.21469100
F	2.52405200	0.91306600	-1.20884500
F	2.68726500	0.87713300	0.93857400
O	-2.61392500	1.83623200	-0.45712100
H	-4.72306600	0.43765500	-0.85517300
O	-4.17364100	-1.02428100	0.43168500

TS16
E(DMSO)[M06-2X/6-311++G(2d,p), SMD (DMSO)] = -1153.949929 a.u.
Gcorr(DMSO)[M06-2X/6-311++G(2d,p)] = 0.028563 a.u.
Hcorr(DMSO)[M06-2X/6-311++G(2d,p)] = 0.085895 a.u.
G = E(DMSO) + Gcorr= -1153.921366 a.u.
H = E(DMSO) + Hcorr= -1153.869987 a.u.

C	-3.66984200	0.41110800	-0.07539200
C	-2.65505100	-0.73185400	-0.15294500
C	-1.01222400	0.32267500	0.00742600
F	-0.79581500	1.08969000	-1.11368800
C	0.10262100	0.13949200	0.71679700
F	0.07331900	-0.62380700	1.85300500
C	1.50282700	0.56857700	0.42739700
F	1.56033400	1.75987300	-0.21061200
F	2.22560200	0.69186000	1.57201800
C	2.28685700	-0.41674600	-0.45168900
F	1.71418700	-0.53142300	-1.64538800
F	3.54300600	-0.00813000	-0.63171700
F	2.31977100	-1.61788500	0.12117300
O	-2.75490800	-1.48928500	0.88369200
H	-4.69187000	0.04478600	-0.33162800
O	-3.52417900	1.57457600	0.22808600
O	-2.52127500	-1.16602900	-1.36191000

TS17
E(DMSO)[M06-2X/6-311++G(2d,p), SMD (DMSO)] = -1591.9986 a.u.
Gcorr(DMSO)[M06-2X/6-311++G(2d,p)] = 0.058518 a.u.
Hcorr(DMSO)[M06-2X/6-311++G(2d,p)] = 0.12484 a.u.
G = E(DMSO) + Gcorr= -1591.940082 a.u.
H = E(DMSO) + Hcorr= -1591.87376 a.u.

C	-4.15546600	-0.13610900	-0.38700500
C	-2.82725300	0.49947000	-0.27002000
C	-1.63881000	-0.31453200	-0.01755300
C	-0.34544500	0.49493900	0.15124500
F	-0.33687800	1.13878900	1.33604600
O	-5.08051500	0.23364800	-1.01706100

O	-1.93895100	-0.64097900	-1.29695700
O	-1.56999400	-1.30901700	0.94162700
H	-2.36137600	-1.85751100	0.86913800
F	-4.25627300	-1.27861400	0.33667100
F	-0.26848100	1.43005600	-0.81944800
F	-3.49297300	1.32660600	1.24805500
H	-2.70492800	1.43508400	-0.78954500
C	0.94052000	-0.36377700	0.08074200
C	2.19487000	0.45964200	-0.30160000
C	3.52313300	-0.25016100	0.04191000
F	1.16930400	-0.93130600	1.27579100
F	0.79261900	-1.33245400	-0.83284400
F	2.18434000	1.63216300	0.34818600
F	2.18797100	0.68832500	-1.61967200
F	3.74286700	-0.23173300	1.34728700
F	3.49385400	-1.50876700	-0.37761100
F	4.52061500	0.37986800	-0.56321300

TS18
E(DMSO)[M06-2X/6-311++G(2d,p), SMD (DMSO)] = -1567.471645 a.u.
Gcorr(DMSO)[M06-2X/6-311++G(2d,p)] = 0.056442 a.u.
Hcorr(DMSO)[M06-2X/6-311++G(2d,p)] = 0.12331 a.u.
G = E(DMSO) + Gcorr= -1567.415203 a.u.
H = E(DMSO) + Hcorr= -1567.348335 a.u.

C	-3.86474600	-1.04640000	-0.09984100
C	-3.61878500	0.10148600	-0.93497800
C	-1.51987200	0.91241500	0.43175000
C	-0.45982900	-0.07746700	-0.07828200
F	-0.56361100	-0.34721600	-1.39058500
O	-3.32280900	-2.14411400	-0.47468700
O	-1.92788900	0.85627700	1.55963200
O	-1.55238200	1.99749600	-0.36133200
H	-2.40683400	2.43323700	-0.19146700
F	-0.53482400	-1.22240300	0.61475100
F	-4.08418900	1.37738800	-0.48216900
H	-2.80794400	0.21677900	-1.63421700
C	0.96653500	0.49356100	0.14262200
C	2.07257600	-0.58981300	0.12417200
C	3.48282400	-0.01683500	-0.13633400
F	1.23582200	1.39747000	-0.81355300
F	1.02198000	1.11112300	1.33334800
F	1.81936400	-1.49213600	-0.83284400
F	2.09859800	-1.20800800	1.31035700
F	3.62034900	0.33352000	-1.40569100

F	3.69570400	1.04328600	0.63344900
F	4.38889800	-0.94175500	0.14814600
O	-4.62445000	-0.93129900	0.91315600

TS19
E(DMSO)[M06-2X/6-311++G(2d,p), SMD (DMSO)] = -1591.486114 a.u.
Gcorr(DMSO)[M06-2X/6-311++G(2d,p)] = 0.043743 a.u.
Hcorr(DMSO)[M06-2X/6-311++G(2d,p)] = 0.110753 a.u.
G = E(DMSO) + Gcorr= -1591.442371 a.u.
H = E(DMSO) + Hcorr= -1591.375361 a.u.

C	3.83242000	-0.88441800	-0.39115700
C	2.61306900	-0.23798000	0.27359900
C	1.63649900	0.40306200	-0.38716100
C	0.32321900	0.83935600	0.14865900
F	2.27698200	-0.73066400	1.47312000
F	0.32366600	0.95088200	1.49077800
F	-0.02558000	2.05509600	-0.36483700
O	4.11209000	-2.01162300	0.05723700
C	-0.83174600	-0.12212600	-0.22372500
F	-0.70200900	-1.24000500	0.51220300
F	-0.72138200	-0.45641000	-1.52008000
C	-2.25311500	0.45157600	-0.01427000
F	-2.30799400	1.16543500	1.11814700
F	-2.55452000	1.25162600	-1.04498300
C	-3.34645700	-0.63528600	0.06684400
F	-3.28196600	-1.28315800	1.21972700
F	-4.53907200	-0.06363700	-0.03054600
F	-3.20383400	-1.50181300	-0.92837700
F	1.77905100	0.78294300	-1.68350700
O	4.06272700	1.19444400	1.33250700
H	4.53097900	1.33053800	0.50362400
O	4.35463500	-0.25635800	-1.32914100

TS20
E(DMSO)[M06-2X/6-311++G(2d,p), SMD (DMSO)] = -1591.539641 a.u.
Gcorr(DMSO)[M06-2X/6-311++G(2d,p)] = 0.046228 a.u.
Hcorr(DMSO)[M06-2X/6-311++G(2d,p)] = 0.111416 a.u.
G = E(DMSO) + Gcorr= -1591.493413 a.u.
H = E(DMSO) + Hcorr= -1591.428225 a.u.

C	4.12862000	-0.67177500	0.07167400
C	2.92697400	0.33786600	0.22099400
C	1.60156400	-0.28342800	-0.07055200

C	0.40095800	0.40888100	0.05321700
F	2.94127100	0.72900000	1.58440500
F	0.32827800	1.16720000	1.17052200
F	0.04981100	1.54012500	-1.04542500
O	4.04817600	-1.75148400	0.66527900
C	-0.90614000	-0.38299500	-0.08364100
F	-1.06050300	-1.13580500	1.03709400
F	-0.86288700	-1.22734500	-1.12820200
C	-2.21714800	0.43702500	-0.23885800
F	-2.18987200	1.56895200	0.47674400
F	-2.42197500	0.73745200	-1.52790600
C	-3.46849300	-0.34456300	0.22740100
F	-3.53112900	-0.41140200	1.54953600
F	-4.55754900	0.28217000	-0.20645100
F	-3.46559600	-1.57602500	-0.27018800
F	1.70100100	-1.03489000	-1.25104900
O	3.21211800	1.46148400	-0.52152000
H	4.13989800	1.29683800	-0.79720200
O	5.07526200	-0.21722200	-0.61700200

TS21
E(DMSO)[M06-2X/6-311++G(2d,p), SMD (DMSO)] = -1591.539641 a.u.
Gcorr(DMSO)[M06-2X/6-311++G(2d,p)] = 0.046228 a.u.
Hcorr(DMSO)[M06-2X/6-311++G(2d,p)] = 0.111416 a.u.
G = E(DMSO) + Gcorr= -1591.493413 a.u.
H = E(DMSO) + Hcorr= -1591.428225 a.u.

C	4.07605900	0.59013100	0.36860000
C	3.64548700	-0.74330400	-0.31489600
C	1.37119400	-0.33971500	0.05851400
C	0.37087400	0.52730300	-0.09467200
F	3.56674300	-0.61815300	-1.69831300
F	0.54121600	1.58402800	-0.95427800
O	4.09141300	0.54546500	1.60861300
C	-1.01373900	0.54244400	0.46510700
F	-1.47554700	1.81519500	0.58254900
F	-1.06453300	-0.01863200	1.69266000
C	-2.02277700	-0.21832900	-0.41923300
F	-1.95696800	0.27494700	-1.66795300
F	-1.67260200	-1.51390500	-0.44598300
C	-3.50101300	-0.16020400	0.00778500
F	-3.96782900	1.07881600	-0.05586200
F	-4.21805000	-0.91958900	-0.81626900
F	-3.65630700	-0.61895500	1.24221700
F	1.03374300	-1.38360500	0.89722500

O	3.79662000	-1.84797100	0.11384600
O	4.39630200	1.51359800	-0.39885600

TS22
E(DMSO)[M06-2X/6-311++G(2d,p), SMD (DMSO)] = -1403.378123 a.u.
G_{corr}(DMSO)[M06-2X/6-311++G(2d,p)] = 0.042692 a.u.
H_{corr}(DMSO)[M06-2X/6-311++G(2d,p)] = 0.105958 a.u.
G = E(DMSO) + G_{corr} = -1403.335431 a.u.
H = E(DMSO) + H_{corr} = -1403.272165 a.u.

C	3.13720700	-0.50396000	-0.67834000
C	2.17523700	0.39481000	-0.49616700
C	0.98949100	0.30998700	0.39261000
C	-0.32811800	0.05375300	-0.37590700
C	-1.61301700	0.29979600	0.44898800
F	2.29175800	1.60482400	-1.09853700
F	0.81766000	1.47700100	1.06894700
F	1.13065000	-0.67868100	1.29362200
F	-0.36796800	0.86385500	-1.44543200
F	-0.32208100	-1.21881000	-0.80580300
F	-1.84569500	1.61624800	0.50776500
F	-1.45915000	-0.17048200	1.69358500
F	2.99862800	-1.74400600	-0.22231700
H	3.95752400	-0.34313000	-1.35621800
O	5.04261000	-0.26550200	0.69727400
H	5.06462000	0.68489500	0.85028300
C	-2.86734500	-0.36896700	-0.15354900
F	-3.94628300	0.10658900	0.45211000
F	-2.82856800	-1.68095100	0.01806100
F	-2.94936700	-0.10117200	-1.45067400

TS23
E(DMSO)[M06-2X/6-311++G(2d,p), SMD (DMSO)] = -1403.428673 a.u.
G_{corr}(DMSO)[M06-2X/6-311++G(2d,p)] = 0.047464 a.u.
H_{corr}(DMSO)[M06-2X/6-311++G(2d,p)] = 0.107915 a.u.
G = E(DMSO) + G_{corr} = -1403.381209 a.u.
H = E(DMSO) + H_{corr} = -1403.320758 a.u.

C	3.31962800	-0.11971700	-0.29628100
C	2.30369300	0.77647100	0.04043600
C	1.05235400	0.42805100	0.70457800
C	-0.20399100	0.37431200	-0.21566600
C	-1.38657300	-0.42690700	0.38130100
F	2.05688900	1.74325500	-0.94844600

F	0.68441900	1.34230000	1.68589200
F	1.13354300	-0.76739200	1.33810000
F	-0.63627400	1.62395700	-0.47610200
F	0.10970000	-0.20763500	-1.38349200
F	-1.53714000	-0.15534900	1.68522400
F	-1.14319500	-1.73705200	0.23731700
F	2.89383200	-1.32401100	-1.40455900
H	4.06286200	0.31643100	-0.96084400
O	3.79950200	-0.90325400	0.71024000
H	4.32637200	-1.60021000	0.29863400
C	-2.73973900	-0.13377400	-0.30214000
F	-3.62695400	-1.04136600	0.08657400
F	-2.61712300	-0.19517300	-1.62207500
F	-3.19075200	1.06504200	0.03567000

TS24
E(DMSO)[M06-2X/6-311++G(2d,p), SMD (DMSO)] = -1302.977232 a.u.
G_{corr}(DMSO)[M06-2X/6-311++G(2d,p)] = 0.033502 a.u.
H_{corr}(DMSO)[M06-2X/6-311++G(2d,p)] = 0.091771 a.u.
G = E(DMSO) + G_{corr} = -1302.94373 a.u.
H = E(DMSO) + H_{corr} = -1302.885461 a.u.

C	3.82554900	-0.01249400	-0.40244400
C	2.51451900	0.50175700	-0.06904800
C	1.35412300	-0.18481100	-0.05147800
C	-0.00198900	0.48932200	0.00402500
C	-1.24718300	-0.37416300	0.38995600
F	2.51724800	1.79699600	0.34179500
F	0.96405700	-0.89317800	1.77842200
F	1.33141400	-1.37791500	-0.61942500
F	0.00922200	1.54711700	0.82358300
F	-0.23967000	0.97246400	-1.25299200
F	-1.55644800	-0.18937200	1.67678900
F	-1.07236900	-1.67794500	0.15534800
H	4.61497300	0.75596500	-0.31531700
O	4.08443200	-1.14614600	-0.74937300
C	-2.51546200	0.03708500	-0.39788900
F	-2.71213600	1.34837600	-0.31685300
F	-2.43906900	-0.31837000	-1.67210100
F	-3.56533200	-0.57783800	0.13783100

TS25
E(DMSO)[M06-2X/6-311++G(2d,p), SMD (DMSO)] = -1278.926456 a.u.
G_{corr}(DMSO)[M06-2X/6-311++G(2d,p)] = 0.042154 a.u.
H_{corr}(DMSO)[M06-2X/6-311++G(2d,p)] = 0.103303 a.u.

$G = E(DMSO) + G_{corr} = -1278.884302$ a.u.
$H = E(DMSO) + H_{corr} = -1278.823153$ a.u.

C	-4.21059700	0.08318200	0.25786800
C	-2.02834100	0.01529200	0.08377900
C	-0.94069500	0.78017700	0.10932400
C	0.41471800	0.57884400	-0.48496700
C	1.37992900	-0.15999500	0.46399900
F	-1.85104900	-1.15368800	-0.62661400
F	-0.97892600	1.94611800	0.83061600
F	0.35236900	-0.14222400	-1.62492300
F	0.99112200	1.77079500	-0.78662600
F	0.87657000	-1.37810500	0.71793300
F	1.45594900	0.52770600	1.61628600
H	-4.19005300	0.88000200	1.00318600
O	-4.57701800	0.23989200	-0.89967000
O	-4.36364800	-1.12330100	0.88158900
H	-4.48725000	-1.77602400	0.17666200
C	2.82279100	-0.36560400	-0.03391800
F	2.84119100	-1.06092900	-1.16253000
F	3.42996900	0.79621200	-0.23095700
F	3.50233700	-1.04234100	0.88773500

TS26
E(DMSO)[M06-2X/6-311++G(2d,p), SMD (DMSO)] = -1326.914735 a.u.
G_{corr}(DMSO)[M06-2X/6-311++G(2d,p)] = 0.020814 a.u.
H_{corr}(DMSO)[M06-2X/6-311++G(2d,p)] = 0.078772 a.u.
$G = E(DMSO) + G_{corr} = -1326.893921$ a.u.
$H = E(DMSO) + H_{corr} = -1326.835963$ a.u.

C	3.60592000	-0.12298600	-0.55430600
C	2.54871600	0.23672500	-0.05364100
C	1.28207700	-0.06174600	0.62605800
C	-0.01009700	0.38254700	-0.12303400
C	-1.21070200	-0.56166300	0.12994600
F	2.18789900	2.00901900	-0.08717400
F	1.20415900	0.44738600	1.87821700
F	1.20349000	-1.41822500	0.77099200
F	-0.39685400	1.60428700	0.27100700
F	0.21502300	0.40137400	-1.44483600
F	-1.29283200	-0.85387700	1.43685000
F	-1.05154700	-1.69233700	-0.56806300
F	4.43662900	-1.08917600	-0.87211100
C	-2.57102200	0.04702600	-0.28267400

F	-3.48371100	-0.91617900	-0.30679400
F	-2.95871900	0.97011100	0.58388200
F	-2.49346500	0.59101500	-1.49020300

TS27

E(DMSO)[M06-2X/6-311++G(2d,p), SMD (DMSO)] = -1403.376233 a.u.

G_{corr}(DMSO)[M06-2X/6-311++G(2d,p)] = 0.045144 a.u.

H_{corr}(DMSO)[M06-2X/6-311++G(2d,p)] = 0.106635 a.u.

G = E(DMSO) + G_{corr} = -1403.331089 a.u.

H = E(DMSO) + H_{corr} = -1403.269598 a.u.

C	2.76935500	1.39111200	0.35338600
C	2.36289300	0.12813900	0.45499000
C	1.15858200	-0.42684700	-0.26239100
C	-0.15018800	0.19009200	0.29856700
C	-1.43575900	-0.56646600	-0.12078800
F	2.63820900	-0.52627500	1.59342300
F	1.02764200	-1.75246200	-0.07534900
F	1.17975500	-0.15354600	-1.57655800
F	-0.10158200	0.17739000	1.64200500
F	-0.24915200	1.46732200	-0.10604300
F	-1.59459200	-1.63260000	0.67335100
F	-1.34566500	-0.98354400	-1.39039600
F	2.38097300	2.14727600	-0.70739500
H	3.51611600	1.84590000	0.98642000
C	-2.71123600	0.29488700	-0.00269400
F	-3.77717000	-0.48681700	-0.10681400
F	-2.74061400	0.90633200	1.17518500
F	-2.75779000	1.20283700	-0.96517200
O	3.56663200	-1.31986300	-0.69224900
H	4.04882700	-0.64570300	-1.18097400

TS28

E(DMSO)[M06-2X/6-311++G(2d,p), SMD (DMSO)] = -1254.436548 a.u.

G_{corr}(DMSO)[M06-2X/6-311++G(2d,p)] = 0.042355 a.u.

H_{corr}(DMSO)[M06-2X/6-311++G(2d,p)] = 0.102135 a.u.

G = E(DMSO) + G_{corr} = -1254.394193 a.u.

H = E(DMSO) + H_{corr} = -1254.334413 a.u.

C	3.29765300	-1.15580600	0.18540900
C	2.15803000	-0.40054400	0.42682200
C	1.36933400	0.39248600	-0.46138800

C	-0.07502900	0.73057000	0.00828000
C	-0.97489200	-0.53040600	-0.07186400
F	1.78385400	-0.36085600	1.76819100
F	-0.22532300	1.18930700	1.26605600
F	-0.64128400	1.63257500	-0.82521900
F	-0.69666000	-1.34430700	0.96264300
F	-0.74923800	-1.20959600	-1.21068800
H	3.66685500	-1.62541500	1.12442500
O	3.91643700	-1.37675800	-0.87619000
O	1.55826400	0.48341300	-1.67588900
O	1.88757400	2.47288300	0.29470300
H	2.35113400	2.54184100	-0.54503700
C	-2.49374400	-0.26222400	-0.03070500
F	-2.82018900	0.53263100	0.98090900
F	-2.91404700	0.29038100	-1.16156400
F	-3.13759200	-1.41871000	0.12414800

TS29
E(DMSO)[M06-2X/6-311++G(2d,p), SMD (DMSO)] = -1254.442007 a.u.
G_{corr}(DMSO)[M06-2X/6-311++G(2d,p)] = 0.045413 a.u.
H_{corr}(DMSO)[M06-2X/6-311++G(2d,p)] = 0.10266 a.u.
G = E(DMSO) + G_{corr} = -1254.396594 a.u.
H = E(DMSO) + H_{corr} = -1254.339347 a.u.

C	-3.36582900	-0.56023400	-0.63110900
C	-2.36581700	0.44288700	-0.40274000
C	-1.06906600	-0.42029400	0.65363900
C	0.05800300	0.72949300	0.65974300
C	1.24331000	0.53654600	-0.30923000
F	-1.79425000	0.83455900	-1.63179700
F	-0.38199800	2.00577900	0.41856900
F	0.64914500	0.80637000	1.89194900
F	0.86058600	0.62890200	-1.58962600
F	2.09311300	1.58532400	-0.09908500
H	-3.19146600	-1.16541100	-1.54431500
O	-4.29398600	-0.84757400	0.11460200
O	-0.59359200	-1.41112300	-0.04140000
O	-1.61589000	-0.52279600	1.81127900
H	-2.67457700	1.32806100	0.14495000
C	2.10890700	-0.75514300	-0.16133200
F	1.86205700	-1.64151400	-1.11038800
F	3.40657700	-0.41933000	-0.30018100
F	1.99774200	-1.32789500	1.02830200

TS30

E(DMSO)[M06-2X/6-311++G(2d,p), SMD (DMSO)] = -1254.434562 a.u.
G_{corr}(DMSO)[M06-2X/6-311++G(2d,p)] = 0.042018 a.u.
H_{corr}(DMSO)[M06-2X/6-311++G(2d,p)] = 0.10211 a.u.
G = E(DMSO) + G_{corr} = -1254.392544 a.u.
H = E(DMSO) + H_{corr} = -1254.332452 a.u.

C	-2.94947900	-0.83186100	-0.50895000
C	-1.79047700	0.00799900	-0.23720500
C	-0.82230800	-0.10847600	0.72505300
C	0.35932300	0.89796200	0.64962200
C	1.46716500	0.52158800	-0.35002800
F	-1.66427500	1.02111400	-1.17423700
F	0.00777000	2.17295100	0.33295800
F	0.96670700	0.97848000	1.85752200
F	2.50533300	1.37105300	-0.19589800
F	1.01442200	0.65100400	-1.60738600
H	-3.30167100	-0.71166200	-1.54613900
O	-3.26409700	-1.82909600	0.14974900
O	-0.70171500	-0.95439100	1.65018100
C	2.03829900	-0.90181600	-0.22358300
F	2.46299600	-1.14456400	1.00779900
F	1.13978600	-1.81069200	-0.56732700
F	3.07759100	-1.01571500	-1.05205100
O	-4.44585200	0.66875800	-0.14247100
H	-4.81311800	0.10443800	0.54460400

TS31
E(DMSO)[M06-2X/6-311++G(2d,p), SMD (DMSO)] = -2028.318027 a.u.
G_{corr}(DMSO)[M06-2X/6-311++G(2d,p)] = 0.046131 a.u.
H_{corr}(DMSO)[M06-2X/6-311++G(2d,p)] = 0.122854 a.u.
G = E(DMSO) + G_{corr} = -2028.271896 a.u.
H = E(DMSO) + H_{corr} = -2028.195173 a.u.

C	-4.39319500	0.23205400	-0.39490300
C	-3.17431800	-0.43710900	0.27884800
C	-1.83542900	0.26559700	-0.05632900
C	-0.60919000	-0.64468800	0.20270100
C	0.72273400	0.12654300	0.34367300
F	-4.33387600	1.54845100	-0.24010200
F	-4.42615600	-0.05339400	-1.68664400
F	-5.50334300	-0.21834800	0.16967900
F	-3.13005300	-1.71327500	-0.12518400
F	-3.36296400	-0.40251300	1.60123700

F	-1.84727100	0.61869000	-1.34977900
F	-1.74932500	1.37453800	0.68855500
F	-0.51345400	-1.50260900	-0.82065500
F	-0.82055500	-1.34156400	1.33171600
F	0.75790600	1.06039400	-0.63896500
F	0.69439000	0.80684000	1.50868000
O	1.72250000	-0.74704500	0.28102700
C	3.03126900	-0.13706400	0.43209100
F	3.42246700	-0.51526100	1.73993300
C	3.36540000	2.32149000	-0.15069900
O	3.08131200	2.77256400	0.88345000
O	3.70126300	2.16403800	-1.25396000
C	3.88900500	-1.00274200	-0.44275400
F	5.18251900	-0.65295000	-0.32815500
F	3.85534200	-2.33693700	-0.17921500
F	3.55012300	-0.87883500	-1.73331400

TS32
E(DMSO)[M06-2X/6-311++G(2d,p), SMD (DMSO)] = -1839.701735 a.u.
G_{corr}(DMSO)[M06-2X/6-311++G(2d,p)] = 0.037908 a.u.
H_{corr}(DMSO)[M06-2X/6-311++G(2d,p)] = 0.107841 a.u.
G = E(DMSO) + G_{corr} = -1839.663827 a.u.
H = E(DMSO) + H_{corr} = -1839.593894 a.u.

C	-4.03551600	-0.41415100	-0.11800400
C	-2.78242600	0.33257300	0.39004400
C	-1.47811300	-0.11668600	-0.31179900
C	-0.21129300	0.27973800	0.48792200
C	1.07061700	0.29725400	-0.37189100
F	-4.05642300	-0.41660100	-1.44418900
F	-4.04444300	-1.66209600	0.32124700
F	-5.11772700	0.20375500	0.33029300
F	-2.67984700	0.11680800	1.70754900
F	-2.96326300	1.63798900	0.17017600
F	-1.49517300	-1.44881800	-0.45181400
F	-1.44116600	0.44253000	-1.52725200
F	-0.05649100	-0.59963300	1.48302300
F	-0.38455600	1.50268900	1.01046700
F	1.08638200	-0.80641900	-1.14123000
F	1.02984300	1.35132800	-1.20086300
O	2.13321100	0.35160700	0.46174100
C	3.34553400	0.51262200	-0.18516000
F	3.77587300	1.79883100	-0.14941400
C	4.26494700	-0.47583700	-0.12867300

F	5.42768500	-0.29281800	-0.72165500
F	5.04939500	-0.69049600	1.55127700
F	3.85789100	-1.72659600	-0.18967900

TS33
E(DMSO)[M06-2X/6-311++G(2d,p), SMD (DMSO)] = -1815.633022 a.u.
G_{corr}(DMSO)[M06-2X/6-311++G(2d,p)] = 0.04642 a.u.
H_{corr}(DMSO)[M06-2X/6-311++G(2d,p)] = 0.11902 a.u.
G = E(DMSO) + G_{corr} = -1815.586602 a.u.
H = E(DMSO) + H_{corr} = -1815.514002 a.u.

C	-4.03659100	-0.42531600	-0.11705200
C	-2.79122200	0.33980100	0.38283300
C	-1.47975200	-0.12304100	-0.29666000
C	-0.22137600	0.29610300	0.50468300
C	1.06696800	0.28859900	-0.34518600
F	-4.04206900	-0.46575600	-1.44278600
F	-4.04577300	-1.66012300	0.35775700
F	-5.12568700	0.20126900	0.30087900
F	-2.69804100	0.15854300	1.70610700
F	-2.97426900	1.63823700	0.12776900
F	-1.49090300	-1.45785800	-0.40454700
F	-1.43081900	0.40725000	-1.52445200
F	-0.07196900	-0.55502300	1.52383400
F	-0.39679300	1.53297900	0.98971800
F	1.10264000	-0.83901900	-1.07249100
F	1.04208100	1.31378300	-1.20624400
O	2.12482300	0.37364900	0.50369800
C	3.33640800	0.52545200	-0.11352000
F	3.71957200	1.79892700	-0.25531400
C	4.17856500	-0.47239300	-0.30263000
F	5.32636300	-0.30848700	-0.91097000
F	3.81089700	-1.72566500	-0.21967800
O	5.26455600	-0.59648300	1.75651000
H	6.03990500	-1.14406400	1.91729300

TS34
E(DMSO)[M06-2X/6-311++G(2d,p), SMD (DMSO)] = -1815.694019 a.u.
G_{corr}(DMSO)[M06-2X/6-311++G(2d,p)] = 0.049543 a.u.
H_{corr}(DMSO)[M06-2X/6-311++G(2d,p)] = 0.120059 a.u.
G = E(DMSO) + G_{corr} = -1815.644476 a.u.
H = E(DMSO) + H_{corr} = -1815.57396 a.u.

C	-4.04779700	-0.36684300	-0.15750000
C	-2.77170800	0.20803500	0.49579300
C	-1.50007800	-0.00443400	-0.36236900
C	-0.20089100	0.12190700	0.47151700
C	1.05981100	0.38251700	-0.38046800
F	-4.11162700	0.00072900	-1.43049800
F	-4.05476400	-1.68799800	-0.08421900
F	-5.10936400	0.10199700	0.48057700
F	-2.61679100	-0.38338500	1.68686100
F	-2.95530000	1.51897000	0.67726800
F	-1.54357800	-1.22744300	-0.90871400
F	-1.50289000	0.90441600	-1.34489700
F	-0.03686600	-1.01763400	1.15331200
F	-0.34057000	1.13333500	1.34255200
F	1.03330300	-0.45526500	-1.43639400
F	0.99641000	1.63104700	-0.87933800
O	2.13434500	0.20178700	0.40370900
C	3.35043200	0.51660700	-0.20997400
F	3.75718400	1.76612100	0.19435800
C	4.31688600	-0.46255700	-0.18032000
F	4.87659800	-0.91244300	1.47041500
F	5.53236800	-0.04947000	-0.57492000
O	3.99805600	-1.70038200	-0.56392400
H	4.38384500	-2.28939700	0.10438600

TS35
E(DMSO)[M06-2X/6-311++G(2d,p), SMD (DMSO)] = -1791.667119 a.u.
G_{corr}(DMSO)[M06-2X/6-311++G(2d,p)] = 0.061139 a.u.
H_{corr}(DMSO)[M06-2X/6-311++G(2d,p)] = 0.132465 a.u.
G = E(DMSO) + G_{corr} = -1791.60598 a.u.
H = E(DMSO) + H_{corr} = -1791.534654 a.u.

C	-4.05217100	-0.42067700	-0.07234500
C	-2.79349800	0.36393800	0.35898400
C	-1.49819600	-0.14058000	-0.32304800
C	-0.22179200	0.30575900	0.43303200
C	1.06254300	0.24453700	-0.42222700
F	-4.08106100	-0.54365700	-1.39270100
F	-4.06260100	-1.62396900	0.47829300
F	-5.13048400	0.23883900	0.32329600
F	-2.67601800	0.25394700	1.68848500
F	-2.97874900	1.64783700	0.03850800
F	-1.52522800	-1.47988200	-0.36725400
F	-1.47621800	0.32907700	-1.57605300
F	-0.07236200	-0.49578400	1.49513200

F	-0.38813300	1.56663200	0.86140400
F	1.06933900	-0.94085800	-1.07288800
F	1.00227200	1.20110400	-1.36511800
O	2.11329200	0.39207800	0.39591300
C	3.36528500	0.45899700	-0.27938500
F	3.72945300	1.79779900	-0.33733100
C	4.33953700	-0.34509800	0.35838800
F	5.17132900	-1.34134000	-0.98460300
O	3.95471800	-1.38997300	1.09633600
H	3.06049800	-1.65615100	0.83729400
O	5.47352200	0.22573700	0.75760300
H	6.16315900	-0.45554700	0.74095400

TS36
E(DMSO)[M06-2X/6-311++G(2d,p), SMD (DMSO)] = -1767.684371 a.u.
G_{corr}(DMSO)[M06-2X/6-311++G(2d,p)] = 0.069563 a.u.
H_{corr}(DMSO)[M06-2X/6-311++G(2d,p)] = 0.140758 a.u.
G = E(DMSO) + G_{corr} = -1767.614808 a.u.
H = E(DMSO) + H_{corr} = -1767.543613 a.u.

C	-3.90941700	0.17972700	-0.42937500
C	-2.68932700	-0.32777100	0.37072400
C	-1.34795400	0.26630900	-0.12665400
C	-0.12672900	-0.57042000	0.32950600
C	1.21590200	0.19244900	0.26652200
F	-3.84754100	1.49768000	-0.56674600
F	-3.94747000	-0.38187000	-1.62708400
F	-5.01761700	-0.13394300	0.22466400
F	-2.65885200	-1.66282000	0.27124100
F	-2.86541200	0.01257200	1.65090000
F	-1.36430100	0.30844100	-1.46652600
F	-1.24889500	1.51708000	0.33949800
F	-0.05163200	-1.64835800	-0.46046100
F	-0.32571300	-0.97313000	1.59463600
F	1.26559000	0.83757400	-0.92507300
F	1.20988500	1.15270400	1.21042600
O	2.20280200	-0.69709200	0.41967000
C	3.56805700	-0.23810300	0.55490800
F	3.67274700	0.33733200	1.81033700
C	3.91457200	0.79798600	-0.49280000
O	4.10686500	0.25673400	-1.69365200
H	4.23657100	-0.74060700	-1.57471700
O	4.63328100	-2.10661800	-0.81239800
H	4.25680800	-1.39766700	0.05772600
H	4.00531000	-2.83243800	-0.88764300

O	4.10250100	1.97201300	-0.28045300

TS37
E(DMSO)[M06-2X/6-311++G(2d,p), SMD (DMSO)] = -1767.18454 a.u.
G_{corr}(DMSO)[M06-2X/6-311++G(2d,p)] = 0.059671 a.u.
H_{corr}(DMSO)[M06-2X/6-311++G(2d,p)] = 0.131506 a.u.
G = E(DMSO) + G_{corr} = -1767.124869 a.u.
H = E(DMSO) + H_{corr} = -1767.053034 a.u.

C	-4.07189600	-0.26333400	0.00627800
C	-2.76368300	0.55417600	-0.08191700
C	-1.49128700	-0.32925200	-0.08055500
C	-0.21492100	0.46166800	0.29673200
C	1.12072300	-0.20142100	-0.12552400
F	-4.03652400	-1.28043900	-0.84514200
F	-4.25031000	-0.72907000	1.23224900
F	-5.09445600	0.52066700	-0.30404500
F	-2.73841800	1.39590100	0.96016200
F	-2.80000500	1.26317500	-1.21520600
F	-1.66638100	-1.32254900	0.80588600
F	-1.36648100	-0.86574400	-1.30121500
F	-0.22456000	0.62032100	1.62946200
F	-0.28804200	1.68044600	-0.27281200
F	0.97361500	-1.55863600	0.13870100
F	1.15540600	-0.15176400	-1.50787800
O	2.12741900	0.34146100	0.44688300
C	3.66416200	-0.44252300	0.09152700
H	3.34157100	-1.02099600	-0.75331000
F	3.75094100	-1.10556400	1.23919900
C	4.46260300	0.85338500	-0.06608300
O	4.92434300	1.34055700	0.97872100
O	4.50246000	1.28912300	-1.23421200
O	5.44498900	-1.48349900	-0.59467900
H	5.69747700	-0.87703200	-1.29740100

TS38
E(DMSO)[M06-2X/6-311++G(2d,p), SMD (DMSO)] = -1767.149035 a.u.
G_{corr}(DMSO)[M06-2X/6-311++G(2d,p)] = 0.062824 a.u.
H_{corr}(DMSO)[M06-2X/6-311++G(2d,p)] = 0.132234 a.u.
G = E(DMSO) + G_{corr} = -1767.086211 a.u.
H = E(DMSO) + H_{corr} = -1767.016801 a.u.

C	-3.11871500	-1.11399600	0.10349100

C	-2.33131800	0.19477700	-0.13981300
C	-0.78212500	-0.01958500	-0.07919900
C	-0.03320200	1.31969400	0.20752200
C	1.52078700	1.45717800	0.05892600
F	-2.60450700	-2.10867300	-0.60875100
F	-3.10701200	-1.44585800	1.38562300
F	-4.38090200	-0.93397600	-0.26879100
F	-2.75321400	1.07967100	0.77390800
F	-2.68012300	0.63911900	-1.35461000
F	-0.57137900	-0.93016800	0.88158000
F	-0.45858500	-0.52251400	-1.27750100
F	-0.34590000	1.63700400	1.47559400
F	-0.66378000	2.16192300	-0.64744600
F	2.05003000	1.64007500	-1.17432600
F	2.30322600	1.52898500	1.15906800
O	1.72284100	-0.22639700	-0.00044300
C	2.94470600	-0.67121300	-0.33653100
H	3.74176400	0.05414100	-0.14420400
F	3.01144300	-0.88003400	-1.75583600
C	3.25497400	-2.01203600	0.37258900
O	3.95407100	-1.89189300	1.40314900
O	2.76698000	-3.04840200	-0.11600400
O	1.34368500	3.24565100	0.25248300
H	1.03331200	3.59527600	-0.58778600

References and Notes

1. A. Leeson, T. Thompson, H. F. Stroo, R. H. Anderson, J. Speicher, M. A. Mills, J. Willey, C. Coyle, R. Ghosh, C. Lebrón, C. Patton, Identifying and managing aqueous film-forming foam-derived per- and polyfluoroalkyl substances in the environment. *Environ. Toxicol. Chem.* **40**, 24–36 (2021). doi:10.1002/etc.4894 Medline

2. A. M. Calafat, L.-Y. Wong, Z. Kuklenyik, J. A. Reidy, L. L. Needham, Polyfluoroalkyl chemicals in the U.S. population: Data from the National Health and Nutrition Examination Survey (NHANES) 2003-2004 and comparisons with NHANES 1999-2000. *Environ. Health Perspect.* **115**, 1596–1602 (2007). doi:10.1289/ehp.10598 Medline

3. United Nations Stockholm Convention, "Perfluorooctanoic acid (PFOA), its salts and PFOA-related compounds" (UN, 2017); http://chm.pops.int/Implementation/Alternatives/AlternativestoPOPs/ChemicalslistedinAnnexA/PFOA/tabid/8292/Default.aspx.

4. "C-8 Medical Monitoring Program" (GCG, 2022); http://www.c-8medicalmonitoringprogram.com/.

5. N. Rich, "Rob Bilott v. DuPont," *New York Times Magazine*, 17 January 2016; https://hnbpjs.blogspot.com/2016/01/rob-bilott-v-dupont.html.

6. A. Maimaiti, S. Deng, P. Meng, W. Wang, B. Wang, J. Huang, Y. Wang, G. Yu, Competitive adsorption of perfluoroalkyl substances on anion exchange resins in simulated AFFF-impacted groundwater. *Chem. Eng. J.* **348**, 494–502 (2018). doi:10.1016/j.cej.2018.05.006

7. M. Ateia, A. Alsbaiee, T. Karanfil, W. Dichtel, Efficient PFAS removal by amine-functionalized sorbents: Critical review of the current literature. *Environ. Sci. Technol. Lett.* **6**, 688–695 (2019). doi:10.1021/acs.estlett.9b00659

8. D. Bond, J. Enck, "First in the nation testing reveals toxic contamination in soil and water near Norlite incinerator" (Bennington University, 2020); https://www.bennington.edu/sites/default/files/sources/docs/Norlite%20News%20Release%20%5Bdb%20final%20updated%5D.pdf .

9. C. D. Vecitis, H. Park, J. Cheng, B. T. Mader, M. R. Hoffmann, Kinetics and mechanism of the sonolytic conversion of the aqueous perfluorinated surfactants, perfluorooctanoate (PFOA), and perfluorooctane sulfonate (PFOS) into inorganic products. *J. Phys. Chem. A* **112**, 4261–4270 (2008). doi:10.1021/jp801081y Medline

10. J. Cheng, C. D. Vecitis, H. Park, B. T. Mader, M. R. Hoffmann, Sonochemical degradation of perfluorooctane sulfonate (PFOS) and perfluorooctanoate (PFOA) in groundwater: Kinetic effects of matrix inorganics. *Environ. Sci. Technol.* **44**, 445–450 (2010). doi:10.1021/es902651g Medline

11. R. K. Singh, S. Fernando, S. F. Baygi, N. Multari, S. M. Thagard, T. M. Holsen, Breakdown products from perfluorinated alkyl substances (PFAS) degradation in a plasma-based water treatment process. *Environ. Sci. Technol.* **53**, 2731–2738 (2019). doi:10.1021/acs.est.8b07031 Medline

12. C. E. Schaefer, C. Andaya, A. Urtiaga, E. R. McKenzie, C. P. Higgins, Electrochemical treatment of perfluorooctanoic acid (PFOA) and perfluorooctane sulfonic acid (PFOS) in groundwater impacted by aqueous film forming foams (AFFFs). *J. Hazard. Mater.* **295**, 170–175 (2015). doi:10.1016/j.jhazmat.2015.04.024 Medline

13. A. M. Trautmann, H. Schell, K. R. Schmidt, K. M. Mangold, A. Tiehm, Electrochemical degradation of perfluoroalkyl and polyfluoroalkyl substances (PFASs) in groundwater. *Water Sci. Technol.* **71**, 1569–1575 (2015). doi:10.2166/wst.2015.143 Medline

14. M. J. Krause, E. Thoma, E. Sahle-Damesessie, B. Crone, A. Whitehill, E. Shields, B. Gullett, Supercritical water oxidation as an innovative technology for PFAS destruction. *J. Environ. Eng.* **148**, 05021006 (2022). doi:10.1061/(ASCE)EE.1943-7870.0001957

15. M. J. Bentel, Z. Liu, Y. Yu, J. Gao, Y. Men, J. Liu, Enhanced degradation of perfluorocarboxylic acids (PFCAs) by UV/sulfite treatment: Reaction mechanisms and system efficiencies at pH 12. *Environ. Sci. Technol. Lett.* **7**, 351–357 (2020). doi:10.1021/acs.estlett.0c00236

16. M. J. Bentel, Y. Yu, L. Xu, Z. Li, B. M. Wong, Y. Men, J. Liu, Defluorination of per- and polyfluoroalkyl substances (PFASs) with hydrated electrons: Structural dependence and implications to PFAS remediation and management. *Environ. Sci. Technol.* **53**, 3718–3728 (2019). doi:10.1021/acs.est.8b06648 Medline

17. M. J. Bentel, Y. Yu, L. Xu, H. Kwon, Z. Li, B. M. Wong, Y. Men, J. Liu, Degradation of perfluoroalkyl ether carboxylic acids with hydrated electrons: Structure–reactivity relationships and environmental implications. *Environ. Sci. Technol.* **54**, 2489–2499 (2020). doi:10.1021/acs.est.9b05869 Medline

18. H. Hori, A. Yamamoto, E. Hayakawa, S. Taniyasu, N. Yamashita, S. Kutsuna, H. Kiatagawa, R. Arakawa, Efficient decomposition of environmentally persistent perfluorocarboxylic acids by use of persulfate as a photochemical oxidant. *Environ. Sci. Technol.* **39**, 2383–2388 (2005). doi:10.1021/es0484754 Medline

19. X. Liang, J. Cheng, C. Yang, S. Yang, Factors influencing aqueous perfluorooctanoic acid (PFOA) photodecomposition by VUV irradiation in the presence of ferric ions. *Chem. Eng. J.* **298**, 291–299 (2016). doi:10.1016/j.cej.2016.03.150

20. B. N. Nzeribe, M. Crimi, S. Mededovic Thagard, T. M. Holsen, Physico-chemical processes for the treatment of per- and polyfluoroalkyl substances (PFAS): A review. *Crit. Rev. Environ. Sci. Technol.* **49**, 866–915 (2019). doi:10.1080/10643389.2018.1542916

21. Q. Zhuo, S. Deng, B. Yang, J. Huang, G. Yu, Efficient electrochemical oxidation of perfluorooctanoate using a Ti/SnO2-Sb-Bi anode. *Environ. Sci. Technol.* **45**, 2973–2979 (2011). doi:10.1021/es1024542 Medline

22. H. Hori, E. Hayakawa, H. Einaga, S. Kutsuna, K. Koike, T. Ibusuki, H. Kiatagawa, R. Arakawa, Decomposition of environmentally persistent perfluorooctanoic acid in water by photochemical approaches. *Environ. Sci. Technol.* **38**, 6118–6124 (2004). doi:10.1021/es049719n Medline

23. B. Wu, S. Hao, Y. Choi, C. P. Higgins, R. Deeb, T. J. Strathmann, Rapid destruction and defluorination of perfluorooctanesulfonate by alkaline hydrothermal reaction. *Environ. Sci. Technol. Lett.* **6**, 630–636 (2019). doi:10.1021/acs.estlett.9b00506

24. D. Kong, P. J. Moon, E. K. J. Lui, O. Bsharat, R. J. Lundgren, Direct reversible decarboxylation from stable organic acids in dimethylformamide solution. *Science* **369**, 557–561 (2020). doi:10.1126/science.abb4129 Medline

25. S. Zhou, B. T. Nguyen, J. P. Richard, R. Kluger, J. Gao, Origin of free energy barriers of decarboxylation and the reverse process of CO_2 capture in dimethylformamide and in water. *J. Am. Chem. Soc.* **143**, 137–141 (2021). doi:10.1021/jacs.0c12414 Medline

26. H. K. Liberatore, S. R. Jackson, M. J. Strynar, J. P. McCord, Solvent suitability for HFPO-DA ("GenX" parent acid) in toxicological studies. *Environ. Sci. Technol. Lett.* **7**, 477–481 (2020). doi:10.1021/acs.estlett.0c00323 Medline

27. C. Zhang, A. C. McElroy, H. K. Liberatore, N. L. M. Alexander, D. R. U. Knappe, Stability of per- and poly fluoroalkyl substances in solvents relevant to environmental and toxicological analysis. *Environ. Sci. Technol.* **56**, 6103–6112 (2022). doi:10.1021/acs.est.1c03979 Medline

28. D. A. Dixon, T. Fukunaga, B. E. Smart, Structures and stabilities of fluorinated carbanions: Evidence for anionic hyperconjugation. *J. Am. Chem. Soc.* **108**, 4027–4031 (1986). doi:10.1021/ja00274a029

29. T. Chatterjee, E. Boutin, M. Robert, Manifesto for the routine use of NMR for the liquid product analysis of aqueous CO_2 reduction: From comprehensive chemical shift data to formaldehyde quantification in water. *Dalton Trans.* **49**, 4257–4265 (2020). doi:10.1039/C9DT04749B Medline

30. J. D. LaZerte, L. J. Hals, T. S. Reid, G. H. Smith, Pyrolyses of the salts of the perfluoro carboxylic acids. *J. Am. Chem. Soc.* **75**, 4525–4528 (1953). doi:10.1021/ja01114a040

31. R. N. Haszeldine, 817. The reactions of metallic salts of acids with halogens. Part III. Some reactions of salts of fluorohalogenoacetates and of perfluoro-acids. *J. Chem. Soc.* 4259 (1952). doi:10.1039/jr9520004259

32. X. Zhang, U. Gross, K. Seppelt, Fluorocarbonate, $[FCO_2]^-$: Preparation and structure. *Angew. Chem. Int. Ed.* **34**, 1858–1860 (1995). doi:10.1002/anie.199518581

33. M. J. Pellerite, Unusual reaction chemistry in thermal decomposition of alkali metal 2-alkoxy-2,3,3,3-tetrafluoropropionate salts. *J. Fluor. Chem.* **49**, 43–66 (1990). doi:10.1016/S0022-1139(00)80362-0

34. Y. Ge, Z. Liu, H. Liu, J.-K. Feng, D. Liu, X. Ge, Theoretical study on the degradation reaction mechanism of elimination hydrogen fluoride from perfluoropropionic acid. *Comput. Theor. Chem.* **1029**, 33–40 (2014). doi:10.1016/j.comptc.2013.12.013

35. G. McGrath, "Denied by Trump EPA, NC activists hope Biden EPA will force 'forever chemical' study," *Fayetteville Observer*, 17 January 2021; https://www.fayobserver.com/story/news/2021/01/27/denied-by-trump-epa-nc-activists-hope-biden-epa-force-forever-chemical-study/4265453001/.

36. Y. Zhao, D. G. Truhlar, The M06 suite of density functionals for main group thermochemistry, thermochemical kinetics, noncovalent interactions, excited states, and transition elements: Two new functionals and systematic testing of four M06-class functionals and 12 other function. *Theor. Chem. Acc.* **120**, 215–241 (2008).

doi:10.1007/s00214-007-0310-x

37. A. V. Marenich, C. J. Cramer, D. G. Truhlar, Universal solvation model based on solute electron density and on a continuum model of the solvent defined by the bulk dielectric constant and atomic surface tensions. *J. Phys. Chem. B* **113**, 6378–6396 (2009). doi:10.1021/jp810292n Medline

38. M. J. Frisch, G. W. Trucks, H. B. Schlegel, G. E. Scuseria, M. A. Robb, J. R. Cheeseman, G. Scalmani, V. Barone, G. A. Petersson, H. Nakatsuji, X. Li, M. Caricato, A. V. Marenich, J. Bloino, B. G. Janesko, J. V. O. R. Gomperts, B. Mennucci, H. P. Hratchian, A. F. Izmaylov, J. L. Sonnenberg, D. Williams-Young, F. Ding, F. Lipparini, F. Egidi, J. Goings, B. Peng, A. Petrone, D. R. T. Henderson, V. G. Zakrzewski, J. Gao, N. Rega, G. Zheng, W. Liang, M. Hada, M. Ehara, K. Toyota, R. Fukuda, J. Hasegawa, M. Ishida, T. Nakajima, Y. Honda, O. Kitao, H. Nakai, T. Vreven, K. Throssell, J. J. A. Montgomery, J. E. Peralta, F. Ogliaro, M. J. Bearpark, J. J. Heyd, E. N. Brothers, K. N. Kudin, V. N. Staroverov, T. A. Keith, R. Kobayashi, J. Normand, K. Raghavachari, A. P. Rendell, J. C. Burant, S. S. Iyengar, J. Tomasi, M. Cossi, J. M. Millam, M. Klene, C. Adamo, R. Cammi, J. W. Ochterski, R. L. Martin, K. Morokuma, O. Farkas, J. B. Foresman, D. J. Fox, "Gaussian 16, Revision A.03" (Gaussian Inc, 2016).

39. N. Mardirossian, M. Head-Gordon, How accurate are the minnesota density functionals for noncovalent interactions, isomerization energies, thermochemistry, and barrier heights involving molecules composed of main-group elements? *J. Chem. Theory Comput.* **12**, 4303–4325 (2016). doi:10.1021/acs.jctc.6b00637 Medline

40. G. Luchini, J. Alegre-Requena, IFunes, J. Rodríguez-Guerra, J. Chen, R. Paton, "bobbypaton/GoodVibes: GoodVibes v3.0.0," Zenodo (2019); https://doi.org/10.5281/ZENODO.3346166.

41. S. Grimme, Supramolecular binding thermodynamics by dispersion-corrected density functional theory. *Chemistry* **18**, 9955–9964 (2012). doi:10.1002/chem.201200497 Medline

42. Y.-P. Li, J. Gomes, S. Mallikarjun Sharada, A. T. Bell, M. Head-Gordon, Improved force-field parameters for QM/MM simulations of the energies of adsorption for molecules in zeolites and a free rotor correction to the rigid rotor harmonic oscillator model for adsorption enthalpies. *J. Phys. Chem. C* **119**, 1840–1850 (2015). doi:10.1021/jp509921r

43. C. Y. Legault, "CYLview20: Visualization and analysis software for computational chemistry" (CYLview, 2020); http://www.cylview.org.

44. C. Dai, L. Sun, H. Liao, B. Khezri, R. D. Webster, A. C. Fisher, Z. J. Xu, Electrochemical production of lactic acid from glycerol oxidation catalyzed by AuPt nanoparticles. *J. Catal.* **356**, 14–21 (2017). doi:10.1016/j.jcat.2017.10.010

45. C. Butch, E. D. Cope, P. Pollet, L. Gelbaum, R. Krishnamurthy, C. L. Liotta, Production of tartrates by cyanide-mediated dimerization of glyoxylate: A potential abiotic pathway to the citric acid cycle. *J. Am. Chem. Soc.* **135**, 13440–13445 (2013). doi:10.1021/ja405103r Medline

46. T. M. Rangarajan, S. Sathyamoorthi, D. Velayutham, M. Noel, R. P. Singh, R. Brahma, Products formed at intermediate stages of electrochemical perfluorination of propionyl

and n-butyryl chlorides. Further evidence in support of NiF 3 mediated free radical pathway. *J. Fluor. Chem.* **132**, 107–113 (2011). doi:10.1016/j.jfluchem.2010.12.004

47. L. V. Saloutina, A. Y. Zapevalov, V. I. Saloutin, M. I. Kodess, V. E. Kirichenko, M. G. Pervova, O. N. Chupakhin, Synthesis of 2,3-bis(perfluoroalkyl)quinoxalines and 2,3-bis(perfluoroalkyl)-1,4-benzoxazines from oxides of internal perfluoroolefins. *J. Fluor. Chem.* **126**, 976–983 (2005). doi:10.1016/j.jfluchem.2005.05.001

48. A. Foris, 19F and 1H NMR spectra of halocarbons. *Magn. Reson. Chem.* **42**, 534–555 (2004). doi:10.1002/mrc.1368 Medline

49. T. Hogan, A. Sen, High-yield, radical-initiated oxidative functionalization of ethane by perfluorocarboxylic acid anhydrides. Role of metal ions in catalytic alkane oxidations in the presence of perfluorocarboxylic acid anhydrides. *J. Am. Chem. Soc.* **119**, 2642–2646 (1997). doi:10.1021/ja964068j

50. M. Iznaden, C. Portella, Hydro-2-oxo-3-perfluoroesters. Synthese et Properties Remarquables: Hydrate, equilibre cent-enolique. *J. Fluor. Chem.* **43**, 105–118 (1989). doi:10.1016/S0022-1139(00)81639-5

51. S. Garcia-Segura, A. B. Nienhauser, A. S. Fajardo, R. Bansal, C. L. Conrad, J. D. Fortner, M. Marcos-Hernández, T. Rogers, D. Villagran, M. S. Wong, P. Westerhoff, Disparities between experimental and environmental conditions: Research steps toward making electrochemical water treatment a reality. *Curr. Opin. Electrochem.* **22**, 9–16 (2020). doi:10.1016/j.coelec.2020.03.001

52. M. Panizza, G. Cerisola, Direct and mediated anodic oxidation of organic pollutants. *Chem. Rev.* **109**, 6541–6569 (2009). doi:10.1021/cr9001319 Medline

53. Z. Liu, M. J. Bentel, Y. Yu, C. Ren, J. Gao, V. F. Pulikkal, M. Sun, Y. Men, J. Liu, Near-quantitative defluorination of perfluorinated and fluorotelomer carboxylates and sulfonates with integrated oxidation and reduction. *Environ. Sci. Technol.* **55**, 7052–7062 (2021). doi:10.1021/acs.est.1c00353 Medline

54. N. Watanabe, S. Takemine, K. Yamamoto, Y. Haga, M. Takata, Residual organic fluorinated compounds from thermal treatment of PFOA, PFHxA and PFOS adsorbed onto granular activated carbon (GAC). *J. Mater. Cycles Waste Manag.* **18**, 625–630 (2016). doi:10.1007/s10163-016-0532-x

55. N. Watanabe, M. Takata, S. Takemine, K. Yamamoto, Thermal mineralization behavior of PFOA, PFHxA, and PFOS during reactivation of granular activated carbon (GAC) in nitrogen atmosphere. *Environ. Sci. Pollut. Res. Int.* **25**, 7200–7205 (2018). doi:10.1007/s11356-015-5353-2 Medline

56. F. Xiao, P. C. Sasi, B. Yao, A. Kubátová, S. A. Golovko, M. Y. Golovko, D. Soli, Thermal stability and decomposition of perfluoroalkyl substances on spent granular activated carbon. *Environ. Sci. Technol. Lett.* **7**, 343–350 (2020). doi:10.1021/acs.estlett.0c00114

57. S. Hao, Y.-J. Choi, B. Wu, C. P. Higgins, R. Deeb, T. J. Strathmann, Hydrothermal alkaline treatment for destruction of per- and polyfluoroalkyl substances in aqueous film-forming foam. *Environ. Sci. Technol.* **55**, 3283–3295 (2021). doi:10.1021/acs.est.0c06906 Medline